



TAMPEREEN TEKNILLINEN YLIOPISTO
TAMPERE UNIVERSITY OF TECHNOLOGY

JETTE-BRITT NAAMS
A RAPID CELL CULTURE PROTOCOL FOR SCREENING
MATERIAL CYTOCOMPATIBILITY
Master of Science Thesis

Examiners: Professor Minna Kellomäki,
Doctoral student Janne Koivisto
Examiner and topic approved by the
Council of the Faculty of Natural
Sciences on 12th August 2015

ABSTRACT

JETTE-BRITT NAAMS: A rapid cell culture protocol for screening material cytocompatibility

Tampere University of technology

Master of Science Thesis, 76 pages, 22 Appendix pages

June 2016

Master's Degree Programme in Biotechnology

Major: Tissue Engineering

Examiners: Professor Minna Kellomäki, Doctoral student Janne Koivisto

Keywords: cytotoxicity, 3D cell culture, hydrogel, gellan gum, biomaterial, BioStation CT, fibroblast

Hydrogels differ from many other cell culture substrates in that they provide a three-dimensional, soft environment for cells, opposed to a two-dimensional surface on which cells are traditionally cultured. This geometry better represents the *in vivo* environment of cells. In addition, hydrogels are easily modified for enhanced cell viability and growth. Therefore, new hydrogels are continuously developed for cell culture and tissue engineering purposes.

Applicability of a hydrogel as cell culture substrate depends on several chemical and physical attributes. Together these attributes affect cytocompatibility of the hydrogel, i.e. cell attachment, viability and cell specific response. The objective of this thesis was to create a protocol for first-step, short-term cell culture screening of new hydrogels. Cytocompatibility testing and analysis methods need to be adjusted for macroscopic 3D hydrogels compared to 2D culturing systems. Another challenge in this screening is adequate stability of cells and their representativeness of the cells intended to be used in the final application.

An interview was conducted with Regenerative Medicine professionals in BioMediTech Institute (University of Tampere) who are working with cardiomyocytes, bone and cartilage cells, corneal and retinal epithelial cells, and neuronal cells. Knowledge was gathered on the properties of representable cell models of each cell type and on tissue-specific aspects of analyzing. A commercial human embryonic fibroblast cell line WI-38 was chosen as a representative first-step cell model and acquired for the first-step cytocompatibility testing. In addition, tissue specific cell lines were recommended for further testing.

Cells were cultured on top and encapsulated in PuraMatrix[®] and gellan gum hydrogels, and on poly(dimethylsiloxane) (PDMS) and uncoated well plate. Cells were stained with Live/dead viability/cytotoxicity kit. The suitability of Nikon BioStation CT cell culture observation system was evaluated for the screening of hydrogels and compared with two other imaging systems. It was possible to assess cell attachment and viability from fluorescence images taken with BioStation CT, even though it was not an optimal imaging system for 3D hydrogel screening. As the result of this thesis, a first-step cytocompatibility testing protocol was created for assessing attachment and viability of cells that were cultured on top and encapsulated in hydrogels.

TIIVISTELMÄ

JETTE-BRITT NAAMS: Nopea soluviljelyprotokolla materiaalien sytokompatibiliteettitestaukseen

Tampereen teknillinen yliopisto

Diplomityö, 76 sivua, 22 liitesivua

Kesäkuu 2016

Biotekniikan koulutusohjelma

Pääaine: Kudosteknologia

Tarkastajat: professori Minna Kellomäki, tohtorikoulutettava Janne Koivisto

Avainsanat: sytotoksisuus, 3D soluviljely, hydrogeeli, gellaanikumi, biomateriaali, BioStation CT, fibroblasti

Hydrogeelit eroavat monista muista soluviljelyalustoista niin, että ne tarjoavat soluille kolmiulotteisen, pehmeän kasvuympäristön. Perinteinen kasvualusta on sen sijaan kaksiulotteinen ja kova pinta. Hydrogeelien kolmiulotteinen (3D) ympäristö kuvastaa paremmin ympäristöä, jossa solut kasvavat kehossa. Lisäksi hydrogeelit ovat helposti kemiallisesti muokattavissa, jolloin solujen kasvua ja elinkykyisyyttä materiaalissa voidaan parantaa. Uusia hydrogeelejä kehitetäänkin jatkuvasti soluviljelyn ja kudosteknologian tarpeisiin.

Hydrogeelin soveltuvuus soluviljelyn kasvualustaksi on riippuvainen monista sen kemiallisista ja fysikaalisista ominaisuuksista. Nämä ominaisuudet vaikuttavat yhdessä hydrogeelin sytokompatibiliteettiin, eli solujen kiinnittymiseen, elinkykyisyyteen ja solutyypistä riippuvaan vasteeseen. Tämän diplomityön tarkoituksena oli kehittää lyhytaikaiseen soluviljelyyn perustuva protokolla uusien hydrogeelien alkuvaiheen seulontaan. Koe- ja analysointimenetelmiä on säädettävä sytokompatibiliteetin testaamiseksi, kun soluja kasvatetaan 3D-materiaalissa verrattuna kaksiulotteisella materiaalilla kasvattamiseen. Lisäksi seulonnan haasteena on solujen riittävä stabiilius sekä edustavuus verrattuna soluihin, joita on tarkoitus käyttää lopullisessa sovelluksessa.

Diplomityössä haastateltiin BioMediTech -instituutin (Tampereen yliopisto) Regeneratiivisen lääketieteen tutkimusryhmiä, jotka tutkivat kardiomyosyyttejä, luu- ja rustosoluja, verkkokalvon ja sarveiskalvon soluja sekä hermoston soluja. Haastattelussa kerättiin tietoa kutakin solutyypistä edustavien solujen ominaisuuksista sekä näiden solutyypien analysoimisesta. Kaupallinen ihmisen embryonaalinen fibroblastisolulinja WI-38 valittiin edustavaksi ensimmäisen vaiheen solumalliksi ja se hankittiin ensimmäisen vaiheen sytokompatibiliteettitestausta varten. Lisäksi jatkotutkimuksia varten ehdotettiin kudoskohtaisia solulinjoja.

Soluja kasvatettiin PuraMatrix[®]- ja gellaanikumihydrogeelien päällä ja sisällä, sekä polydimetyylisiloksaanilla (PDMS) ja päällystämättömällä kuoppalevyllä. Solut värjättiin Live/dead viabiliteetti/sytotoksisuus -kitillä. Nikon BioStation CT -kuvantamisjärjestelmän soveltuvuutta hydrogeelien seulontaan arvioitiin, ja sitä verrattiin kahteen muuhun kuvantamisjärjestelmään. BioStation CT:n avulla saaduista fluoresenssikuvista oli mahdollista määrittää solujen elinkykyisyys ja kiinnittyminen, mutta se ei kuitenkaan ollut optimaalinen 3D-hydrogeelien seulontaan. Diplomityön tuloksena tuotettiin sytokompatibiliteetin testausprotokolla, jota voidaan käyttää hydrogeelien päällä ja sisällä kasvatettujen solujen kiinnittymisen ja elinkykyisyyden määrittämiseksi.

PREFACE

This Master's thesis was done in Biomaterials research group in BioMediTech Institute, Tampere University of Technology. The thesis was part of the Human Spare Parts project funded by Finnish Funding Agency for Innovation (TEKES). Part of the practical work was done in premises of BioMediTech Institute, University of Tampere, and an interview was conducted with BioMediTech Regenerative Medicine research groups. In this thesis, a macro for FiJi software was written by MSc Boris Kashentsev (Appendix 5).

I would like to thank Professor Minna Kellomäki for offering me this topic and for encouraging advice along the project. I would like to express my gratitude to my supervisor Janne Koivisto for all the advice and help with the thesis and for creating a nice working atmosphere. In addition, I would like to thank all the staff members of BioMediTech who were helping me along the way, and who gave their valuable time and knowledge. Especially, I would like to thank Outi Paloheimo and Risto-Pekka Pölönen for teaching me using imaging systems and Henna Venäläinen for teaching me how to culture cells, Joose Kreuzer for instructing with PDMS and Olli Koskela for help with image analysis.

I am grateful for being able to end my studies to such interdisciplinary project and for learning so much during the thesis. I would like to thank my family and friends for patience and understanding, and never losing faith in me during my long process of graduation. Special thanks go to Noora, your company during this spring was invaluable help for me. Finally, my boyfriend Boris, I cannot thank you enough for your endless support, in so many meanings of the word.

Tampere, 25th May 2016

JETTE-BRITT NAAMS

TABLE OF CONTENTS

1. Introduction	1
THEORETICAL BACKGROUND	3
2. Cytotoxicity and biocompatibility tests of materials	4
2.1 Definitions.....	4
2.2 Standards for testing cytotoxicity and biocompatibility	5
2.3 Standards for testing hydrogel compatibility for cell culture.....	7
3. Mammalian cell culture and repeatability.....	9
3.1 Culture types	9
3.1.1 Primary cell, cell line and cell strain.....	10
3.1.2 Formation of cell line.....	10
3.1.3 Finite and continuous cell lines	11
3.1.4 Stem cells.....	12
3.2 Advantages and disadvantages of cell lines	13
3.3 Growth characteristics.....	14
3.4 Environmental conditions of cell culture	15
3.4.1 Culture substrate	15
3.4.2 Culture medium	15
4. Selecting fibroblast cell line.....	17
5. Hydrogels as cell culture substrates	21
5.1 Puramatrix® hydrogel.....	22
5.2 Gellan gum hydrogels	22
6. Methods for testing cytocompatibility	24
6.1 Cell viability.....	24
6.2 Proliferation.....	25
6.3 Cell attachment.....	26
6.4 Morphology.....	26
EXPERIMENTAL PART.....	27
7. Interview on expert perspective	28
7.1 General requirements for all cell models	28
7.2 Criteria for different cell models.....	29
7.3 Representative cell lines.....	30
7.4 Culture environment.....	33
7.5 Analysis methods	34
7.6 Conclusion	35
8. Development of cytotoxicity protocol to study novel hydrogels.....	37
8.1 Research methods and materials	38
8.1.1 Sample preparation	39
8.1.2 Imaging systems	44
8.1.3 Image acquisition settings in BioStation CT	46
8.1.4 Image analysis.....	48

8.1.5	Assessment of attachment and viability.....	49
8.2	Experimental results.....	51
8.2.1	Sample parameters.....	51
8.2.2	Choice of imaging system.....	52
8.2.3	Focusing range and sample volume in BioStation CT	53
8.2.4	Image acquisition in BioStation CT.....	56
8.2.5	Image analysis.....	61
8.2.6	Assessment of attachment and viability.....	64
8.2.7	Cell behavior.....	65
9.	Discussion and future recommendations	67
10.	Conclusions	71
	References	72
	Appendices.....	77

TERMS AND DEFINITIONS

Aneuploidy	Having a chromosome number that is not an exact multiple of the haploid number, caused by one chromosome set being incomplete; not euploid
ARPE-19	Commercial retinal pigment epithelial cell line
BrdU	5-bromo-2'-deoxyuridine
Biocompatibility	The ability of a foreign material to fulfil its intended function with an appropriate host organism response
Ca-AM	Calcein-AM, calcein acetoxymethyl
CCD-1112Sk	Commercial human foreskin fibroblast cell line
Confluence	Approximate proportion of the cell culture surface covered by cells in monolayer
CE	Corneal epithelium
CNS	Central nervous system
DAPI	4,6-diamidino-2-phenylindole
Dil	1'-dioctadecyl-3,3,3',3'-tetramethylindocarbocyanine perchlorate
Diploid	Containing two complete sets of chromosomes, one from each parent
DPBS	Dulbecco's Phosphate-Buffered Saline; a commercial saline solution
ECM	Extracellular matrix
EFR	Effective focus range
ELISA	Enzyme-linked immunosorbent assay
END2	Clonal cell line from mouse embryonal carcinoma
EthD-1	Ethidium homodimer-1
FAK	Focal adhesion kinase
FBS	Fetal bovine serum
GG	Gellan gum
Haploid	Having a single set of unpaired chromosomes
Hydrogel	A three dimensional network of polymer chains that retains water within the spaces between the macromolecules
Immortalization	Acquisition of infinite life span of a cell line
HCE-T	Commercial corneal epithelial cell line
hESC	Human embryonic stem cell
hFF	Human foreskin fibroblast
hNP1	Commercial human neural progenitor cell line
hTERT	(Human) telomerase reverse transcriptase; subunit of the enzyme telomerase
iCell® Neurons	Commercial human cerebral cortical neurons
iPS cell	Induced pluripotent stem cell

Ki-67	Nuclear protein associated with cell proliferation and ribosomal RNA transcription
L929	NCTC clone 929 (commonly known as L929 or L-929), commercial fibroblast cell strain
MRC-5	Commercial human fetal fibroblast cell line
MSC	Mesenchymal stem cell
MTS	3-(4,5-dimethylthiazol-2-yl)-5-(3-carboxymethoxyphenyl)-2-(4-sulphophenyl)-2H-tetrazolium
MTT	3-(4,5-dimethylthiazol-2-yl)-2,5-diphenyltetrazolium bromide
PA6	Commercial cell line from mouse bone marrow, also named MC3T3-G2/PA6
PEG	Poly(ethylene glycol)
PEO	Poly(ethylene oxide)
PM	PuraMatrix [®] Peptide Hydrogel
Proliferation	The process whereby cells reproduce themselves by growing and then dividing into two equal copies
PDL	Population doubling level of cells
PVA	Poly(vinyl alcohol)
RPE	Retinal pigment epithelium
SAOS-2	Commercial osteosarcoma cell line
SH-SY5Y	Commercial human neuroblastoma cell line
Senescence	The phenomenon leading to cell death due to its age
SPD	Spermidine; N-(3-aminopropyl)-1,4-diaminobutane
Telomeres	Terminal regions of the chromosomes, which maintain the proliferative capacity of cells and are progressively shortened during cell division
WI-38	Commercial human embryonal fibroblast cell line
WSTs	Water Soluble Tetrazolium Salts
XTT	2,3-bis-(2-methoxy-4-nitro-5-sulphophenyl)-2H-tetrazolium-5-carboxanilide

1. INTRODUCTION

Over the past decades, interest in hydrogels has grown in biomedical research due to their soft and tissue-like physical properties, hydrophilicity, possibility to fabricate from biocompatible and biodegradable polymers, and ease of further functionalization [1], [2]. Hydrogels are hydrophilic polymer networks that retain water within the spaces between the macromolecules. They are able to absorb from 10-20 % up to thousands of times their dry weight in water without losing their structural integrity. [1], [3] Hydrogels have been used in many biomedical applications, such as drug delivery systems, cell encapsulation, wound dressings and contact lenses. In tissue engineering they have been used as cell culture environments and tissue engineering scaffolds. [2], [3]

In the body, cells are surrounded by extracellular matrix (ECM), which they produce and secrete. The ECM serves as a support to the tissue, and cells have complex interactions with the ECM and adjacent cells. [4], [5] In a cell culture *in vitro*, the culture substrate takes the role of the ECM and should mimic the properties of natural ECM. Hydrogels differ from many other cell culture substrates in that they provide a three-dimensional (3D) environment to cells, opposed to a two-dimensional (2D) surface on which cells are traditionally cultured. On a surface, cells grow mostly in a monolayer along the surface, and the 2D geometry changes the interactions between cells and between surrounding matrix and cells. This constitutes many of the differences in cell behavior seen *in vitro* compared to the behavior *in vivo*. For this reason, cell culture substrates such as hydrogels have been prepared to allow cells to migrate and re-aggregate into more natural 3D structures. [6, p. 3-9]

A variety of synthetic and natural polymers as well as cross-linking agents and fabrication methods can be used to manufacture hydrogels, and also a variety of modifications can be made to the polymers. The applicability of a hydrogel for tissue engineering applications depends on several factors, such as mechanical, kinetical, biological and mass transport properties. [3] New hydrogels are constantly developed to provide better physical or biological properties for different applications. These new hydrogels have to be tested for the above mentioned properties as well as the toxicity and biocompatibility of the raw material itself. One way to test cell reaction with a new hydrogel is to culture cells on top or encapsulated in the new hydrogel *in vitro*.

To select the best ones among all possible hydrogels, there is a need for fast and simple cytocompatibility screening process. Currently, there is no widely used or standardized protocol for such high-throughput screening of hydrogels with cells [3]. One of the challenges in the screening process is the stability of cells: when growing cells on hydrogels,

there is often biological variation in cell behavior [7], thereby making it difficult to determine if the observed difference is a result of an unfavorable hydrogel or only due to the varying biological factors. In addition, some analysis methods need adjustment when cells are cultured in 3D hydrogels compared the traditional 2D culturing systems [8], [9].

The objective of this thesis is to create a protocol for repeatable, short-term cell culture screening of cytocompatibility of new hydrogels. The results from this screening should be applicable to culturing of cardiomyocytes, bone and cartilage cells, and corneal, retinal, and neuronal cells. More specifically, this thesis has two aims. The first aim is to find cell lines and their culturing techniques resulting in minimal biological variation in their attachment, proliferation, viability, and cell type specific thriving when grown on hydrogels that are cytocompatible. The cell lines should be, however, sensitive enough to show variation in these results due to adverse change in culturing conditions such as unfavorable hydrogel. The second aim is to select appropriate analyzing methods that would easily reveal the cytocompatibility of chosen hydrogels.

This protocol is meant to be used in future studies as a fast and simple, first step *in vitro* test, where new hydrogels are studied as possible cell culture or tissue engineering materials. The protocol can also be applied when investigating other factors affecting cell growth, such as coatings, fibers, fluid flow in bioreactor or molecules incorporated to the hydrogel (or other materials) and in the growth medium.

THEORETICAL BACKGROUND

2. CYTOTOXICITY AND BIOCOMPATIBILITY TESTS OF MATERIALS

Hydrogels that are designed to be used as cell culture substrates are formed from polymeric biomaterials. Polymeric biomaterials are studied for, or are already in use, as medical devices or as parts of medical devices. A biomaterial is a material that is exploited in contact with living tissues, organisms, or microorganisms. The exploitation can include usage both in applications and for fundamental research. [10]

There are several biological hazards that are involved when materials come to contact with cells or tissues. [11] This chapter introduces terminology related to safety of biomaterials and key standards for testing biological hazards, especially cytotoxicity.

2.1 Definitions

According to International Union of Pure and Applied Chemistry (IUPAC), the term biocompatibility is used to refer to the ability (of a material, for example) to be in contact with a living system without producing an adverse effect [10]. There are, however, several slightly different definitions for biocompatibility. Perhaps the most known definition was given in Williams Dictionary of Biomaterials in 1987, which states that “biocompatibility refers to the ability of a material to perform with an appropriate host response in a specific situation” [12 In: 13]. This definition does not only state that the material has to be safe (causes no biological hazards) but also that it has to be able to perform in the function given to it in the specific application. Thus, biocompatibility is a rather broad term. The same definition is accepted by IUPAC when referred to polymers of biological and biomedical interest [10].

Toxicity, in contrast, is the “consequence of adverse effects caused by a substance on a living system”, as defined by IUPAC [10]. When the living system is specifically cells, term cytotoxicity is used. Toxicity can be acute or chronic, depending on the time period needed for the reactions to occur. Several factors affect the nature and degree of the adverse effects and they can be quantified by the observed physiological response or by a viability test. [10] The physiological response may be, for example, change in proliferation rate, morphology or attachment of the cells. [14, p. 9]

Often biocompatibility of a material *in vitro* is only assessed by testing cytotoxicity (such as in [15]). In this thesis, however, the purpose of the screening is to ultimately select materials that surpass their control materials as a cell culture substrate. Therefore, a more specific term, cytocompatibility, is used here to describe a material that is not cytotoxic

and is able to fulfill its intended function with an appropriate cellular response. The intended function in this case is to act as a cell culture substrate, which supports normal cell behavior. In more detail, this means that the material does not cause significant cell death or decrease in proliferation rate, and the material enables cells to grow in their normal morphology. Other cell specific responses may also be tested to ensure normal behavior of cells.

It must be noted that also the definitions of positive and negative controls are opposite depending on whether cytotoxicity or cytocompatibility is tested. When testing cytotoxicity (in accordance with ISO 10933-5), a positive control is the material that causes a reproducible cytotoxic response in cells and a negative control is the material that does not cause a cytotoxic response [14]. On the contrary, when testing cytocompatibility, such as in this thesis, a positive control is a material that supports cell growth or other desired cellular functions and does not cause a cytotoxic response; a negative control is a material that does not support cell growth or other desired cellular functions or causes a cytotoxic response. Optimally, controls should be selected so that they can be prepared by the same procedure as the test sample [14].

2.2 Standards for testing cytotoxicity and biocompatibility

The International Organization for Standardization (ISO) describes *in vitro* cytotoxicity testing of medical devices in Part 5 of standard 10993 “Biological evaluation of medical devices”. [14] Testing of cell culture substrates can be conducted following this standard, because the cell substrate material can be classified as a medical device according to ISO 10993-1; it fulfills the criteria of a material intended by the manufacturer to be used alone, or in combination, for human beings for the purpose of providing information for medical purposes by means of *in vitro* examination of specimens derived from the human body. [11]

Standard ISO 10993-5 describes the general principles and decisions to be made when conducting an *in vitro* cytotoxicity study. In general, cytotoxicity is tested by imposing cells to the test material or its extracts. After an exposure time, cytotoxic effects are evaluated. This can be done by assessing cell damage as indicated by cell morphology, or by measuring cell damage, cell growth or specific aspects of cellular metabolism. [14]

There are three main categories of cytotoxicity tests: extract test, direct contact test, and indirect contact test. The category that is chosen for testing depends on the device that is tested and the intended nature and site of use of the device. Direct contact test can be used to test materials with many shapes, sizes and physical states, including solids, liquids and gels, and the materials can be tested as such without any modifications. The direct contact cytotoxicity test is conducted by placing a test sample of a previously cultured, subconfluent cell layer in a culture vessel. The sample should cover a ratio, such as 1/10, of the

cell layer surface. However, with appropriate specimens, the specimen can be placed in the vessel first and cell suspension can be then pipetted on the sample. The samples are incubated in normal cell culture environment over a period of time, which depends on the following assay. [14]

The purpose of extract test is to assess cytotoxic effects of substances that might extract from the test material or device in clinical conditions (i.e. leachables). To obtain the extract, the sample is incubated in 37 °C or heightened temperature over 1 to 72 hours in cell culture medium or other solute. Cells are then exposed to the extract. Indirect contact tests, namely agar diffusion and filter diffusion tests, also assess cytotoxicity of leachables from the sample material. In indirect contact tests, an agar gel or a porous filter is separating cells from the sample. Agar diffusion test is only suitable for leachables that can diffuse through agar and which do not react with agar. According to ISO 10993-5, using agar diffusion test for cytotoxicity testing must be justified. After an incubation period, samples are removed and cytotoxic effects to cells are assessed (by an appropriate staining method). [14]

In this thesis, the aim is to culture cells directly on top or encapsulated inside hydrogels. This sample setup is closest to the direct contact testing. Therefore, the protocol presented in this thesis relies on similar principles than in direct contact test presented in ISO 10933-5 [14], especially when testing cell behavior on top of hydrogels.

Both indirect contact tests allow only qualitative assessment of cytotoxicity, whereas extract test and direct contact test allow qualitative and quantitative assessment of cytotoxicity. Quantitative assessment is preferred, but qualitative assessment can be useful especially for screening purposes. [14] In general, qualitative assessing occurs by evaluating morphological aspects of cells microscopically (after cytochemical staining if appropriate). These morphological aspects may include general morphology, such as shape and size, vacuolization, detachment, cell lysis, or cell membrane integrity. A change from normal morphology is graded descriptively or numerically. In extract test, the condition in the whole cell layer is observed, whereas in indirect and direct tests the size of a reactivity zone around and under the sample area can be evaluated, if the sample only covered a part of the cell layer. [14]

Quantitative assessing occurs by measuring a parameter indicating cell death, inhibition of cell growth, cell proliferation (the process whereby cells reproduce themselves by growing and then dividing into two equal copies), or colony formation. This measurable parameter may be, for example, the number of cells, amount of a certain protein, release of enzymes, release of vital dye, or reduction of vital dye. In general, 30% reduction in cell viability is considered a cytotoxic effect. Other evaluation criteria must be determined and described, based on the application. [14]

The standard ISO 10993-5 leaves open the specific test method (assay or staining method) by which cytotoxicity has to be assessed. Therefore, the standard remains applicable to many types of devices and allows new methods to be used. Nonetheless, some example methods were given for extract test, such as XTT ((2,3-bis-(2-methoxy-4-nitro-5-sulphophenyl)-2H-tetrazolium-5-carboxanilide) assay and MTT (3-(4,5-dimethylthiazol-2-yl)-2,5-diphenyltetrazolium bromide) assay. These and other commonly used assays for determining cytotoxicity and cytocompatibility are described in Chapter 6.

Cytotoxicity testing is one part of assessing biological effects of a medical device. Depending on the device, its nature of body contact and contact duration (limited, prolonged, permanent), additional tests may be needed along with cytotoxicity testing. These tests include assessing some or all of the following biological effects [11]:

- sensitization
- irritation or intracutaneous reactivity
- systemic toxicity (acute)
- subchronic toxicity (subacute toxicity)
- genotoxicity
- implantation
- haemocompatibility
- chronic toxicity
- carcinogenicity
- biodegradation
- toxicokinetics
- immunotoxicity and
- reproductive / developmental toxicity or other organ-specific toxicities.

The current protocol focuses on testing cytotoxic effects of material on mammalian cells *in vitro*. Should the material be considered as a candidate for *in vivo* use (or bringing it into contact with human or animal tissue), a full risk assessment according to ISO 10993-1 should be done, and the biological hazards mentioned above should be evaluated and tested for, if necessary. Standards for testing these affects are found in respective parts of ISO 10993. In addition, several methods for assessing cytotoxicity may be needed. [11]

2.3 Standards for testing hydrogel compatibility for cell culture

In addition to considering cytotoxicity of the raw materials that hydrogels are comprised of (polymers and crosslinkers), other factors have to be taken into account for characterizing suitability of hydrogels in regenerative medicine. Many properties of hydrogels ultimately affect their applicability to act as cell culture substrates: permeation of dissolved

gases, nutrients and biomolecules; ability to sustain cell growth and migration; degradation; release of drugs and/or biologics at an appropriate rate; and ability to maintain their shape [3].

The key factors that affect the suitability of hydrogels for regenerative medicine use, and attributes that are related to these factors are presented in Table 2.1. Many of the attributes presented in this table are interconnected with each other. For example, environmental stability is assessed by testing different properties such as swelling, mechanical properties, gelling time, and ability to encapsulate cells in response to different environmental conditions. [3]

Table 2.1 Key factors and attributes to be considered in hydrogel characterization (modified from [3]). For further information on each attribute, refer to listed ISO and ASTM standards.

Key factors	Attribute	Standards
Biological properties	Biocompatibility	<i>ISO 10993, F748, F895</i>
	Adventitious agents	<i>F2383, ST72, ISO 22442, 21 CFR 210, 21 CFR 221, 21 CFR 610, 21 CFR 820</i>
Kinetics	Gelling time	<i>F2315</i>
	Swelling rate	<i>ISO 10993, F2214</i>
	Matrix degradation	<i>F2150</i>
Physical and chemical stability	Environmental stability	<i>D4516</i>
	Mechanical properties	<i>F2150</i>
	Cell encapsulation	<i>F2315</i>
Mass transport	Cell migration	<i>F2315</i>
	Transport of nutrients and waste	<i>F2450</i>
	Release rate of bioactive agents	<i>F2450</i>

Cell response towards a hydrogel can be assessed by testing biocompatibility and cell migration. It must be noted, however, that all attributes presented in Table 2.1 ultimately affect also response of cells. For example, transport of nutrients and waste products is essential for the cells to survive and function inside a hydrogel. Likewise, both biochemical and physical properties of the cell environment affect cell function and tissue morphogenesis. Therefore, also attributes such as mechanical properties and environmental stability impact the ability of hydrogels to support cells in their attachment, migration, differentiation, and other functions. Different tissues have distinct mechanical properties (e.g. stiffness), hence, optimally hydrogels for tissue-engineered constructs would be designed to roughly correlate with these mechanical properties. [2], [16]

3. MAMMALIAN CELL CULTURE AND REPEATABILITY

A cell culture refers to growing cells *in vitro*, i.e. in an artificial environment suitable for the cell in question. Cell culturing was first established as a method for studying cells in a controlled manner. Unlike *in vivo*, physiological and physical conditions can be kept constant in a cell culture, without systemic variations affecting the cells, such as changes in hormone levels in the organism. [6, pp. 1–6], [17] In addition, cells and their behavior in a culture can often be analyzed more easily than *in vivo*, for example by observing with a microscope (and immunostaining) or by electrophysiological measurements. However, cell culture has its limitations, which stem from various differences in *in vivo* and *in vitro* conditions. The major differences are that *in vitro* cells are detached from the 3D geometry surrounding them *in vivo* and that cells lack interactions with their natural ECM and adjacent heterotypic cells. Nevertheless, if these limitations are kept in mind, cell cultures are very useful models for studying cells. [6, pp. 1–31]

Nowadays, cell culturing is used for various research and production purposes. It is an excellent method for studying cellular and molecular biology: intracellular activity, genomics, cell products, and cell-cell interactions, for example. It also enables research on cell-matrix interactions, which is a fundamental concern in tissue engineering. In addition, cell culture is a useful model for immunological, toxicological, and pharmacological studies. Beyond this, cell culturing can be used for large scale manufacturing of biologicals such as vaccines and hormones; however, cell cultures for production are out of the scope of the protocol developed in this thesis. [6, p. 4], [17], [18]

3.1 Culture types

The general term of tissue culture refers to both cell culture and organ culture. Organ culture means culturing of a three-dimensional, undisaggregated tissue, which retains some or all of the histological features it possessed *in vivo*. Cell culture, on the other hand, refers to culture of disaggregated cells. A cell culture can be initiated from cells dispersed from the original tissue, from a primary culture, or from already existing cell line or cell strain. [6, p. 3], [19, p. 862]

Cells are traditionally cultured on a two-dimensional plastic or glass surface. However, there are histotypic cultures, in which cells are re-aggregated or grown to re-create a three-dimensional structure with tissue-like cell density. This can be achieved, for example, with the help of a three-dimensional matrix, such as collagen gel. Furthermore, an organ culture must not be confused with an organotypic culture. In an organotypic culture, a

tissue equivalent is attempted to achieve by combining cells from different lineages in the culture. [6, p. 3]

3.1.1 Primary cell, cell line and cell strain

A primary culture is established either by allowing outgrowth of cells from a tissue explant, or by enzymatically or mechanically dispersing tissue and culturing the subsequent cell suspension [6, p. 39], [19, p. 865]. Cells in this culture are called primary cells. Cells proliferate in or on their culture substrate, until they have used all the available space, i.e. reached confluence [6, p. 40]. In order to maintain healthy growth of the cells, the culture must be subcultured (i.e. passaged) before reaching confluence [19, p. 865]. This involves enzymatic disaggregation, dilution, transfer to a new culture vessel and adding fresh culture media. After the first subculture, the culture is known as a secondary culture, and at the same time, starts a new cell line. The cell line can be further propagated and subcultured several times. [6, p. 41], [17], [19, p. 862]

A cell strain or subline, on the other hand, is formed by selecting cells from a culture by cloning or other means [17]. The resulting cell population in one culture flask is, thus, derived from a single cell. The purpose of forming cell strains is to obtain genetically homogenous cultures. [19, p. 866] A cell strain has certain characteristics and a sustained marker is required to recognize these characteristics. The cell strain can also be finite or continuous (see Chapter 3.1.3), depending on how it was derived. [20, p. 31]. However, cell strains often acquire genetic changes after the selection, distinguishing the cells from the parent cell line [17]. Thousands of cell lines and cell strains are nowadays in regular use in research and commercially available through several cell repositories [19, pp. 866–867], [21]–[24].

3.1.2 Formation of cell line

Formation of a cell line from a primary culture consists of a selective process. With each passage, cells or cell lines which have the highest growth capacity will become more predominant, and “weaker” cells will dilute out. The growth capacity of the cells is influenced by attributes such as proliferation rate, ability to adhere to the substrate, and ability to grow under the chosen culture conditions. Equally, cells have varying abilities to withstand the enzymatic handling during passage. These selective circumstances lead to a certain level of genotypic and phenotypic uniformity in the cell population. By the third passage, the cell line can be assumed to be rather stable and to consist mainly of a hardy, rapidly proliferating cell. The cell line can be characterized, and these characteristics will apply for the most of the life span of this finite cell line. [6, pp. 9, 41], [17], [19, p. 865]

The predominance of these hardy cells is problematic, if a cell line is wished to be formed from a more fragile cell, or a cell with lower proliferation rate. In addition, in the past

decades, phenotypic loss of characteristics was noticed in cell lines, which was interpreted as dedifferentiation. Nowadays it is understood that this phenomenon, too, is in fact overgrowth of undifferentiated cells of the same or different lineage. For that reason, several selective media and substrates have been developed, that allow isolating these more fragile cell lineages and maintaining or restoring many of the specialized characteristics of the cells. [6, pp. 7, 41], [25, p. 318]

3.1.3 Finite and continuous cell lines

Cell lines can be either finite or continuous. Cell lines derived from normal tissue (e.g. not tumors) are finite. Finite cell lines can be subcultured and maintained for a limited number of population doublings before the cells cease to proliferate and die due to senescence. [6, p. 41], [17], [19, p. 862] Senescence is a natural phenomenon, which occurs at least partly due to the incapability of the cell to replicate the terminal sequences of DNA in the telomeres during cell division [6, p. 41].

Another possible fate of the cell line, instead of senescence, is becoming immortal through a process called transformation. When a cell line becomes immortal, i.e. it can divide indefinitely, the cell line is said to be a continuous (or as previously called, established) cell line. The transformation giving rise to continuous cell lines can occur spontaneously or it can be chemically or virally induced. [6, pp. 9, 41], [17], [19, pp. 882, 866] Transformation can also occur after exposure to ionizing radiation or chemical carcinogens [6, p. 291].

It must be noted, that the term transformation is used differently in different sources and fields. Freshney [6] uses the term immortalization to describe acquisition of infinite life span, and the term transformation implying to three phenotypic changes: immortalization, alterations in growth characteristics and malignancy (growth of invasive tumors *in vivo*). A cell line can go through one or more of these three phenotypic changes during transformation. The alterations in growth characteristics may be loss of anchorage dependence, loss of contact inhibition and loss of density limitation of growth (see Chapter 3.3), and these alterations often, but not necessary correlate with tumorigenicity. It is possible, however, to achieve immortalization, without aberrant alterations in growth control and malignancy. [6, pp. 41, 291] In addition, when untransformed cells become continuous, cell lines often lose differentiated properties of the phenotype. [6, p. 375]

Some cell types are capable of giving rise to continuous cell lines. Cells that are more prone to genetic change, i.e. are genetically unstable, are more likely to transform. Normal, finite human cells are genetically quite stable. For example, human fibroblasts remain predominantly euploid (having a chromosome number that is an exact multiple of the number of single (haploid) set of unpaired chromosomes) throughout their lifespan in culture and never give rise to continuous cell line. [26 In: 6] Fibroblasts from other spe-

cies, especially mouse, are genetically unstable and, thus, transform easily. Genetic instability is a common feature of continuous cell lines, especially those derived from tumors, still after the transformation. Continuous cell lines are usually aneuploid (i.e. have a chromosome number that is not an exact multiple of the haploid number) and have chromosome number between diploid and tetraploid values. In addition, the chromosome number may vary among the cell population, i.e. there is heteroploidy. [6, pp. 41, 291–292]

In addition to transformed cells, germ cells and stem cells have extended life spans compared to normal finite cells. Life span of germ cells and some tumor cells is indefinite. These cells often express telomerase, an enzyme which gives them the capability of replicating the terminal sequences of telomeres. [6, p. 41]

3.1.4 Stem cells

Stem cells are cells that have the ability both for self-renewal (making identical copies of themselves) and for differentiation. For *in vitro* research, specialized cells are often differentiated from embryonic stem cells (ESC), induced pluripotent stem cells (iPS) or adult stem cells. ESCs and iPS cells are pluripotent, i.e., they are able to differentiate into cells of any of the three germ layers (but not form an entire new organism). Both embryonic and iPS cells can be differentiated into several cell lineages and cell types *in vitro*, for example, neuronal precursor cells, glial cells and neurons. [27]–[29]

Embryonic stem cells are obtained from the inner cell mass of a blastocyst. Both mouse and human ESCs have been used extensively in research. Human ESCs are obtained from embryos that are left over from artificial insemination. Several embryonic stem cell lines are also available commercially. [28] iPS cells have been reprogrammed into stem cells from adult differentiated cells, such as fibroblasts, and are similar to embryonic stem cells in properties. [27]

In addition to embryos and fetuses, stem cells are present in many adult tissues. Most of these adult stem cells (also called organ- or tissue-specific stem cells or somatic stem cells) are multipotent, meaning that they have the ability to give rise to limited cell types. [28] For example, bone marrow contains two types of adult stem cells: haematopoietic stem cells and bone marrow stromal cells [30, p. 17]. It is possible to harvest adult stem cells in connection with surgeries, but some adult stem cells, like mesenchymal stem cells, are also available commercially. [30, p. 18]

The difficulty in differentiating pluripotent and multipotent stem cells is in obtaining uniform populations of cells. Differentiation can be induced in several ways: by changing the constitution of culture media, with added growth factors, cytokines or other proteins; by changing the substrate, for example into a 3D matrix, and utilizing mechanotransduction of the cell; or by co-culture with cells that already have differentiated phenotype. [30,

p. 6] Another challenge with stem cells is that cells from one patient might behave differently than cells from another patient. Therefore, cells have to be harvested from multiple patients for a single experiment, in order to obtain validated results. [30, p. 18]

Different types of stem cells offer a great potential in tissue engineering and are extensively studied. Therefore, hydrogels are also studied as possible *in vitro* substrates for stem cells and precursor cells, either serving as differentiating substrate or a substrate that remains cells in undifferentiated state. Even though ultimately a goal in hydrogel research is to provide suitable hydrogel candidates as 3D matrices for stem cells, this protocol does not extend to testing differentiation of stem cells.

3.2 Advantages and disadvantages of cell lines

The source of cells for a cell line determines the composition of cells in the population. When the source is an embryo, more stem cells and precursor cells are present than when the source is adult tissue, and thus the cells have greater self-renewal capacity. Furthermore, cells from adult tissues that have a good self-renewal capacity *in vivo*, such as intestinal epithelium and epidermis, contain some amount of stem cells. Thus cultures derived from these tissues, given the appropriate environment, will also have a longer life span *in vitro* than cells derived from tissues with slow renewal rate (or which renew only under stress). The latter rely their self-renewal ability only on precursor cells, which have a limited life span. [6, p. 42]

The selection process that occurs during formation of cell lines produces advantages and disadvantages of cell lines. The uniform constitution of cell lines offers a great advantage of repeatability for experiments, as at each subculture, replicate samples are identical to each other [6, p. 6]. Cell lines are also a renewable source of cells for repeated experiments [19, p. 866], unlike primary cells, which have to be isolated from animals or humans for each experiment. Furthermore, primary cultures are less stable than cell lines, and therefore unsuitable for some studies [6, p. 39].

On the other hand, the loss of heterogeneity and diversity of the culture in cell lines makes them less representative of the tissue of origin. Ideally, the cell line should reflect the properties of tissue from which they were derived. [19, pp. 865–866] However, primary cultures express more strongly some aspects of specialized functions, which are apparent *in vivo* [6, p. 40]. Therefore, a cell line should be considered merely as a model of its tissue of origin.

3.3 Growth characteristics

Cells can be cultured either in an adherent culture or in a suspension culture. In adherent cultures, cells attach to a solid or semi-solid substrate and propagate as a monolayer. This means that given the opportunity, cells will propagate on the two-dimensional surface, on which cells are traditionally cultured. Adherent cells are anchorage dependent, meaning that attachment to, and to some extent spreading onto, the substrate is a prerequisite for proliferation. Most normal cells, with the exception of haematopoietic cells, are anchorage dependent. Cells from malignant tumors and some transformed cell lines, on the other hand, are anchorage independent. They do not attach to a substrate; instead they are cultured in a suspension within the growth medium. [6, p. 9], [17], [19, p. 862]

Different types of cells have different levels of contact inhibition, which means stopping migration when cells are in confluence, together with a reduction of plasma membrane ruffling. Based on their morphology, adherent cells are described either as fibroblast-like or epithelial-like, but they also have different growth characteristics. Fibroblast-like cells require mainly attachment and spreading on the surface for their migration and proliferation. At low densities, they migrate as single cells with distinctive polarity in the movement. When encountering another cell, polarity reverses. In confluence, directional movement ceases and eventually cells withdraw from the division cycle. In contrast, epithelial-like cells may require also adhesion with other cells in order to survive and grow optimally. Unless transformed, epithelial-like cells in low densities migrate until they encounter another cell. This leads to the cells growing in patches and even the whole patch can show coordinated movement. [6, pp. 31, 34]

Cells in monolayer culture proceed to proliferate and migrate until all the available growth area on the surface has been occupied, i.e. the culture is confluent. After reaching confluence, both epithelial-like and fibroblast-like cells may differentiate, depending on their environment. In addition, epithelial cells may form increasing amount of desmosomes and complete junctional complexes, if they are left at confluence for too long. This makes disaggregating cells difficult. Cells that are sensitive to contact inhibition and density limitation of cell proliferation stop dividing at confluence, but transformed cells that have lost sensitivity to density limitation will overgrow. Therefore, frequent subculturing before reaching confluence is necessary in order to keep the phenotype of the culture normal, especially in cultures which easily transform (such as mouse fibroblasts). [6, pp. 33, 40], [17], [19, p. 865]

Passage number indicates the number of times a cell culture has been subcultured. For diploid cells, passage number is roughly the same as number of population doublings since the culture was started, i.e. population doubling level (PDL). Continuous cell lines are subcultured in a higher split ratio (i.e. into higher amount of new vessels) and therefore

their passage number does not equal PDL. PDL is usually not determined for continuous cell lines, although it can be estimated by calculations. [20, p. 4]

3.4 Environmental conditions of cell culture

As stated before, one of the main advantages of cell culture is that environmental conditions surrounding cells can be kept rather constant. However, these conditions may not be fully determined and some variation might occur, especially when using animal derived substances like serum and natural substrates. There are at least five environmental aspects to consider which influence cell growth in a culture. These include physicochemical and physiological composition of the culture medium, the constitution of the gas phase, the incubation temperature, the degree of contact with other cells, and the nature of the culture substrate [6, pp. 6, 31].

Degree of contact with other cells was shortly described in the previous chapter, and it is also related to the choice of culture substrate. The required culture conditions vary for each cell type [17], and some common considerations are introduced here.

3.4.1 Culture substrate

Cells are traditionally cultured in culture vessels: glass petri dishes, plastic culture flasks or plastic multiwell and microtiter plates. [6, p. 31], [14] Thus, usually the culture substrate for adherent cells is a glass or plastic (most commonly polystyrene) surface. Cells adhere to glass with a slight negative charge, and also plastic vessels are treated by irradiation or chemically to produce a negatively charged surface. [6, p. 31], [19, p. 862] Extracellular matrix (ECM) proteins and proteoglycans, which cells secrete, attach to the negative charge of the surface and cells then attach to these proteins via specific receptors. Cell attachment is often improved by coating the surface with ECM proteins, such as collagen, laminin, or fibronectin, before adding cells; or the surface can be pre-conditioned with other cells. [6, p. 31], [19, p. 862]

However, in monolayer, which cells form on this type of 2D surface, cells lack three-dimensional cell-cell and cell-matrix interactions which are present *in vivo*. Therefore, several 3D structures have been attempted to create as cell culture substrates. [6, p. 31] One example of such 3D environments is hydrogels, which are looked into in more detail in Chapter 5.

3.4.2 Culture medium

Several culture media are available commercially for different cells. Most of these so called basal media require additional serum supplement, most frequently 5–20 % of the

volume. Fetal or newborn calf are most typical sources of sera, but human and equine sera are sometimes used. Serum adds important components to the medium, including hormones, growth factors, transport (binding) proteins, enzyme cofactors, lipids, and attachment factors. Serum has some level of batch-to-batch variation: concentrations of serum components vary and they are affected by the age and health of the donor animal. [19, p. 864]

Serum-free media offer the opportunity to culture cells without any animal derived ingredients, which decreases the risk of introducing contaminants to the culture. It also allows complete control of the content of media without batch-to-batch variation. Furthermore, certain growth-inhibitory components of serum are avoided. Several serum-free media are available commercially. [19, pp. 862–865] If cells that are regularly cultured in a serum containing medium are transferred into serum-free medium, an adaptation period is required, whereby serum percentage is gradually reduced. [19, pp. 862–865]

In serum free media, cells may express lower attachment levels to a (plastic) surface. [19, pp. 862–865] This is understandable, because several proteins in serum attach to the negative charge in the surface of the vessel and cells attach to the proteins with their specific receptors. This needs to be taken into account when planning tests for cell attachment.

Factors such as pH, osmolality, and ion concentration and composition should be considered not only with growth medium but also with other substances when conducting experiments with cells. For certain cell types like myocytes and neurons, concentration of ions is especially crucial for their normal function and, therefore, using chelating agents such as EDTA in experiments requires careful consideration. [31, p. 4956] Also extracts that may be released due to degradation from biomaterials that are used as cell culture substrates need to be considered, as they may change the pH and ion composition of the culture environment.

4. SELECTING FIBROBLAST CELL LINE

Based on the previous chapter, it can be concluded that primary cells, stem cells, and stem cell derived differentiated cells are more representative of the cells *in vivo* than cell lines. However, these cells can be hard to acquire, expensive, or require time to be differentiated from stem cells. In addition, they have a larger “batch-to-batch variation” (or from patient to patient) than cell lines. Therefore, for the first-step cytocompatibility testing, a cell line was preferred. Properties of a few common fibroblast cell lines were compared in order to choose a fibroblast cell line for the cytocompatibility screening.

The ISO standard 10933:5 [14] includes useful considerations when testing cytocompatibility of new medical materials. The standard recommends cell lines shown in Table 4.1 as suitable cell lines for cytotoxicity tests. Most of these cell lines are fibroblasts, with the exception of Vero, which is a kidney cell with epithelial morphology [32]. As the standard merely provides a recommendation, other cell lines may be used if they can be shown to lead to the same or more relevant results [14].

Table 4.1 Cell lines suggested by ISO 10993-5 [14] for cytotoxicity testing. Information compiled from [6] and [21].

General name	ATCC number	Cell type	Tissue	Species
NCTC clone 929	CCL 1	Fibroblast	Subcutaneous connective tissue: areolar and adipose	Mouse (C3H/An)
Balb/3T3 clone A31	CCL 163	Fibroblast	(Embryonal)	Mouse (BALB/c)
MRC-5	CCL 171	Fibroblast	Lung	Human
WI-38	CCL 75	Fibroblast	Lung	Human
Vero	CCL 81	Epithelial	Kidney	Monkey (Grivet)
BHK-21 (C-13)	CCL 10	Fibroblast	Kidney	Hamster (Syrian)
V-79 379A		Fibroblast	Lung	Hamster (Chinese)

In addition to the recommendation in ISO 10993, NCTC clone 929 (commonly known as L929 or L-929) has been used in standards ASTM F813 [33] and ASTM F895 [34] for cytotoxicity testing of materials intended for biomedical use. These ASTM standards favor L929 because it is widely used in cytotoxicity testing and it is a well-characterized, established cell strain that is readily available and has demonstrated reproducible results in several laboratories. [33], [34] Though in many cases L929 is referred to as a cell line, it is in fact a cell strain. L929 was isolated in 1948 by capillary cloning from a mouse L-

cell, which, in turn, is a fibroblast cell strain derived from subcutaneous connective tissue (areolar and adipose) of a C3H/An mouse (*Mus musculus*) [6, pp. 1, 41], [35]. L929 was the first cloned cell strain ever generated [35]. Figure 4.1 presents the fibroblast-like morphology of L292 cells.

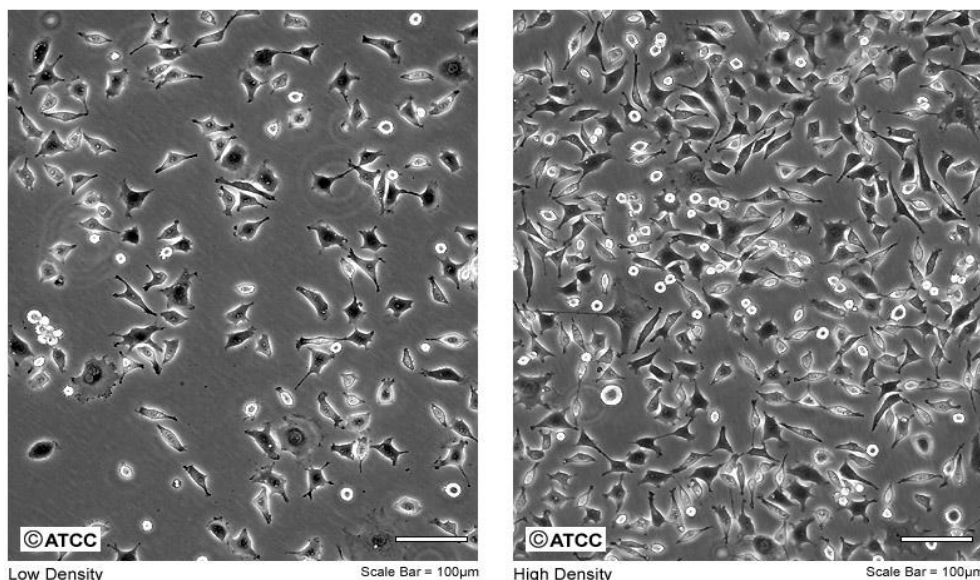


Figure 4.1 NCTC clone 929, also known as L929, in low density (left) and high density (right). [35]

Among the cell lines recommended in ISO 10993-5, only two cell lines are derived from human sources: MRC-5 and WI-38. In the protocol developed in this thesis, human source can be seen as an advantage, as the ultimate aim is to test hydrogels for human tissue applications. MRC-5 and WI-38 are both finite fibroblasts from normal (non-diseased) fetal lung tissue [36], [37]. Although these cells are not immortalized, they proliferate extensively. MRC-5 cells are capable of 42 to 46 population doublings before onset of senescence, and WI-38 cells have an approximate lifetime of 50 ± 10 doublings. They are both commonly used cell lines and, especially, frequently used as feeder cells. [6, pp. 40, 200, 223], [36], [37] Figures 4.2 and 4.3 illustrate the morphology of MRC-5 and WI-38 cells grown on a 2D surface.

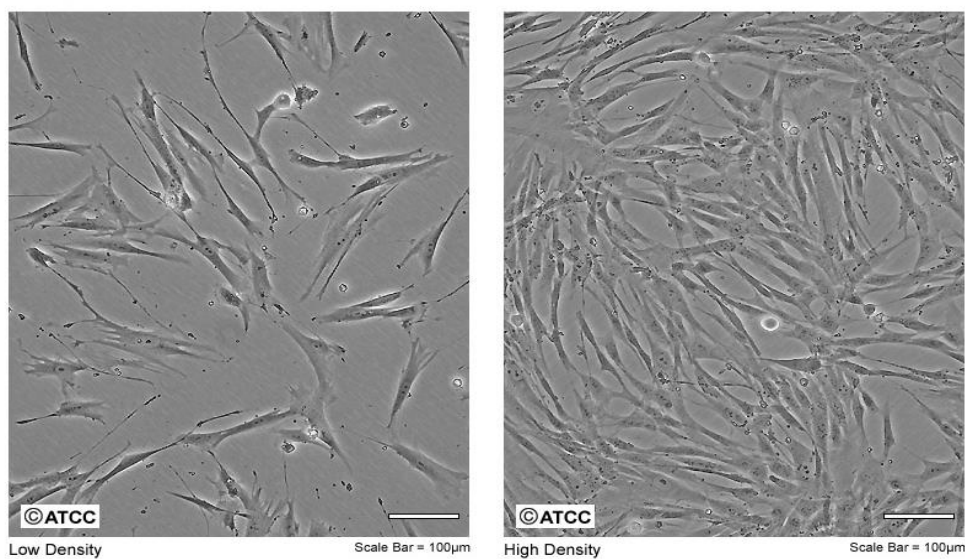


Figure 4.2 Morphology of MRC-5 fibroblasts in low density (left) and high density (right). [37]

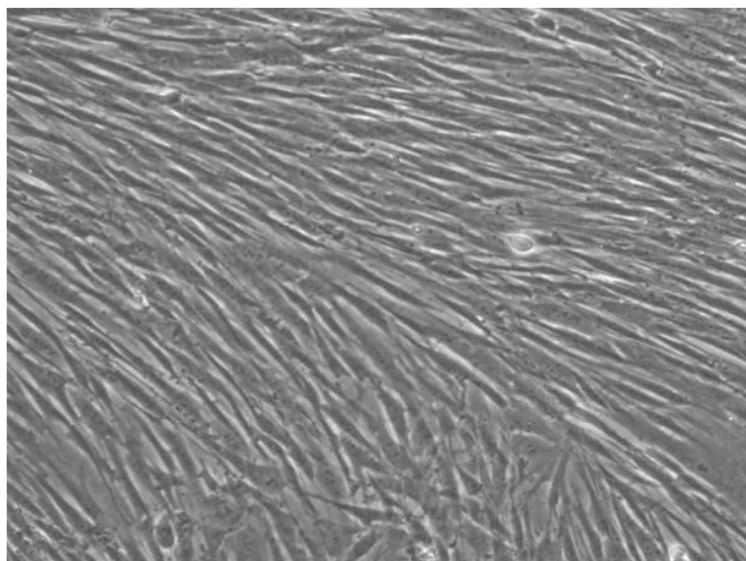


Figure 4.3 WI-38 cells, imaged before cryo-preservation. [38]

In addition to the suggested fibroblasts in [14], human foreskin fibroblasts (hFF) are often used in *in vitro* cell models. They are commonly used as feeder cells [39], [40], but also in biomaterial research [41], [42]. Commercial hFFs are harvested from newborn males, and there are several human foreskin fibroblast lines available commercially (for example, HFF-1, Hs27, Hs68, and CCD-1112Sk) [21]. Also hFF cells go through many population doublings in culture before senescence. One of the commercial hFF lines, CCD-1112Sk (ATCC CRL-2429) has anticipated life span of around 60 population doublings [43]. Further properties of L929, MRC-5, WI-38, and CCD-1112Sk are presented in Table 4.2

Table 4.2 Properties of four fibroblast cell lines.

Property	L929	MRC-5	WI-38	CCD-1112Sk
Age of source tissue	adult	fetal (14 week gestation)	fetal (3 months gestation)	newborn
Species	mouse	human	human	human
Source tissue	clone of L-cell (subcutaneous connective tissue)	lung	lung	foreskin
Culture property	adherent	adherent	adherent	adherent
Immortality	continuous	finite	finite	finite
Ploidy	aneuploid	diploid	diploid	-
Disease	neoplastic	no	no	-
Serum requirement	yes	yes	yes	yes
Reference	[6, p. 201], [35]	[6, p. 200], [37]	[6, p. 200], [36], [38]	[43]

As can be seen in Figures 4.1 - 4.3, the morphology of WI-38 and MRC-5 cells is longitudinally more spread than that of L929. Moreover, it can be seen advantageous, that WI-38 and MRC-5 are diploid and derived from non-diseased sources ([36]–[38]), as they likely better represent normal growth characteristics and attachment to materials. Thus, for the purpose of this protocol, WI-38 and MRC-5 cells seem to be better options than L929. The only practical difference between WI-38 and MRC-5 is found in their maximum population doublings, which is slightly higher for WI-38 [36], [37]. hFF cell line CCD-1112Sk also has very similar properties to WI-38 and MRC-5 cells (Table 4.2). However, literature available on CCD-1112Sk is not as vast as in case of WI-38 cells, which have been used in research extensively. Therefore, WI-38 cells are favored for the screening protocol.

5. HYDROGELS AS CELL CULTURE SUBSTRATES

Hydrogels are hydrophilic polymer networks that absorb large amounts of water, while maintaining their structural integrity in the swollen state [3]. Hydrogels may absorb from 10–20% up to thousands of times their dry weight in water [1]. The network is formed by crosslinking the polymer chains chemically or physically. This water-containing network structure allows hydrogels to form a three-dimensional material. General properties of hydrogels include considerable biocompatibility, soft and tissue-like physical properties, and high permeability of small molecules. [1], [2] Hydrogels can be biodegradable or stable depending on the constituting materials and crosslinking density. [44] Because of these properties, which resemble the ECM of tissues *in vivo*, hydrogels are interesting materials for cell culture substrates.

Hydrogels can be fabricated from natural or synthetic polymers, and even their combination. Natural hydrogel polymers include hyaluronic acid, alginic acid, chitosan, polylysine, collagen (and its derivative gelatin), fibrin, agarose and gellan gum. [1], [45] Examples of synthetic polymers include poly(ethylene oxide) (PEO), poly(vinyl alcohol) (PVA), and polypeptides [44]. Naturally derived hydrogels (such as collagen and Matrigel[®]) are considered as the gold standard for 3D cell culture substrates, because of their physical properties; although, they may suffer from batch-to-batch variation, limited design options and poor handling characteristics. [7] Synthetic polymers, on the other hand, have the advantages of controllable and repeatable chemistry and properties, but they may lack biological cues needed for interactions with cells [7], [44].

When linear polymer chains are crosslinked with an agent that forms covalent bonds between the chains, the hydrogel is called chemically crosslinked, thermosetting, or permanent hydrogel. Disadvantage of using crosslinking agents that form strong permanent hydrogels is that they are mainly toxic and unreacted agent has to be leached out. In addition, it is impossible to leach out partially reacted agents. This limits the usage of chemically crosslinked hydrogels. [2]

In contrast, in physically crosslinked (or irreversible) hydrogels the polymer chains are held together by molecular entanglements or secondary forces, including ion bonding, hydrogen bonding, or hydrophobic forces. [1] Physically crosslinked hydrogels have the advantages of avoiding usage of toxic crosslinking agents, ease of fabrication, and possibilities for modification after crosslinking. The major disadvantage is weak mechanical properties in swollen state, although this can be improved by copolymerization. [2]

Further, there are stimuli responsive hydrogels, or smart hydrogels, which rapidly and notably respond to small environmental changes by changing their network structure, mechanical strength, swelling behavior, or permeability. These environmental changes can be classified as chemical, physical or biomedical. For example, smart hydrogels exist that respond to temperature, pH, ionic factors or glucose level changes in their environment. [2]

5.1 Puramatrix[®] hydrogel

PuraMatrix[®] (registered trademark of 3-D Matrix) is a synthetic, commercial hydrogel. PuraMatrix[®] (PM) is composed of a repeating unit of three common amino acids, arginine – alanine – aspartic acid – alanine, which are coupled as a short peptide chain of 16 amino acids. These peptides, prepared in an aqueous solution, self-assemble into nanofibers when exposed to physiological salt concentration. Therefore, the hydrogel can be formed by adding culture media. The nanofiber density and average pore size (5-200 nm) can be controlled by the concentration of peptide solution when preparing the hydrogel. [46]

PM forms a weak hydrogel. This structure might have its advantages especially when the cells are isolated from the gel for further analysis. However, it is also fragile and needs to be prepared and handled with caution. The hydrogel is colorless and transparent, which is beneficial for observing encapsulated cells microscopically. Because it is fully synthetic and no human or animal source nor recombinant method has been used in the manufacturing, PM is ensured to be pure, well defined, reproducible and lack the risk associated with biogenic sources. [47]

PM has been shown to be biocompatible and to support growth and differentiation of many anchorage-dependent cell types [47]. For example, human progenitor neurons [8], hECS derived neuronal cells [48], and cartilage cells [49] have been cultured with PuraMatrix[®] as the cell culture substrate.

5.2 Gellan gum hydrogels

Gellan gum is an anionic linear polysaccharide. Gellan gum is derived from a fermentation product produced by a bacteria *Sphingomonas elodea* (ATCC 3146, formerly classified *Pseudomonas elodea*; also referred to as *Sphingomonas paucimobilis*). [45], [50] Gellan gum is produced with a high yield with this bacterial strain and it has a wide range of applications. Most commonly gellan gum is known as a gelling, stabilizing and suspending additive in food and personal care products, for which gellan gum has U.S. Food and Drug Administration (FDA) and European Union (EU) approvals (E number E418 in EU). [50] In addition, gellan gum has been used in various controlled drug delivery ap-

plications, plant and bacterial cultures, and studied as a mammalian tissue culture substrate [50]–[52]. Depending on the application area, gellan gum is sold commercially under several product names, such as Gelzan (CP Kelco) [45], [50].

The gellan gum polymer chains consist of a repeating tetrasaccharide unit of 1,3- β -D-glucose, 1,4- β -D-glucuronic acid, 1,4- β -D-glucose, and 1,4- α -L-rhamnose. In water the polymer chains are in random-coil conformation (disordered conformation) at high temperature (> 40 °C). When cooling the temperature, the chains transition into ordered conformation, which is a three-fold left-handed double-helix. [45], [50]

Due to the helical structure, gellan gum may have properties of a weak gel when cooled. However, cations are required to form a true hydrogel network by aggregating helices. Divalent cations, such as Ca^{2+} and Mg^{2+} form bridges between helices by binding carboxyl groups of two double helices. Monovalent cations, such as Na^+ and K^+ , produce weaker gels, and their use is based on suppressing electrostatic repulsions between the negatively charged carboxyl groups. [45], [50], [51] Carboxyl groups in the polymer chain also allow a variety chemical modifications of gellan gum. This way properties, such as stability *in vivo* and mechanical properties, can be altered. [45]

6. METHODS FOR TESTING CYTOCOMPATIBILITY

Common parameters that are evaluated in direct contact cytotoxicity or cytocompatibility testing include attachment of cells to the surface material, and proliferation, viability (cell death, lysis or membrane integrity) and general morphology of cells [14], [33] (see also Chapter 7.5). These parameters can be assessed by various methods (assays), few of which are introduced in this chapter. The presented methods measure cell behavior roughly in two ways: either microscopically (imaging based methods) or by quantification with a plate reader (colorimetric or fluorometric assays).

Imaging based methods may precede staining or labelling cells with a (fluorescent) substance, and are followed by image analysis [9]. Imaging based method allows qualitative assessment of cells, but especially with image analysis software several attributes can be also quantified [9], [14, p. 9]. Colorimetric assays are based on a reagent that is converted into a colored substance and can be therefore measured with a spectrophotometer, i.e. measuring absorbance of light in the sample. Similarly, fluorometric assays are based on a reaction product that is fluorescent (i.e. a fluorophore), and which can be detected with a fluorometer. [9], [52]

6.1 Cell viability

The total number of live cells can be determined by the tetrazolium reduction assays, resazurin reduction assays, and protease activity assays. These assays measure general metabolism or an enzymatic activity of cells, which are indicators of cell viability. In all of these methods, cells are incubated with a reagent, which viable cells convert into a measurable colored or fluorescent substrate. [53]

An example of tetrazolium reduction based assays is MTT (3-(4,5-dimethylthiazol-2-yl)-2,5-diphenyltetrazolium bromide) assay. MTT is yellow until reduced, after which it forms purple formazan. The reduction occurs due to enzymatic reactions in metabolically active cells. For that reason, it can be used as a measure for proliferation or viability of cells, as the formation of formazan is directly correlated to enzymatic activity. The purple color can be quantified with a spectrophotometer. [53], [54] MTT assay is an endpoint assay, because of formazan crystals forming in cells. Similar, newer, versions of MTT assay are MTS ((3-(4,5-dimethylthiazol-2-yl)-5-(3-carboxymethoxyphenyl)-2-(4-sulphophenyl)-2H-tetrazolium), XTT (2,3-bis-(2-methoxy-4-nitro-5-sulfophenyl)-2H-tetrazolium-5-carboxanilide), and WSTs (Water Soluble Tetrazolium Salts) assays. [53]

Another, rezaurin reduction based, viability (and proliferation) assay is alamarBlue assay. The assay uses an oxidation-reduction indicator that changes color and becomes fluorescent as a result of chemical reduction of growth medium due to metabolic activity of cells [9]. It allows the number of living cells to be quantified by fluorometric measurement; also absorbance can be measured, but it is less sensitive than fluorescence measurement. This assay is relatively inexpensive and it is more sensitive than tetrazolium assays. The needed incubation time is 1-4 h. [53]

An imaging based approach, which can also be used as a fluorometric assay, is Live/dead viability assay. Live/dead cell viability assay is conducted by using fluorescent dyes which allow distinguishing live and dead cells. There are several such dyes available commercially. One such option is using calcein-AM (Ca-AM) and Ethidium homodimer-1 (EthD-1). Cells are dyed with both dyes at the same time. The incubation time is short, only about 30 minutes for 2D culture. The dyed cells can be observed or measured with flow cytometry, fluorescence microscopy, and with fluorescence microplate readers. [55] Live/dead assay has been used previously also with hydrogels. [41], [56]

Non-fluorescent calcein-AM enters all cells, after which (in live cells) esterase activity converts it to fluorescent calcein by acetoxymethyl ester hydrolysis. Ubiquitous intracellular esterase activity is characteristic for live cells. Moreover, calcein as a polyanionic dye remains inside live cells well, thereby forming a strong, uniform green fluorescence. Calcein is green-fluorescent (excitation/emission maxima ~494/517 nm). [55], [57] Cell membrane integrity is a sign of cell viability. EthD-1 is cell-impermeant, unless the cell membrane is damaged. Therefore, EthD-1 enters only dead cells. In cells, EthD-1 binds to nucleic acid. EthD-1 is weakly fluorescent until bound, after which it emits red fluorescence (excitation/emission maxima ~528/617 nm). [55], [58]

6.2 Proliferation

Viable cells can be proliferating or non-proliferating. Proliferating cells go through DNA synthesis and mitosis (so called (S) phase and (M) phase in cell cycle) to produce two daughter cells. Therefore, assays that measure viability of cells include both non-proliferating and proliferating cells, but assays that specifically measure proliferation of cells do not detect all viable cells. [9]

One common colorimetric immunoassay for measuring specifically proliferation is based on 5-bromo-2'-deoxyuridine (BrdU). BrdU is a pyrimidine analogue which is incorporated in place of thymine into the synthesized DNA of proliferating cells. Cells are incubated with BrdU usually 2 - 24 h. Fixation of cells and denaturation of DNA is needed after incubation, however this is easy and fast, around 30 min, with a fixing and denaturation solution included in the assay kit. [59]

BrdU is detected by staining with an anti-BrdU antibody conjugated with peroxidase, and a following substrate reaction, such as with TMB (tetramethyl-tetramethyl-benzidine). The reaction product is a colored substance, which can be quantified by measuring the absorbance in specified wavelength by using a scanning multiwell spectrophotometer, such as ELISA (enzyme-linked immunosorbent assay) reader. The absorbance correlates with amount of DNA synthesis in the cells of the sample, and thereby with number of proliferating cells. The benefit of using a multiwell ELISA reader is that a large number of samples can be analyzed simultaneously. [59]

6.3 Cell attachment

The simplest way of assessing attachment of cells to a material, is to count the number of cells on a material microscopically after a short culture time. For example, cell nuclei can be stained with fluorescent DNA stain such as Hoechst 33342 (bisbenzimidazole) or DAPI (4,6-diamidino-2-phenylindole) after a short culture time (for example 10 min). Cells are imaged and the number of cells (nuclei) is counted and compared to a control material [60]. Simultaneously, cells can be stained with other methods, such as with fluorescent dye phalloidin, which allows observing cell morphology (as described later). [61] Attachment of cells inside a hydrogel has been studied by scanning electron microscopy of fixed and dehydrated hydrogels. [62]

In addition, adhesion of cells to the material can be studied by staining adhesion molecules in cells. These molecules include integrins, paxillin, vinculin, focal adhesion kinase (FAK), and tensin [60]. Adhesion studies the interaction between the material and cell more specifically.

6.4 Morphology

Morphology is observed by staining cells with molecules that locate in or bind to specific compartments or structures of cells. The molecules are either fluorescent themselves or are attached to another, fluorescent molecule. For example, cytoskeletal F-actin of fibroblasts can be stained with rhodamine-labelled phalloidin and cell nuclei are commonly stained with DAPI (4',6-diamidino-2-phenylindole). [7] Plasma membranes can be stained, for example, with Dil stain (1'-dioctadecyl-3,3',3'-tetramethylindocarbocyanine perchlorate). [60] After staining, morphology can be observed microscopically and imaged, but the fluorescence can also be measured with a plate reader [7].

EXPERIMENTAL PART

7. INTERVIEW ON EXPERT PERSPECTIVE

This thesis was made in collaboration between Biomaterial research group of BioMed-iTech (Tampere University of Technology) and Regenerative Medicine research groups of BioMediTech Institute (University of Tampere): Heart group, Mesenchymal stem cell group, Ophthalmology group, and Neuro group. The research in each of the Regenerative Medicine groups focuses on cells from the respective tissues (cardiomyocytes, mesenchymal stem cells, corneal epithelial cells, retinal pigment epithelial cells, and neuronal cells).

The aim of the cytocompatibility screening protocol created in this thesis was to offer these research groups a tool for screening hydrogels that could be finally used as a cell culture substrate for their cells of interest. As the cells used by the research groups are different, the interview was conducted in order to discover requirements that each of the research groups have for the screening protocol. In addition, the laboratory work of this thesis includes practical considerations that are difficult or impossible to know only based on the literature. Instead, working with live cells requires experience in cell culture of the particular cell type and its analyzing methods.

For this reason, professionals in the Regenerative Medicine research groups were interviewed to get their perspective on three main topics: criteria of a representable cell line that suits for cytocompatibility screening of their cell type (i.e. determining a suitable cell model); interactions of their cells of interest with surrounding (hydrogel) biomaterial; and analysis methods they would recommend using. One or two persons were interviewed from each Regenerative Medicine group of BioMediTech. The interview was conducted in fall 2015. Interview questions were based on Chapter 3, where effects on cell culture repeatability were investigated. The interview questions are in Appendix 1. Chapter 7.1 introduces the general criteria for the cell line(s) that will be selected for the screening. The results of the interview are presented in chapters 7.2-7.5 and compiled in table form in Appendix 2.

7.1 General requirements for all cell models

In order to use a cell for repeatable testing of material cytocompatibility, the cell (with its culturing techniques) should result in minimal biological variation in attachment, proliferation, viability and cell type specific functions when grown on substrates (such as hydrogels) that are cytocompatible. However, the cell should show decrease or variation in these results due to unfavorable change in culture substrate, such as a cytotoxic hydrogel.

Required properties of the cell model are as follows:

- commonly used and readily available
- not too expensive to acquire or culture
- well characterized and standardized
- relatively easy to culture, yet sensitive enough not to grow in an unsatisfactory hydrogel
- stable; as repeatable growth as possible
- growth rate high enough so that it can be used in short time screening
- adherent i.e. anchorage dependent cell

The cell line should be commonly used in order to have enough literature to compare results with, and readily available so that this protocol could be generally accessible and repeatable. Many cells that are acquired from an acknowledged cell repository, are both readily available and well characterized and standardized by the repository (cell identity, purity, and safety are tested). As the aim is to study cell behavior with a material, adherent cells are required. In addition, because the screening is desired to be rapid, a short culture time is preferred. Therefore, the used cells should have high enough proliferation rate.

7.2 Criteria for different cell models

Most interviewed research groups preferred the species of the cell origin to be human, because animal derived cells can behave differently. Also, some biomarkers are specific for human cells, and therefore it is easier to use analysis methods that have been used with human cells. In cardiomyocyte model the species of the cell origin was not as significant, and animal derived cells are often used in research. It is also noteworthy, that human derived, stable neurons can be restricted in availability and price.

The source of cells was preferred to be young in age, except in case of cell lines, when the age of the cell source has no significance. Especially in neuronal cell model, other than adult cells were required, because young and developing cells mimic the properties of neurons (from central nervous system) the best: they have better abilities to migrate and to form neuronal networks than adult cells. Neuroblastoma cells are an exception to this: they can originate from an adult (or child, more specifically), but because they are tumor cells, these adult cells are acceptable. For mesenchymal stem cell model, required age of the source depends on the application; adult cells might suffice for first step screening if they grow sufficiently. However, cells from a young individual would be better, because they allow producing a long-lasting cell line more easily, without gene transformation. In case differentiation is tested, mesenchymal stem cells would be needed.

All groups agreed that continuous cell lines would be a better option than finite cells, in order to achieve reproducibility. Although, it was suggested that in case finite cells are used, cells should be able to proliferate enough to be subcultured to large quantities and cryopreserved, and then early passages could be used in all experiments. Furthermore,

even though a continuous cell lines would be better for repeatability, continuous cardiomyocyte cell lines do not have the characteristic electrophysiological features, i.e. they do not beat, like primary cardiomyocytes do. Therefore, finite fibroblasts were suggested as the first step cell model for cardiomyocytes.

Transformed and tumor cell lines divided opinions among groups. Some transformed and tumor cells attach and proliferate well on almost any material, which raises a question of representativeness of natural cells, especially when studying attachment to material. Transformed (immortalized) cell lines were considered suitable for corneal epithelial (CE) and retinal pigment epithelial (RPE) cell models (*in vitro*), even though the results should be considered approximate because of their different attachment properties. Tumor cells, on the other hand, were not considered representative cells in applications of the Ophthalmology group. For neuronal model, both transformed and tumor cells would be suitable, as long as it has been proven with a negative control that the cell line does not grow too easily (on any material). Also for cardiomyocyte model transformed cell lines would be acceptable.

Because the transformation to induce immortalization can occur anywhere in the cells, transformed cells were not considered an acceptable option for mesenchymal stem cell model. Commercial tumor cell lines, such as osteosarcomas, have been studied extensively, and because the vast base of earlier research results, tumor cell lines were considered as the best option for the model (in addition to mesenchymal stem cells). Tumor cells and transformed cell lines do, however, behave differently than, for example, osteoblasts. Further, as for natural cells, early passages of finite fibroblasts from a young individual have growth properties nearly equal to those of a continuous cells line, and fibroblasts are used in research related to mesenchymal stem cells.

Cloning cells was not recommended by any of the groups. Cloning would require additional work for characterizing the cells, for example, and compared to the effort, cloning was not seen necessary. Especially if a cell line can be used, cloning would offer no benefits. In addition, further changes might occur in the cells during cloning.

7.3 Representative cell lines

Ideally, the chosen cell model should represent cells of interest of each research group. Research groups identified their ideal cell type, and cells that they are using currently in their studies. Research groups also recommended cells for the screening protocol (Table 7.1)

Table 7.1 Cells that each cell model should represent, cells in use in the research groups currently, and recommended cells for the screening protocol.

Cell model	Should represent	(Mimicking) cells in use	Recommended cells
Neuronal cell model	any young CNS cell	iPS derived neurons, hNP1, hESC derived neurons	SH-SY5Y [63], hNP1 [64], iCell [65], fetal neural progenitors / neural stem cells
Corneal epithelial cell model	corneal epithelial cell	hiPS derived CE cells, HCE-T	HCE-T [66]
Retinal pigment epithelial cell model	retinal pigment epithelial cell	hiPS derived RPE cells, human primary RPE cells, ARPE-19	ARPE-19 [67]
Cardiomyocyte model	differentiated cardiomyocyte	primary rat cardiomyocytes, END2, PA6	fibroblasts, (continuous cardiomyocyte)
Mesenchymal stem cell model	mesenchymal stem cell	fibroblasts, sarcomas mesenchymal stem cells	sarcomas (SAOS-2) [68], fibroblasts

The cells of interest in Neuro group, especially in biomaterial research, are central nervous system (CNS) neurons. Neuro group commonly uses (young) neurons differentiated from hESCs and iPS cells. In addition, hNP1 cells (ArunA Biomedical) have been used. hNP1 cells are commercial human neural progenitor cells, which have been derived from hESCs [64].

For neuronal cell model, four types of cells were recommended (Table 7.1). SH-SY5Y, a human neuroblastoma cell line [63], was recommended because it has been extensively used in research and it is easy to culture. SH-SY5Y cells do not, however, form neuronal networks like hNP1 cells do, which were recommended because of this property. Neither of these cell lines had been used by Neuro group in biomaterial experiments before, therefore, behavior on unfavorable substrates had not been tested. Further, iCell[®] Neurons [65] were recommended because they are iPS derived neurons (“first step” of differentiation completed), and therefore correspond fully the cells of interest in Neuro group. iCell[®] Neurons are mixed populations of human cerebral cortical neurons (glutamatergic and GABAergic neurons) that exhibit native electrical and biochemical activity, including formation of neuronal networks [65]. They are also stated to exhibit long-term viability and demonstrated reproducibility [65]. As the fourth option, fetal neural cells (stem cells

/ progenitor cells) were recommended, that have also gone through the first step of differentiation.

The two cells of interest of Ophthalmology group, that the cell models should represent, were corneal epithelial cell and retinal pigment epithelial cell. In Ophthalmology group, clinically relevant retinal pigment epithelial (RPE) cells and corneal epithelial cells (CE) are produced from human pluripotent stem cells lines. The differentiation of these cells is a long process; at least 3 months for RPE cells. These human pluripotent stem cell line derived cells are challenging to culture, they are slow and suffer from batch to batch variation and variation between cell lines. Ophthalmology group also uses human primary RPE cells, but these can be cultured only for few passages. In addition, the group has commercial immortalized cell lines ARPE-19 (RPE cells) and HCE-T (corneal epithelial cells) in use.

Even though these immortalized cell lines, ARPE-19 [67] and HCE-T [66], behave rather differently on biomaterials compared to the stem cell derived cells and primary cells, they were recommended for the first-step screening model. That is because they are commonly used cell lines in Ophthalmology research and quite stable cells. The most important criteria for both cell types is that they form an epithelial cell layer, have correct morphologies and express correct marker proteins, which can be detected with immunostaining. Corneal epithelial cells form a multilayered structure on the border of material surface and air. RPE cells, however, should stay as a monolayer. ARPE-19 cells should not be cultured too long (3-4 d), because they lack the property of stopping proliferation due to contact inhibition. In addition, ARPE-19 cells do not produce pigment, like RPE cells *in vivo*. Otherwise, ARPE-19 and HCE-T were considered to represent well human retinal pigment epithelial cells and human corneal epithelial cells.

The cardiomyocyte cell model should represent a differentiated cardiomyocyte. The Heart group had used rat primary cardiomyocytes (harvested by the group), END2 cells (from mouse, a clone from P19 embryonal carcinoma cells [69]; and used to differentiate stem cells to cardiomyocytes [70]) and PA6 cells (also named MC3T3-G2/PA6, commercial cell line from mouse bone marrow [71], [72]). However, according to the Heart group, there is not really another cell that mimics differentiated cardiomyocyte very well. Instead, the properties of the chosen cell line are more important to consider. The most important properties are, that the cell has to spread and take contact to other cells. Therefore, quite many cell lines can be used, if the aim is merely to see whether the cell attaches and spreads on a material (in a fibroblast-like manner). PA6 cell line is similar to END2, but it was suggested that a fibroblast would be better option for the screening model. In addition, it was suggested that a continuous human cardiomyocyte cell line could possibly be a good option, if available, although, these cells do not beat.

For mesenchymal stem cell (MSC) model, the cells should represent MSCs that can be used in bone and cartilage applications. The cells that could be used for the model are fibroblasts, osteosarcoma cells (for example, SAOS-2 [68]) and chondrosarcoma cells. Although there are some disadvantages of using tumor cells, they give repeatable results and grow more rapidly than osteoblasts and chondrocytes, hence tumor cells were considered a better option for screening. SAOS-2, which is an osteoblast-like sarcoma, has the advantage of being extensively used in research relating to bone tissue.

7.4 Culture environment

Possible applications of hydrogels in the research areas of Regenerative Medicine research groups included three-dimensional cell culture, disease modeling, and drug and toxicity testing. Further, in future, hydrogels could have tissue engineering applications, such as acting as a scaffold in central nervous system transplantation therapy or heart patch after ischemia.

For these applications, the aim is to ultimately culture neurons, cardiomyocytes, and mesenchymal cells inside the hydrogels (encapsulated in hydrogel or in “sandwich” layout, i.e. cell layer between two hydrogels). In addition, cells could be cultured on top of hydrogels to study their attachment to the hydrogel. In RPE and CE applications, hydrogels have the advantage of being transparent. The role of a hydrogel in CE applications would be to mimic the structure of the stroma of the eye and cells would therefore only be cultured on top of hydrogels. This represents the layout of corneal cells in the eye, where the cells are in the substrate-air interface. Also RPE cells are required to grow only on top of hydrogels. In case of RPE model, the hydrogels do not need to be macroscopic in their thickness. In fact, for retina applications, hydrogels may not be the best approach, as the optimal substrate was described as an extremely thin (4-20 μm) yet mechanically durable biomimetic porous sheet.

Research groups were asked to recommend positive and negative controls, preferably hydrogels, for the screening of new hydrogels based on the cells that are currently used in their research. Many research groups had not tested culturing their cells with hydrogels before, or hydrogels were not in regular use. Therefore, they could only suggest some options to try (Appendix 2 (2/3)), and also recommended two-dimensional controls. For example, collagen was suggested as a potential positive 3D control. However, it must be noted, the positive and negative controls depend on the final application. Especially in MSC model, the difficulty with many hydrogels is that cells form soft tissue or fat tissue, not bone or cartilage.

Commercial hydrogels, PuraMatrix[®] and Matrigel[®], have been used previously by Heart group. Also Neuro group has cultured neuronal cells with PuraMatrix[®] in different lay-

outs with good results [48]. As controls with neuronal cells, uncoated well (negative control) and laminin-coated well (positive control) have been used. A negative hydrogel control was not in regular use of Neuro group. Some options for possible negative hydrogel controls were mentioned to include unmodified PEG (polyethylene glycol), chitosan, and unmodified cellulose.

Many cells require a coating with a biomolecule before plating them on culture flasks. This should be considered separately for each cell that is used, when choosing control materials. In general, for cardiomyocytes gelatin coating is routinely used. The commercial immortalized cell lines HCE-T and ARPE-19 grow almost on everything and do not necessarily need any additional coating. However, with stem cell derived RPE and CE cells additional ECM proteins are needed. MSC cells attach to uncoated well, so coating is not needed, although 3D scaffolds are sometimes incubated in culture medium before inserting cells. Neurons require a laminin coating. According to interview, this coating should be only considered for 2D control, and not with hydrogel, when aim of the screening is to test cell reaction towards hydrogel, and when the location of laminin in the sample (or level of attachment of laminin to hydrogel) is not known.

All other groups except MSC group culture their final cells of interest (for example, in Ophthalmology group hiPS derived RPE and CE cells) in serum free medium or medium with serum replacement. Because proteins in serum can affect attachment of cell to material, this aspect can be taken into consideration when choosing the cell model, so that its requirements for serum would be the same as in final application. However, cell lines are usually adapted to a certain culture medium, and according to the interview, re-adaptation to different serum conditions in medium is time demanding and not recommended.

7.5 Analysis methods

All groups recommended 3-5 parallel samples for experiments. In addition, several cell lines could be used in some cases to better validate the results and give more information, especially if the used cells are derived from stem cells (for example, hiPS derived CE cells) or primary cells (should be collected from several patients). For first step screening, generally one cell line was considered sufficient. Later the results could be proven to be reliable with a more representable cell (for example, starting with a sarcoma cell line and validating results with MSCs or osteoblasts).

Research groups described aspects of cellular behavior that need to be observed in order to determine response of their cells of interest toward a material. In addition, they recommended methods to analyze these aspects. These are listed in Appendix 2 (3/3). All groups needed to observe at least proliferation or viability of cells and morphology cells, even though the methods to detect these varied.

The culture time that is needed to observe cell response to hydrogel differed between cell types. Neuronal cells and MSCs needed 2-week culture time. Culturing for one week was said not to suffice for neuronal cells, because cells might grow well for one week, but retract after that. For differentiation of MSC, 4 weeks is needed, however, testing differentiation is out of the scope of this thesis. To observe response of HCE-T cells and fibroblasts, 1-week culture was recommended. For ARPE-19 cells culture time of 3-4 days was recommended, although proliferation can be detected already after culturing for one day. (Also, detecting formation of mature RPE monolayer would take 28 – 42 days.) In general, attachment of cells, however, can be observed right away.

7.6 Conclusion

Based on the interview, we can conclude that the cytocompatibility testing can be made in different steps. Before using more specialized cells such as stem cells, neural progenitor cells or hiPS / hESC derived differentiated cells, an immortal cell line or a tumor cell line should be used (Table 7.2). These immortalized cell lines and tumor cell lines are easier to culture, have high repeatability and have been used extensively in research, offering a base for comparing results. However, the behavior of these proposed cell lines should be checked on negative controls before taking into use, in order to confirm that they are sensitive enough.

Table 7.2 The proposed cells to be used for each cell model in the three phases of cytocompatibility screening protocol. The first step is common to all cell models.

Cell model	1 st step	2 st step	3 rd step
Neuronal cell model	Fibroblast (WI-38)	SH-SY5Y	iPS derived neurons (eg. iCell®); hNP1 (Aruna) hESC derived neurons; fetal neural progenitors / neural stem cells
CE cell model		HCE-T	hiPS derived CE cells; human primary RPE cells
RPE cell model		ARPE-19	hiPS derived RPE cells; human primary RPE cells
Cardiomyocyte model		END2, PA6, continuous cardiomyocyte	primary rat cardiomyocytes,
Mesenchymal stem cell model		Osteosarcomas, chondrosarcomas (SAOS-2)	Mesenchymal stem cells

For cardiomyocyte model, fibroblasts were considered the best option for the first-step screening. Because no other cell than cardiomyocytes really represent (beating) cardiomyocytes very well, morphology was considered as the most important property. Fibroblasts are rather easy cells to culture, and because of their “fibroblast-like” morphology they should generally spread on their culture substrate. Fibroblasts were mentioned as an option also for MSC model for first-step screening. In addition, a few fibroblasts were recommended by ISO 10993-5 standard for general cytotoxicity testing of materials [14]. Therefore, the cytocompatibility screening could be started by using fibroblasts, regardless of the final cell of interest. This first step would give information about the cytotoxicity of the material in general. Based on comparison made in Chapter 4, it can be concluded that WI-38 would be the most suitable fibroblast for this particular screening protocol. After testing with fibroblasts, testing can be continued with immortal cells and tumor cells (Table 7.2).

Choice of control materials, culture time before analysis, and whether culture medium will be supplemented with serum are aspects that depend on the cell model that is used in each step. Even though using serum-free medium would be desirable in many final applications, a compromise has to be made to choose a suitable cell line.

Within the limits of Master’s Thesis, only the first step was optimized in this thesis. In this case, WI-38 cells are adapted to serum supplemented medium, hence, serum would be used, even though this might affect attachment to materials and can cause some batch-to-batch variation. PuraMatrix[®] has been proven to be cytocompatible with many cell types, including fibroblasts (see Chapter 5.1). Because PuraMatrix[®] was mentioned by two groups and can therefore be useful in further steps as well, it was chosen as positive (3D) control. Attachment and viability were chosen to be studied by Live/dead staining method.

8. DEVELOPMENT OF CYTOTOXICITY PROTOCOL TO STUDY NOVEL HYDROGELS

Based on the results of the interview (Chapter 7) and the literature, the following protocol is recommended for screening hydrogel cytocompatibility for cell culture applications (Figure 8.1). First, attachment, viability, proliferation and morphology of cells are tested by using a general cell line, such as a fibroblast cell line. After that, more tissue-specific cell lines are used to study the same phenomena. The tissue specific cell line depends on the cell type intended to be used in the final application. For example, in case of mesenchymal stem cells, a sarcoma cell line can be used as a representable cell line (Appendix 2). Finally, the same phenomena are studied with the intended cell type for the final application, such as stem cells, differentiated cells or primary cells. Testing specific functions of cells or staining cell-specific structures becomes especially relevant in parts 2 and 3 (Figure 8.1).

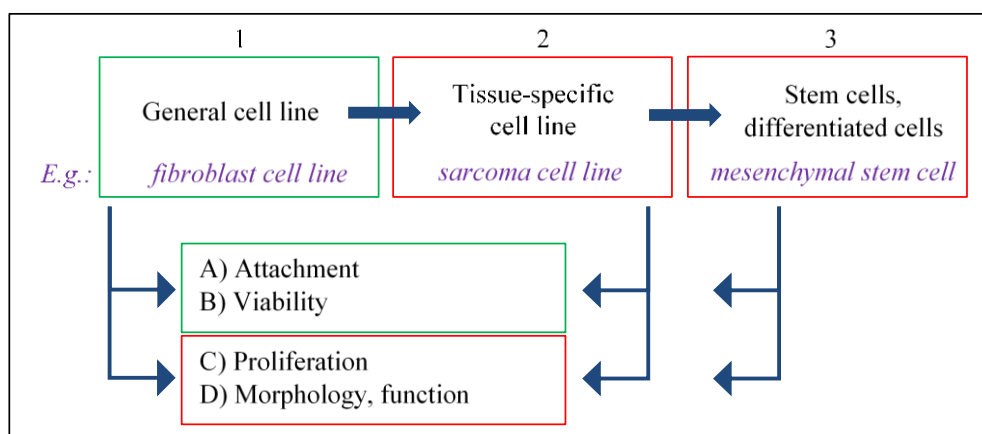


Figure 8.1 Parts of the hydrogel cytocompatibility testing protocol for cell culture applications. First-step cytotoxicity testing protocol, which tests short-term attachment and viability of a general cell line, was created in this thesis (marked with green). Other parts of the protocol (marked with red) were left out of the scope of this thesis.

Within the scope of this Master's thesis, a protocol for screening attachment and viability of a general cell line (steps 1A and 1B in Figure 8.1) was optimized and tested in practise. Morphology of cells was assessed qualitatively only as a reference when needed, in order to validate the protocol. According to definitions in Chapter 2.1, these parts of the protocol, when tested with a short culture time, indicate short-term cytotoxicity of a material. Steps 1A-B can be therefore considered as a "first-step" cytotoxicity protocol. This protocol is based on principles of direct contact cytotoxicity testing in standard ISO 10993-5:2009 [14].

Optimizing and testing of other parts of the cytocompatibility protocol (1C, 1D, 2 and 3) were left for future experiments. However, similar principles as defined in this thesis can be used for testing attachment and viability of the more specialized cells (in steps 2 and 3). In addition, a longer culture time than 1 – 2 days could be later used to better represent the needs of the research groups (Chapter 7).

The purpose of the first-step cytotoxicity protocol would be to screen attachment and viability of cells seeded on top and encapsulated in hydrogels. As stated earlier in Chapter 2.2, cytotoxicity (and, therefore, cytocompatibility) can be evaluated either quantitatively or qualitatively. The analysis method was chosen to be an imaging based, because it can offer both qualitative and quantitative information. Cells were observed qualitatively from fluorescence and phase contrast images. However, even though qualitative assessment would be suitable for screening cytotoxicity [12], a quantitative approach was preferred in this thesis to obtain a more high-throughput protocol, and so that effects of small differences between new hydrogels could be detected. Therefore, attachment and viability were quantified from fluorescence images.

8.1 Research methods and materials

Figure 8.2 represents the workflow of the experiments that were made and the parameters relating to each step. These parameters were optimized for the attachment and viability screening protocol. The experiments for optimizing the parameters are introduced in the following subchapters.

A set of materials and methods were selected based on literature and the conducted interview (cell line, control materials and staining method). The imaging system (equipment) was selected by comparing the suitability of three imaging systems: BioStation CT (Nikon), Cell-IQ (CM Technologies), and ApoTome (Zeiss). Further, other experimental parameters were optimized based on an iterative sequence of several experiments. Each experiment gave results for several parameters, which are, in addition, interconnected with each other. For example, the working distance of imaging system is one of the most important factors in defining the maximum volume of the sample that can be imaged. On the other hand, the material affects the practicalities of sample preparation, such as the minimum volume in which a hydrogel can be formed (as well as maximum volume). Because imaging a three-dimensional, transparent sample is rather different than imaging a monolayer of cells, optimizing the imaging acquisition settings was especially focused on.

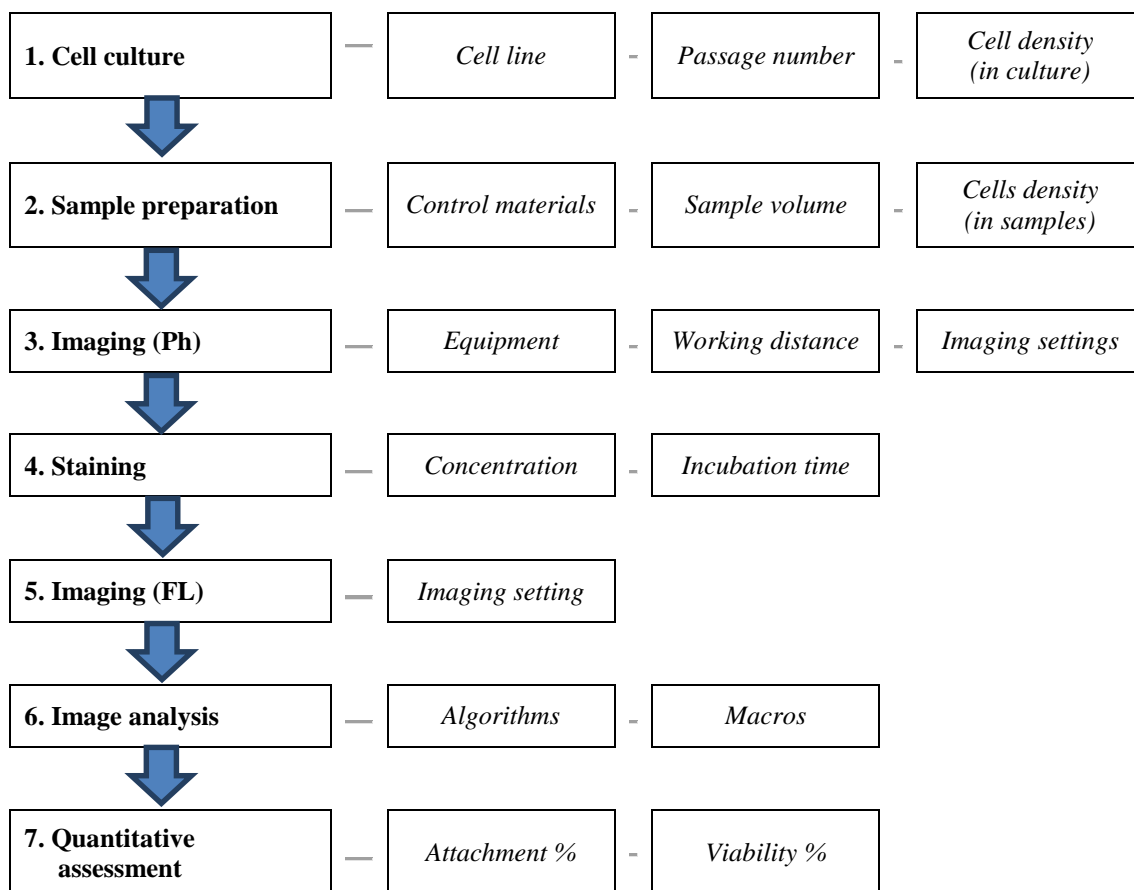


Figure 8.2 Overview of the workflow of experiments and the parameters that were optimized relating to each step.

Briefly, the workflow of the experiments was as follows. Fibroblasts were cultured on top of and encapsulated in 3D macroscopic hydrogels and on control materials. After 2 h – 3 d culture time, cells were imaged with phase contrast microscope of BioStation CT, which was the main imaging system in the experiments. Cells were then stained with LIVE/DEAD[®] viability/cytotoxicity kit (Molecular probes, ThermoFisher Scientific) and phase contrast and fluorescent images were then taken from the same imaging points. Obtained images were analyzed with ImageJ software (FiJi distribution, open source [73], [74]). Cell viability and attachment on top or inside the control and test materials were assessed quantitatively from fluorescence images.

8.1.1 Sample preparation

Sample layouts are schematically presented in Figure 8.3. Cells were plated on top of hydrogels (“OnGel”) or encapsulated inside hydrogels (“3D”). A commercial hydrogel, BD[™] PuraMatrix[™] (BD Biosciences), was used as a positive three-dimensional control (both for OnGel and 3D samples). In addition, gellan gum (GG) hydrogels crosslinked with spermidine (SPD) were tested. SPD is a polyamine which allows physical crosslinking of gellan gum [52]. Cells were always plated also on uncoated well-plate (“2D”),

which acted as the positive (two-dimensional) control and a reference for imaging. Untreated polydimethylsiloxane (PDMS) discs were used as the negative (two-dimensional) control. PDMS does not elicit negative, cytotoxic reactions [75], but it is an inert material because of its high hydrophobicity, and does not support cell attachment or growth, unless treated with suitable plasma treatment [61]. PDMS also has the advantage of being transparent.

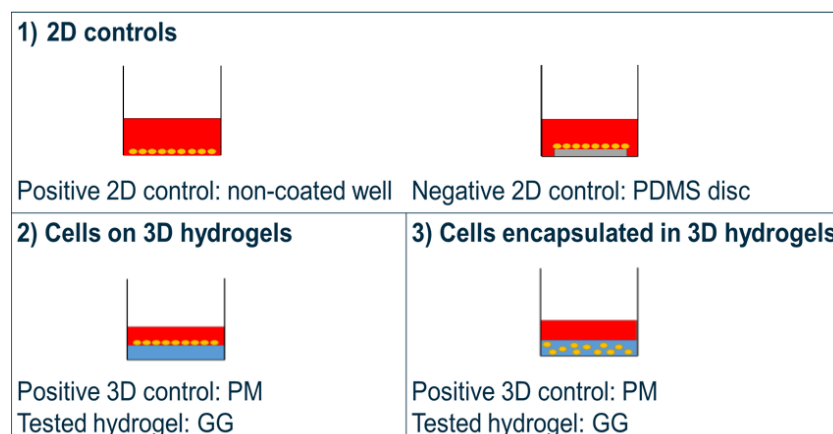


Figure 8.3 Schematic illustration of test and control sample layouts prepared for the experiments.

Test and control samples were prepared according to the following common instructions, unless stated differently in particular experiment. The numbers of replicate samples in experiments varied between 2 and 6.

8.1.1.1 Cell culture

A commercial human embryonic lung fibroblast cell line WI-38 (Sigma-Aldrich / Culture Collections, Public Health England) was chosen based on the literature review and interviews and used for most experiments. WI-38 cells were cultured with DMEM/F-12 growth medium supplemented with 10% FBS (fetal bovine serum), 1.25% Glutamax, and 0.5% Penicillin/Streptomycin. WI-38 cells were subcultured twice a week with 1:2 ratio (or seeding density of $2-4 \times 10^4$ cells / cm^2). WI-38 cells with passages 19-34 were used for experiments (p. 21-27 for attachment and viability assessment tests).

In addition, a few experiments were made with human foreskin fibroblast (hFF) cell line, CCD-1112Sk (a kind gift from the Ophthalmology group, BioMediTech). hFF cells cultured with IMDM growth medium supplemented with 10% FBS and 0.5% Penicillin/Streptomycin. Cells were subcultured once a week with 1:5 ratio. hFF cells with passages 10-13 were used for experiments. All cells were stored in sterile conditions at 37 °C and 5% CO_2 .

After thawing from cryopreservation, cells were cultured at least a week before using for experiments, as is recommended [14] to allow cells retain their normal functions. For preparing samples, cells were washed twice with DPBS and detached with trypsin (5-10 min incubation). Trypsin activity was stopped with full (supplemented) growth medium, unless cells were encapsulated in gellan gum. FBS accelerates gelation of gellan gum, which makes sample preparation difficult, and in that case unsupplemented growth medium was used.

Samples were made to Nunc™ Multiwell plates (Thermo Scientific), treated with Nunclon™ Delta surface treatment, or to CELLSTAR® Cell Culture Multiwall plates (Greiner Bio-one). For initial experiments (testing equipment and Live/dead staining concentration conditions), CCD-1112Sk cells were plated on 2D and on top of hydrogels with density of 5×10^4 cells / cm² and encapsulated in (GG) hydrogel with the density of 100 and 200 cells / μl of hydrogel (in Nunc™ 48 well plate).

Later, different seeding densities of WI-38 were tested on 2D controls and on top of hydrogels (Table 8.1) and encapsulated in hydrogels (Table 8.2). Recommended seeding density of WI-38 cells is $2-4 \times 10^4$ cells / cm². However, in order to be able to distinguish cells from one another well, cell densities slightly under the recommendation were also tested.

Table 8.1 Seeding densities of WI-38 on two-dimensional controls and on top of hydrogels. Seeding densities are announced in (cells / cm²), because in addition to using 24- and 48 well plates, the area of wells in well plates of different manufacturers differ from each other.

Well plate	Cell density (cells / cm ²) × 10 ⁴
Nunc 24 wp	1.7
	2.0
	2.8
	4.0
CELLSTAR® 48 wp	1.5
	1.7

Table 8.2 Cell densities (WI-38) encapsulated inside hydrogels.

Well plate	Cell density (cells / μl of hydrogel)
Nunc 24 wp	350
	600
CELLSTAR [®] 48 wp	500
	600

8.1.1.2 Gellan gum hydrogel

Gellan gum (Gelzan, Sigma-Aldrich) and spermidine (Spermidine trihydrochloride, 85578, BioXtra, $\geq 99.5\%$ (AT), Sigma Aldrich) stock solutions were prepared in 10 % sucrose. The spermidine (SPD) (1.0 mg/ml) stock solution, gellan gum (GG) 5 % stock solution (5 mg/ml) and sucrose solutions were sterile filtered with 0.2 μm filter. GG solution was heated to 60 °C in water bath (or dry bath) prior to sterile filtering in order to decrease viscosity. After sterile filtering, solutions were handled aseptically. Two concentrations of SPD were used to crosslink hydrogels for experiments: 1.0 mg/ml and 0.5 mg/ml. These concentrations correspond to volume ratios of 3% and 1.5% of SPD in the final hydrogel, respectively.

Crosslinker and gellan gum solutions were warmed to 37 °C prior to gelation. Hydrogel samples were prepared by mixing the crosslinker (SPD) and gellan gum in a well-plate in SPD:GG volume ratio 160:1000. The solutions were mixed by stirring with pipette tip or pipetting up and down (if gelation was slow enough). When possible, well-plate was kept on a 37 °C hot-plate during mixing and gelation. Gelation time depends on the crosslinker concentration, and gelation was observed by tilting the well-plate; when no flow was seen, the hydrogel was considered to be gelled. Hydrogel volumes of 145 μl – 290 μl were tested.

When cells were cultured on top of the hydrogel, the hydrogel was prepared first. After the hydrogel had properly gelled, cell suspension (cells in supplemented medium) with correct cell concentration was simply pipetted on the hydrogel. When cells were encapsulated inside the hydrogel, the crosslinker and cell suspension (cells in medium without serum supplement) with correct cell concentration were first pipetted into the well. Thereafter, gellan gum was added and solutions were mixed. Medium without serum supplement was used, because serum decreases the gelation time of GG, which makes it more difficult to prepare homogenous samples. The volume of cell suspension was kept under 10% of the total volume of the hydrogel, in order not to compromise the mechanical properties of the hydrogel. Medium with serum supplement was added on the hydrogel sample after gelation.

8.1.1.3 PuraMatrix™ hydrogel

BD™ PuraMatrix™ peptide hydrogel (PM) stock solution (10 mg/ml, 1 % w/v) was acquired from BD Biosciences. Hydrogels (0.5 % w/v) were prepared according to PuraMatrix™ instructions. Volume of PM hydrogels was 200 μ l. PM stock solution was vortexed to decrease viscosity and bubbles. For OnGel samples, 200 μ l of 0.5% PM solution (diluted in 10% sucrose solution) was pipetted into each well. PM was first crosslinked with WI-38 growth medium and the medium was changed twice during one hour, before adding cells (1.7×10^4 cells in each well).

For 3D encapsulated samples, cells were suspended in 10% sucrose solution to a concentration double the final concentration (in this case 1.2×10^6 cells / ml, to obtain final concentration of 600 cells / μ l of hydrogel). 100 μ l of the cell suspension was mixed slowly with 100 μ l of 1 % PM solution. After mixing, the mixture was immediately transferred into a well and crosslinked by slowly adding WI-38 growth medium. The samples were prepared individually to decrease the time cells must stay in contact with PM and sucrose solution without medium, because the pH of PM is not favorable to cells before adjusting it with growth medium. Samples were stored in incubator and medium was changed twice during one hour to equilibrate pH.

8.1.1.4 Poly(dimethylsiloxane)

A large poly(dimethylsiloxane) (PDMS) disc was prepared from Sylgard® 184 Silicone Elastomer Kit. The disc is made by pouring correct amount of PDMS solution on a plastic disc and then heated for crosslinking. Therefore, the upper and bottom sides of the disc were different, as one faced plastic and the other faced air during preparation. Small discs were cut out with an 8.5 mm diameter biopsy punch. The discs were 820 μ m – 950 μ m thick.

The discs were moved into sterilization bags, while keeping them facing the same direction (air side facing the paper and plastic side facing plastic of the bag or aluminum folio inserted into the bag). The discs were sterilized by autoclaving (Tuttnauer Autoclave 2540ELLB) in 121 °C for 15 min.

8.1.1.5 Live/dead assay

Control cells, and cells on top and encapsulated inside hydrogel were cultured approximately 2 h to 3 d before staining with LIVE/DEAD® viability/cytotoxicity kit (Molecular probes, Thermo Fisher Scientific). In brief, the two dyes of the kit, calcein-AM (Ca-AM,

stock 1 mM, $\lambda^{\text{emission}} = 488 \text{ nm}$) and ethidium homodimer-1 (EthD-1, stock 2 mM, $\lambda^{\text{emission}} = 568 \text{ nm}$) stain live and dead cells, respectively.

Because the staining solution can be assumed to dilute in the water-containing hydrogel, three concentrations (single to triple concentration of EthD-1 and Ca-AM) in the staining solution (in PBS) were tested (Table 8.3).

Table 8.3 Tested concentrations of LIVE/DEAD[®] staining solution.

	EthD-1 (μM)	Ca-AM (μM)
C₁	0.05	0.10
C₂	0.10	0.20
C₃	0.15	0.30

The volume of staining solution in each well was the same as volume of replace medium (e.g. for 48-well plate 500 μl). After 20 min - 1 h incubation at +37 °C the cells were imaged with one of the imaging systems.

8.1.2 Imaging systems

CM Technologies Cell-IQ, Nikon BioStation CT, and Zeiss ApoTome were tested as the possible imaging systems. Cell-IQ and BioStation CT are both cell culture imaging systems, which include an incubator and imaging hardware. They are automated systems, where the imaging points can be set in the operating software. Phase contrast images and fluorescence images can be taken with these systems. Zeiss ApoTome imaging system included Zeiss Axio Imager M2 upright Microscope, which is a wide field fluorescence microscope. It was equipped with ApoTome unit, a structured illumination system, which allows optical sectioning of the sample.

Because Zeiss ApoTome imaging system was equipped an upright microscope, samples could not be prepared in 24- or 48- multiwell plates. Otherwise the objective lens would not reach close enough to the samples (edges of the well are on the way). Therefore, hydrogels were made in Nunc 24-well plates with $\text{Ø} = 13 \text{ mm}$ glass coverslips in the bottom. In addition, similar samples were made into 5 ml cut syringes that had been sterilized (Figure 8.4). 145 - 290 μl GG 1.5% SPD hydrogels were prepared.

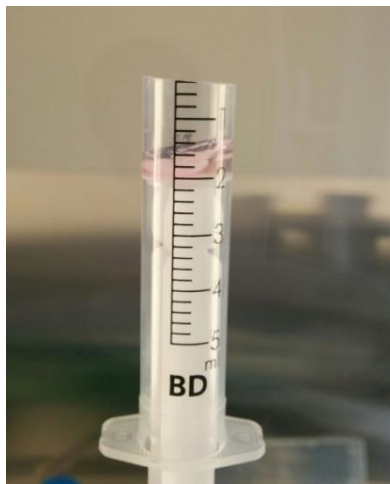


Figure 8.4 Gellan gum hydrogel in a cut syringe. Red color comes from incubation in cell culture medium.

After gelation, WI-38 cells (1.6×10^4 cells / cm^2) were seeded on top of hydrogels. Cells were stained with Live/dead assay solution and after 30 min incubation in room temperature, the staining solution was removed. Before imaging with ApoTome imaging system, samples were lifted together with the cover slip or pushed out from the syringes into a 6-well plate (or on its lid) (Figure 8.5).

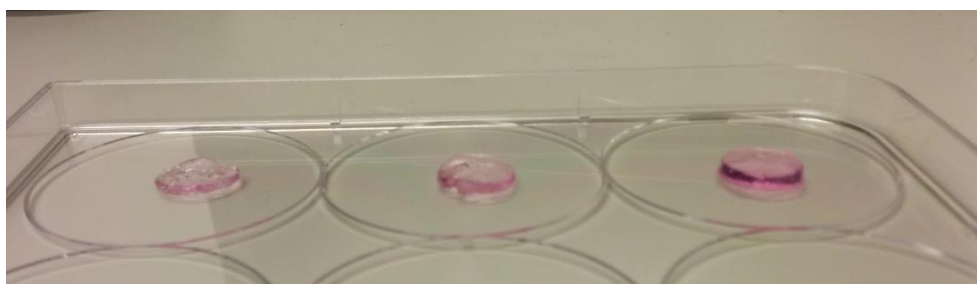


Figure 8.5 Gellan gum hydrogels transferred from 5 ml syringes to well plate lid for imaging with ApoTome. On the left 145 μl , in the middle 200 μl and on the right 290 μl samples.

Both Cell-IQ and BioStation CT were tested with 290 μl gellan gum samples casted in Nunc 48-well plate. CCD-1112Sk cells were encapsulated in (GG 3% SPD) hydrogels (100 and 200 cells / μl gel) and plated on top of hydrogels and uncoated wells (5×10^4 cells / cm^2). After 3 days, cells were first observed with phase contrast microscope in the imaging systems, and after staining, imaged with fluorescence and phase contrast microscopes.

BioStation CT was also tested with thinner hydrogels: gellan gum hydrogels (3% SPD) with volumes of 145 μl and 174 μl were prepared in Nunc 24-well plate. In addition, CELLSTAR[®] (TC treated) 48 well-plates (Greiner Bio-one) well plates were tested with 145 μl , 200 μl , 250 μl , and 290 μl gellan gum (1.5% SPD) hydrogels. Cells were seeded on top and encapsulated in samples.

Usability of the three imaging systems was compared, especially in terms of imaging 3D hydrogels in high-throughput manner. Also the focusing ranges of the systems and sample volumes that could be imaged fully were compared. In well plates used with BioStation CT, focus position of the inner surface of the well was observed (where cells on uncoated wells were in focus).

8.1.3 Image acquisition settings in BioStation CT

Several different test series were conducted to optimize image acquisition settings in BioStation CT. In case of PDMS and uncoated well, the surface on which cells were growing was flat, and therefore this focus plane was the target of imaging. However, in case of hydrogels, cells are located in different focal planes. In encapsulated samples this is because cells are inside the hydrogel, but also cells on top of hydrogels are located in different focal planes to some extent, because of uneven surface. To get a representable set of data from samples, the aim was to image encapsulated samples from several xy coordinates in different planes in Z-axis. In order to prevent distortion of quantitative results, it was attempted to avoid imaging above the surface. For OnGel samples the aim was to image surface of the hydrogel, where cells were in focus (Figure 8.6).

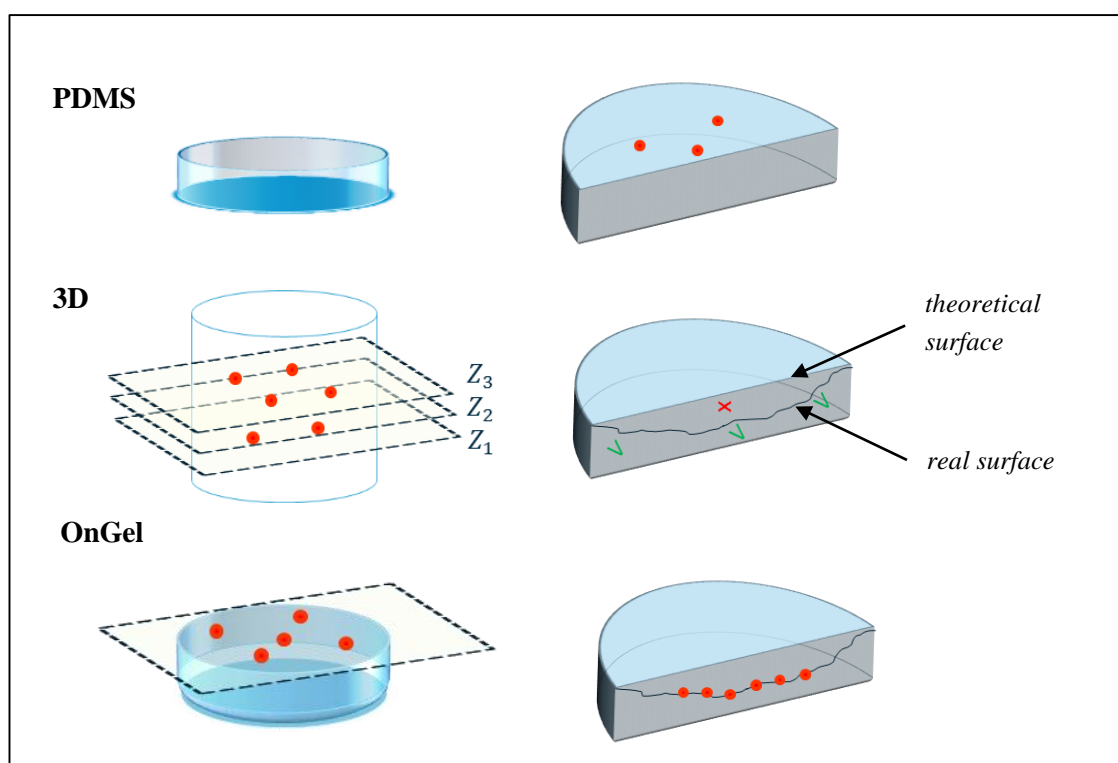


Figure 8.6 Principles of imaging cells on PDMS control, and encapsulated and on top of hydrogels. PDMS was a flat disk, on which cells were in one plane. The uncoated well had a similar layout, only in the bottom of the well. Ideally encapsulated samples would be imaged from several focal planes (middle, left), however the topology should be considered, not to image above the surface (middle, right). Ideally, cells on top of hydrogels would also be imaged in one plane (bottom, left), but in reality the cells reside in different planes (bottom, right). Red dots illustrate possible imaging positions.

Samples were imaged in BioStation CT with phase contrast microscope (Ph channel) before staining. After staining the same coordinates were imaged with phase contrast and fluorescence microscope (green and red channels) of BioStation CT. All samples were imaged with 4× and 10x magnification, and 1-15 images were imaged per sample.

Imaging points were set either manually (custom points, user defines x,y, and Z coordinates) or by using 5 default points. The latter is an option where x,y coordinates are pre-set in the middle of the well and at equal distances around it; Z coordinate is defined by autofocus (i.e. optimal focus point calculated by the equipment).

Custom points of hydrogel samples were set at the same x, y coordinates (Figure 8.7), and Z coordinates varied according to sample. Z coordinates on OnGel samples were set manually where cells on top of hydrogel sample were in focus. Information on Z coordinates in those points was used to estimate the location of sample surface in encapsulated samples of the same experiment. Custom points in encapsulated samples were then set accordingly in 2-4 different planes inside the sample.

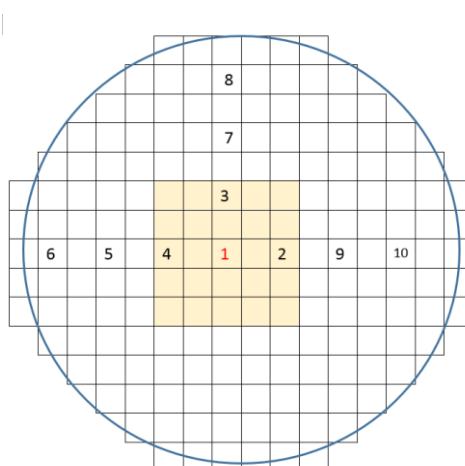


Figure 8.7 Well map of imaging coordinates. Each square represents the area of well that is seen in live mode with 10x magnification on the operating panel of BioStation CT.

Hydrogel samples were also imaged with phase contrast channel by using Z stacking (equal number of images are taken automatically below and above the autofocus or custom set Z coordinate). Range (i.e. total distance of stack) was 200 μm - 400 μm and pitch (distance between images) was 5 μm - 10 μm . In addition, Full scan function was used, which images the entire area of well in one focus plane (autofocus or custom set). Three focus planes with custom set Z coordinates were imaged separately in 3D samples. After imaging a focus plane with Full Scan function, tiling images were retrieved or imaged for some samples (2D and 3D).

8.1.4 Image analysis

Images were analysed with FiJi software. Two fluorescence images were obtained in grayscale from each imaging point, one with each of the two channels they were imaged with (“green channel” and “red channel”). For observing RGB images, the two images (channels) were merged, and green and red colors were added by using FiJi. For efficiently processing all images, a macro was written (Appendix 5). The macro opens images from all coordinates of one sample and merges the channels, and forms a stack in RGB format.

For counting cells from the fluorescence images, the following circumstances were considered to count cells correctly either as dead or live. Usually, live cells are seen as uniform green fluorescent areas and dead cells are seen as uniform red fluorescent areas. However, green and red stains can be located seemingly in the same cell, or in the area of one cell, because of the following reasons.

1. There is bleed-through to the opposite channel. The intensities that are observed should be very low.
2. “False green” is seen, even though the cell is dead. Intensity of the cell (or nucleus) in red channel is high compared to its surrounding. At the same location and/or around the red area, there is an area in the green channel which is visible in low to high intensity. This is the cytosol of the cell, which, for some reason, still remains fluorescent calcein inside it, even though the cytosol is dotted and the edges of the cell are not uniform or clearly defined.
3. Two cells are on top of each other, one is dead and the other is live. Usually, but not always, a live cell is bigger than a dead cell.
 - a. If the cells are in two-dimensional surface, or in the same focus plane in a hydrogel, these cells should have equally high intensity.
 - b. If the cells in hydrogel are apart from each other in Z-axis, the intensity of cells also decreases when cells are located further away from the focus plane.

Cells were counted from RGB images manually. Cells that were far from focus plane (only aberration ring visible) were omitted. “False green” cells were the most prominently double stained, and they were counted in addition to the number of red cells and green cells (include green and red cells that were double stained). To obtain the number of live cells and dead cells, the number of double stained cells was subtracted from the number green cells. The final number of dead cells was the same as number of red cells.

Cells were also counted automatically with FiJi. The set of executed functions are presented in Particle Count algorithm, Appendix 4. The algorithm for counting was based on intensity differences in the image and cell size. It produces numbers of cells in green channel and red channel. In attempt to omit the same cells in automatic counting as in manual counting, high threshold values were used. The values for thresholding green and

red channels were estimated by measuring the minimum intensity of countable cells in a few images (Table 8.4, Threshold 2). Similarly, minimum size of cells that needed to be analyzed was estimated.

The Particle Count algorithm was used to analyze 10x fluorescence images of one experiment (2D and 3D samples). Cells were counted with the algorithm twice, using different threshold values (Table 8.4). The particle size was the same, 40 px^2 - infinity, both times and for both channels.

Table 8.4 Values used in the steps of Particle Count algorithm. Cells were counted twice, with two different threshold ranges.

Step	Red channel	Green channel
Threshold 1	100 – 255	100 – 225
Threshold 2	100 – 255	130 – 225
Analyze particles; size	40 px^2 - infinity	40 px^2 – infinity

The final number of dead and live cells with automatic counting were the numbers of red and green cells, respectively. The numbers of live and dead cells obtained by the different manual counting and Particle Count algorithm were compared to estimate the accuracy of the algorithm.

8.1.5 Assessment of attachment and viability

For assessing attachment and viability of cells, numbers of live cells and dead cells were obtained from fluorescence images by manual counting (according to Chapter 8.1.4). Attachment of cells to a hydrogel was assessed with samples where cells were seeded on top of the hydrogel (OnGel samples). With this layout, unattached cells are removed during medium change. The more cells are present on the material after medium change, the better the material supports attachment of cells.

One approach to assess attachment would be to count cells on the samples before and after medium change. This would require counting cells from phase contrast images. Contrast between cells and hydrogel is low, especially when cells have a spread morphology, which makes counting more difficult than from fluorescence images. Also the image analysis in FiJi was optimized for fluorescence images, thus, another approach was chosen where fluorescence images were utilized. Cells that remained on the sample after the medium change (in this case, change to Live/dead staining solution) were counted from fluorescence images. The number of all cells (live and dead) on the test hydrogel was compared to the number of all cells on the control material.

The attachment in a sample was calculated relative to the positive 2D control (uncoated well plate), hence giving the 2D control a comparison value of 1. Simply, attachment was defined as in Equation 8.1.

$$\text{Attachment} = \frac{\text{cells per image on sample}}{\text{cells per image on 2D}} \quad (8.1)$$

The area covered by each image, when imaged with the same magnification, was assumed equal (cells assumedly in one focus plane). Because the number of images analyzed per sample can vary, average number of cells per image in each sample was used for the calculations instead of total number of cells in the sample. The attachment for each material was calculated according to equations 1-4 in Appendix 3.

Using OnGel samples, also viability of cells on the materials was calculated. This assessment is coherent with more traditional direct contact cytotoxicity testing methods and is useful for cells that are only cultured on top of the hydrogels, not encapsulated in hydrogels (such as corneal and retinal cells). As the main focus in this protocol was to test viability of cells when they are encapsulated inside the hydrogel (3D), viability was also assessed using encapsulated samples. Viability was calculated in the same way for both sample layouts.

The viability of cells in a sample was defined as in Equation 8.2 [56, p. 1388].

$$\text{Viability} = \frac{\text{live cells in sample}}{(\text{live cells} + \text{dead cells}) \text{ in sample}} \quad (8.2)$$

The viability was calculated for each image according to Equations 1-4 in Appendix 3. Finally, the average viability in each material were compared. Especially, viability of cells in different materials is compared with that of the positive 3D control PM, to assess the properties of material in terms of supporting cell viability (i.e. “cell survival”). Standard deviations for viability and attachment were calculated by using (sample) standard deviation formula.

Attachment and viability were assessed for cells on top of 2D, PDMS, PM and GG 1,5 % SPD. Samples were prepared according to the general instructions and parameters shown in (Table 8.5). Similarly, viability was assessed for cells encapsulated in PM and GG hydrogels, and cells on 2D for reference (Table 8.5).

Table 8.5 Sample preparation values and imaging settings of the assessed samples. Attachment and viability was assessed from OnGel samples, and viability was assessed from 3D (encapsulated) samples.

	Attachment and viability	Viability
Sample layout of hydrogels	OnGel	3D
Cells	WI-38 p. 21	WI-38 p. 21-27
Culture time	5 h	48 h
Seeding density	$1.7 \times 10^4 / \text{cm}^2$	600 / μl (gel)
Staining	c_1 , 500 μl / well	c_1 , 500 μl / well
Incubation	1h 20 min, +37 °C	30 - 60 min, +37 °C
Imaging	Custom points, 10x, FL	Custom points, 10x, FL

The (theoretical) volume of both 3D and OnGel hydrogel was 200 μl and samples were made in CELLSTAR[®] 48 plate. The numbers of all parallel samples was 2, and samples were imaged with BioStation CT. At least 3 images (10x magnification) were evaluated for the cytotoxicity analysis per sample.

8.2 Experimental results

The results from experiments are presented in the following subchapters. The parameters that were found the best based on these results, were used to create a set of instructions for the first-step screening of hydrogel cytocompatibility. This protocol is found in Appendix 3, supplemented with Appendices 4-5 for image analysis.

8.2.1 Sample parameters

Cell density of $2.0 - 2.8 \times 10^4$ cells / cm^2 was suitable for seeding WI-38 cells on uncoated well, PDMS, and on top of hydrogels. In these densities it was possible to separate cells from one another for counting, yet cells were presumably densely enough not to suffer. Although, especially at higher densities cells grew on top of each other in the middle of the well. In higher cell densities (4×10^4 cells / cm^2) it was impossible to count cells, because they were overlapping each other.

In encapsulated samples, 600 cells / μl (gel) was a better density than 350 cells / μl (gel) and cells could still be separated from each other. 350 cells / μl (gel) was too low density for effective observation. In fact, even in samples with 600 cells / μl cells were quite scarce. Encapsulating 100 – 200 cells / μl was definitely too low cell density, although in that experiment the whole hydrogel was not visible due to focus range restrictions.

Staining concentration of 0.10 μM EthD-1 and 0.20 μM Ca-AM (double concentration) in PBS together with approximately 40 min incubation time in 37 °C produced the best imaging results. After 20 minutes of incubation in BioStation CT, condensation droplets under the well plate were interfering with imaging, and therefore minimum incubation time was limited already by the equipment. At least the double concentration is recommended, because with single concentration cells were stained unevenly.

In general, the hydrogel samples were difficult to prepare in a way that the thickness would be uniform throughout the sample. Gellan gum samples were thicker on the edges of the sample. PM become uneven easily because of its fragile structure and way of cross-linking by adding culture medium on top of the PM solution. PM samples were slow to prepare and often did not succeed.

8.2.2 Choice of imaging system

Key advantages and disadvantages of BioStation CT, Cell-IQ, and ApoTome system for hydrogel screening purposes are summed in Table 8.6. ApoTome imaging system is more manual than BioStation CT and Cell-IQ systems, as it is possible to image only one x, y coordinate at a time. In BioStation CT and Cell-IQ systems, several imaging coordinates (imaging points) can be set first, after which the system will move the well plate and objective lens to image all set points automatically. In addition, several imaging rounds at separate time points can be taken from the same coordinates, which allows time-lapse imaging with these systems.

Table 8.6 Advantages and disadvantages of tested imaging systems for hydrogel screening purposes.

Equipment	Advantages	Disadvantages
Cell-IQ	Imaging in incubator conditions. Time-lapse imaging, automated	Cells move out of the focus and are hard to find after removing the plate from equipment. Image size is large. Z coordinate not visible when operating.
BioStation CT	Imaging in incubator conditions. Imaging points stable after removing plate out of equipment. Time-lapse imaging, automated	Imaging setting limitations.
ApoTome system	Flexible imaging range and pitch. Less automated. Z stack of fluorescence images is possible.	Not usable with hydrogels in high-throughput because of temperature and humidity issues. Time-lapse imaging not possible. Sample preparation more time-consuming.

However, operating ApoTome system to obtain images at desired Z coordinates was easy. For example, to image a stack of images in one x, y coordinate, starting and ending coordinates in Z axis could be entered numerically. This was faster opposed to Cell-IQ and BioStation, where Z coordinates of imaging points were set by first moving to the desired location in the sample by scrolling. It would be possible to add a motorized stage in the ApoTome system, which would make imaging even faster and more repeatable, when the same coordinates could be images in all replicate samples. Another advantage of ApoTome system was high focusing range. It was possible to image all sample volumes, 145 - 290 μl , fully with the ApoTome upright microscope.

As the aim is to analyze the number of live and dead cells, live cells have to remain live during imaging. Because of that, also temperature, humidity and gas composition are of importance. The disadvantage of ApoTome system was the lack of incubator unit. When imaging hydrogels, it is important to retain the humidity stable. Now samples were removed from culture medium, which caused samples to dry and shrink quickly. This was an unacceptable problem, as with the used experiment setup, the imaging was not fast enough to go through all samples before hydrogels suffered. In addition, the preparation of samples for imaging adds a slow step in the process, comparing to imaging samples in a well plate. Therefore, the system was not usable with hydrogels in high-throughput manner. Another type of sample preparation and preserving arrangements should be made to avoid temperature and humidity issues, in order for this system to be suitable for cytocompatibility screening in the desired scale.

BioStation CT and Cell-IQ systems do have an incubator unit and well plates (or other culture flasks) are imaged below the well plate. Between these two similar imaging systems, BioStation CT was chosen, because of more informed operation (Z coordinate values were visible) and smaller image size. In addition, cells were noticed to move off their earlier imaging points in Cell-IQ after the well plate had been removed from the equipment for medium change. In both systems, the focusing range was too small for 290 μl samples (in Nunc 48 well plates) that they were tested with. This issue was later resolved in BioStation CT, which became the main imaging system in further experiments.

8.2.3 Focusing range and sample volume in BioStation CT

The focusing range of BioStation CT did not cover the whole hydrogel with the initial experimental setup of 290 μl GG samples in Nunc™ 48-well plate (ThermoFisher Scientific). The upper limit (maximum focusing position) was reached before cells on top of the hydrogel were seen.

The problem was related to the moving range and working distance of the objective lens (Figure 8.8). The upper limit, i.e. maximum focusing position when the objective lens was at its uppermost position, was reached at $Z = 4700 \mu\text{m}$ (distance from the holder

surface). The focus position of the inner surface of the well bottom (where cells on uncoated wells were in focus) shall be defined here as the zero level (as it is the reference focusing position to compare different experimental setups). Further, the distance between the zero level and maximum focusing position shall be defined here as effective focusing range (EFR). In order to observe and image a hydrogel sample throughout its thickness, the sample should fit in between maximum focusing position and focusing position of the inner surface of the well bottom, that is, within the EFR.

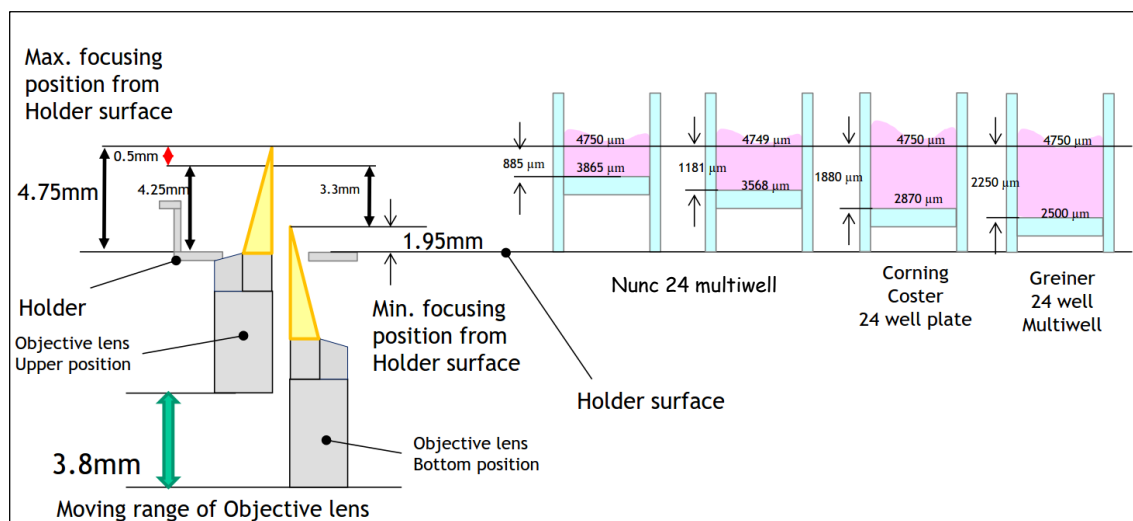


Figure 8.8 Focusing range in BioStation CT, and effective focusing ranges when using well plates from different manufacturers. (Picture: Yasujiro Kiyota, Nikon, reproduced with permission.)

The obstacle of too short effective focusing range was approached with two possible solutions: first, thickness of the samples was decreased, and second, a well plate with lower well bottom was tested. Decreasing sample size to 174 μl or lower in 24 well plate, was not a good solution for imaging full thickness of hydrogel. Smaller hydrogel volumes (145 μl and 174 μl) were difficult to prepare in a 24-well (Nunc) plate in practice, because the gelation requires mixing of the crosslinker and gellan gum solution, and gellan gum gellates rather quickly. Therefore, it was difficult to obtain homogenous samples. Instead, the hydrogels tended to gelate more on the edges of the well and leave the middle of the well nearly or entirely empty. It was impossible to know, if the cells were then attached to a thin hydrogel layer, or rather the plastic well plate bottom. In either case, this made the setup unreliable.

The problem with focusing range in BioStation CT was solved by using Greiner CELLSTAR[®] 48-well plate, in which bottom of the well plate was lower than in Thermo Scientific[™] Nunc[™] multiwall plate - and therefore closer to the objective lens in BioStation CT. Hydrogels with volume of up to 250 μl were entirely visible with CELLSTAR[®] 48 well plate. Even 290 μl hydrogels were partially visible (in the central area of well), but on the edges of the well the hydrogel surface was above the upper limit (Table 8.7). 200

– 250 μl hydrogels were the most successful volumes both from preparation and imaging perspectives.

Table 8.7 Theoretical thickness of hydrogels in CELLSTAR[®] 48 well plate and volumes that were visible in BioStation CT.

Volume (μl)	Theoretical thickness (μm)	Visible
145	1422	Yes
200	1961	Yes
250	2451	Yes
290	2843	Partially

The zero level in CELLSTAR[®] 48 well plate was on average at $Z = 3136.12 \mu\text{m}$, which gives EFR of approximately $1600 \mu\text{m}$ (counted from the upper limit, $4750 \mu\text{m} - 3136.12 \mu\text{m} = 1613.88 \mu\text{m}$). This EFR value was consistent in repeated experiments and between imaging rounds; only small changes were seen due to human effect because of placing the well plate in holder. In Nunc well plates, the EFR (shown in Figure 8.8) was observed to be $885\text{-}1180 \mu\text{m}$ (there were differences between well plates and wells in single well plate). Thus, EFR in CELLSTAR[®] well plate was at least $420 \mu\text{m}$ longer than in Nunc well plates, which was a significant increase in the EFR.

In both CELLSTAR[®] 24- and 48- well plates, the distance between the lower edge of the well plate (frame) and the inner surface of the well is $19 \text{ mm} - 16.5 \text{ mm} = 2.5 \text{ mm}$ ($\pm 0.15 \text{ mm}$) [76], [77] (shown in Figure 8.8). According to Figure 8.8, this should leave a moving range of $4750 \mu\text{m} - 2500 \mu\text{m} = 2250 \mu\text{m}$ above the well surface before upper limit is reached. The EFR, however, does not directly correspond to the moving range of objective lens (as noted, EFR was $1600 \mu\text{m}$ versus $2250 \mu\text{m}$ ($\pm 150 \mu\text{m}$)).

Table 8.8 indicates example volumes of hydrogels and their corresponding thicknesses calculated by the area of well in Nunc and CELLSTAR[®] well plates. ($A(\text{Nunc } 24) = 180 \text{ mm}^2$, $A(\text{Nunc } 48) = 113 \text{ mm}^2$, $A(\text{CELLSTAR}^{\text{®}} 24) = 194 \text{ mm}^2$, $A(\text{CELLSTAR}^{\text{®}} 48) = 102 \text{ mm}^2$.) According to Table 8.8, hydrogels with a volume of $100 \mu\text{l} - 200 \mu\text{l}$ that are prepared in CELLSTAR[®] 48 well plate should theoretically be thin enough to be visible within the effective focus range (EFR) of $2250 \mu\text{m}$. Similarly, only $100 \mu\text{l}$ hydrogels would be visible in Nunc 48 well plate, within EFR of $885 - 1180 \mu\text{m}$.

Table 8.8 Theoretical volumes and corresponding thicknesses of hydrogel samples prepared in Nunc and CELLSTAR® 24 and 48 well plates. Thickness is announced in micrometers.

Volume (μ l)	Nunc well plate		CELLSTAR® well plate	
	24	48	24	48
100	556	884	515	980
145	806	1282	747	1422
200	1111	1768	1031	1961
250	1389	2210	1289	2451
290	1611	2564	1495	2843

From Table 8.7 it is also visible, that theoretical thickness of the hydrogel is not directly corresponding to the thickness that is seen optically in the microscope. Volumes that can be imaged fully, should be calculated according to physical volume (moving distance) above the surface of well plate volume. However, even though thicknesses counted in Table 8.8 are closer to moving range of 2250 μ m, larger volumes were visible than can be estimated based on theoretical thickness.

There are several factors that have to be taken into consideration to estimate the volume of hydrogel that can be imaged. First, real volume of hydrogel may differ from its theoretical volume, i.e. the sum of volumes of its components. This is because of the water containing structure of hydrogels. Second, the surface of the hydrogel can be curved, so that the difference in thickness between middle of the sample and edges can be several hundred micrometers (this was noticed especially in case of gellan gum hydrogels). Third, the working distance of the objective lens, its moving range in the equipment, and finally the diffraction of light in different materials, affect the effective focusing range. The plastic bottom of the well and the water-containing hydrogels diffract light because of different refractive indexes than that of air. This changes the distance that objective has to be moved compared to the distance seen in the sample.

8.2.4 Image acquisition in BioStation CT

Imaging with phase contrast channel at the same position as with fluorescence channels was very beneficial. Phase contrast images provided additional information, and allowed to interpret the fluorescence images from a different view point, if there was any uncertainty, for example, about the health of cells or whether they were inside hydrogels. A round of phase contrast imaging before staining also allowed saving the imaging points. This made imaging faster after staining, especially when custom points were used, and decreased incubation times with the staining solution, which would have been too long otherwise.

Magnification

Cells could be counted from fluorescence images taken with both 4x and 10x magnifications. However, from time to time, in 4x magnification images it was not entirely possible to separate cells from one another accurately, whereas counting cells from 10x images was easier. In addition, with 10x magnification it is easier to avoid overlapping of the areas that are imaged. In 4x images taken with 5 default points, the imaged areas were noticed to partially overlap each other; same cells were visible in the images. Therefore, 10x magnification is recommended.

Coordinates in x,y plane

During experiments cells were noticed to mostly reside in the central area (when cultured on 2D or on hydrogel) due to slight curving of the well bottom and hydrogel surface. In addition, samples in well plates are generally imaged in the middle of the well rather than on the edges for higher image precision, because of light diffracts due to the sides of the well and a slight curving of the well bottom. Only images from the centre of the well (coloured area in Figure 8.9), gave images with high enough precision and enough cells for counting. When images are taken from this area in all samples, results will be comparable, because attachment and viability are counted by comparing average number of cells per image. Images that are taken with 5 default points also locate in this area.

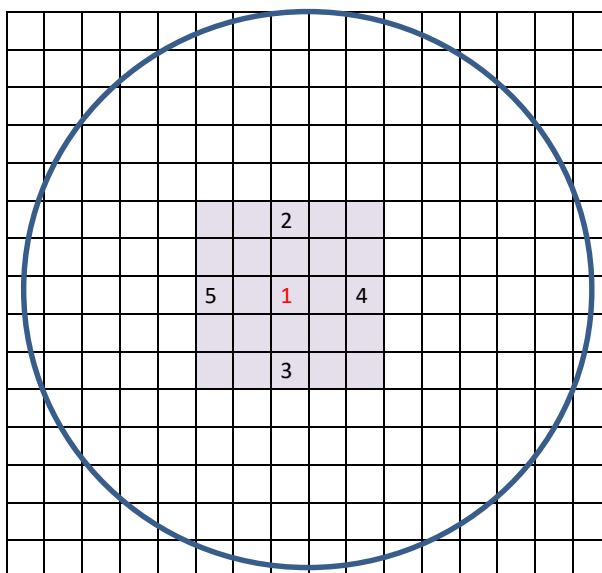


Figure 8.9 Recommended map of imaging points in a well. The colored area corresponds to the area where cells were mostly located. In imaged points outside this area, cells were usually not present, hence images should be acquired from coordinates 1-5, or other points with similar distance from the center of the well (point 1).

Focusing and Z coordinates

Uncoated wells were successfully imaged with 5 default points with automatic focusing, which was a useful setting for these controls. Also tiling images could be taken from these 2D controls with autofocus, to increase the number of images per well. Because autofocus works well with uncoated wells, it is beneficial to use it instead of custom focus, in order to save time in setting the imaging points. Autofocusing with PDMS controls worked well only after changing medium, otherwise unattached cells that were floating in the medium above PDMS shifted the focus level too high. With PDMS it also has to be checked that the autofocusing has not focused on the surface of the well (zero level). On the other hand, custom points were focused correctly, and as the discs were flat, it was not time-consuming to set custom points manually. Therefore, custom points are recommended.

Because of uneven topology of hydrogels, imaging points were set manually (10 custom points) on gellan gum OnGel samples. The Z values of these custom points are shown in Table 8.9. The table shows that surface of the hydrogel samples had a significant topological variation in the range of hundreds of micrometers, especially, but not limited to, rising toward the edges of well.

Table 8.9 Average Z coordinates of 10 imaging points (set according to Figure 8.7) where cells on top of gellan gum hydrogels were in focus (if visible).

Point	145 μl	200 μl	250 μl	290 μl
1	3200	3507	3836	4032
2	3200	3571	3748	4126
3	-	3596	3900	4099
4	3250	4254	3895	4113
5	3750	3815	4148	4345
6	4110	4453	4671	4750
7	3500	3908	4200	4317
8	-	4468	4662	4576
9	3400	3844	4198	4415
10	3890	4403	4683	4658

Schematic illustration of the topology of hydrogels is presented in Figure 8.10. The topological variations of surface were bigger than expected and caused a challenge in imaging, because it was hard to predict the location of the surface of samples. Because of this, setting custom points was very time-consuming, but this allowed to estimate the needed coordinated for encapsulated samples.

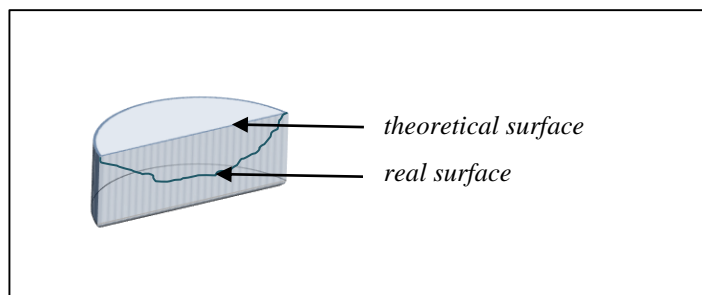


Figure 8.10 Schematic illustration of the shape of a hydrogel sample, cut into half. Hydrogels could be theoretically imagined to form a cylinder shaped sample with flat surface when gellated into a well plate. In reality, the surface of the hydrogels curved down from the edges to the middle of the sample: difference in the thickness was up to several hundred micrometers. In addition, the surface topography was uneven in smaller (micrometer) scale.

Imaging hydrogels with autofocus gave conflicting results. In one experiment where cells on top of (145 μ l) hydrogels were imaged with autofocus, cells were in focus in the resulting images. On the other hand, in another experiment, autofocus focused in the well bottom and no information was retrieved from these images. In addition, the setback with autofocus is that information on the Z coordinate where the cells are imaged is not added to the data of images. Even theoretically, using 5 default points to image OnGel samples is not feasible when samples have large topological variation between the imaging coordinates (distance from the center corresponds to points 1-4 in Table 8.9). That is because the Z coordinates for imaging all 5 points are equal, and defined by autofocusing in the center of the well (point 1).

Similar, conflicting results were obtained for autofocusing in 3D samples. It can be concluded that autofocusing is an unreliable way of setting imaging points in hydrogels, and whether it can be used depends largely on the samples. The more homogenous the sample is, the more likely autofocus will work, because uneven structures of hydrogel that are visible, would not distract the focusing. However, if autofocusing is an option due to homogenous samples, it is recommended to be used, because setting imaging points would be significantly faster.

Because of problems with autofocusing, custom points were mostly used for setting the imaging points in hydrogels. In 3D samples (but not OnGel samples), it was possible to set custom points in one sample and copy them to all replicate samples. However, cells encapsulated in samples were not always distributed in the hydrogel evenly. Therefore, the number of visible cells in each image was not very high. Adding to this, copying imaging coordinates without focusing to certain cells further decreased the amount of cells in focus in images. To obtain enough data for analysis, the number of custom points could be increased. The colored area in Figure 8.9 covers 25 tiles (in 10x magnification), and the maximum number of custom points that can be set per well in BioStation CT is 26.

Another way to increase the number of images obtained from a sample was to image the sample with Full Scan function. Imaging several planes in 3D samples with Full Scan gave successful results. However, because the Full Scan function images all tiles at the same Z coordinate (defined by user of autofocus in the center tile of the well), this function was not convenient for OnGel samples. It must be noted, that only one Z coordinate per sample can be imaged with Full Scan at one time.

Examples of images obtained from 2D, PDMS, GG and PM (OnGel and 3D) samples are presented in Appendix 6. The samples had been prepared according to Table 8.5 and imaged (more specifically) with settings described in Table 8.10.

Table 8.10 Imaging settings that were chosen for attachment and viability assessment setup.

Setting	2D	PDMS	OnGel	3D
Observation points	5 default	custom	custom	custom
Z coordinate	autofocus	custom	custom	custom
Focusing	autofocus	custom	custom	custom
Copying points	automatically set, no need	no	no	yes
Magnification	10x	10x	10x	10x
Channels	Ph, FL	Ph, FL	Ph, FL	Ph, FL

Limitations of BioStation CT

A very big limitation in BioStation CT was that it is impossible to capture a Z stack of fluorescence images. This would have been useful in order to screen through the hydrogel in different depths. Z stacking is only possible with phase contrast channel, but in that case the information on cell viability is not obtained (other than by qualitative evaluation). It is also not possible to register custom points with different Z values to the same x,y coordinate for imaging in one experiment.

Imaging a Full scan of one Z coordinate (custom set) was possible with fluorescent channels, but only one Full scan coordinate could be set per well at a time. Therefore, to image several Z values with Full scan, one needs to image one Z level, then return to the sample to update the Z scan value (by moving to the desired location), and schedule a new imaging for this Z coordinate.

Even more useful than a Full Scan of a level would be a tile of, for example, 4 x 4 images, because not all images in the Full Scan contain useful information (Figure 8.9). Tiling images were possible to obtain after imaging a Full scan. To obtain Tiling image with

custom focus, however, an additional step was needed (choosing a desired tiling to be downloaded from the list of Full Scan images).

In addition, setting custom imaging points by entering coordinates numerically was not possible. This makes setting points slow when many points are set and when there are many samples to screen. Map of the well for planned moving in the operating panel and copying settings makes this a little faster. It must be remembered that copying settings to all parallel samples is an easier option than setting individual options, and it randomized the points, although in that case cells will not be in focus in all images.

8.2.5 Image analysis

The macro for opening images and converting to RGB was very helpful. The macro allows processing images faster, and can be used before counting cells manually. If algorithms are used in FiJi to process images, recording or writing macros is recommended for achieving more high-throughput protocol.

Step for separating cells (watershed) in Particle count algorithm was not used in the calculation of cells. Watershed function separates areas that should be counted as individual particles. Using Watershed function makes a 1 px line between these areas based on a narrower area between them. This function is beneficial in samples where many cells are close to each other. However, when cells were longitudinal, individual cells were cut to smaller pieces, because the outline of their morphology was not simply convex. This resulted in cell numbers increasing falsely.

Table 8.11 presents total numbers of green and red cells counted manually and automatically by Particle Count algorithm in FiJi software with two threshold ranges. When counting cells manually, it was seen that approximately half of the cells that were stained red were also stained with green (double stained), and therefore, the number of double stained cells were counted as well. (In Table 8.11, double stained cells are counted as red, green and double stained.) Based on the high intensities of red and green, and dotted appearance of green in the same location, these cells were identified as dead cells. The green in these cells can be described as “false green”. Thus, the number of double stained cells was subtracted from the number of green cells to obtain the number of live cells.

Table 8.11 Total numbers of green and red cells counted manually and by Particle Count algorithm (two threshold ranges). Double stained cells were counted manually. Threshold 1: red and green 100-255, threshold 2: red 100-255, green 130-255. Number of analyzed images was $n = 15$ for 2D and $n = 20$ for 3D (encapsulated) samples.

Approach	Sample layout	Red	Green	Double stained	Dead	Live
Manual	2D	40	839	18	40	821
	3D	47	71	32	47	39
Particle count Threshold 1	2D	38	674	-	38	674
	3D	44	84	-	44	84
Particle count Threshold 2	2D	38	692	-	38	692
	3D	44	57	-	44	57

Error of the total number of green, red, live and dead cells obtained by different automatic counting methods was calculated comparing to manual counting (Table 8.12). In both sample types, Particle Count algorithm produced a small error (5 - 6 %) in number of red cells. The error was slightly higher in number of green cells (18 - 20 %). Because of double staining, the error became large after the interpretation to live and dead cells. The error was especially large in 3D sample calculated with threshold values 100 - 255 for both channels. Rising the threshold of green channel to 130 - 255, which was the estimated threshold range for green channel, decreased the error. This shows that some double stained cells were filtered out (84 cells versus 57 cells). However, the error was still 46% with this thresholding.

Table 8.12 Error in numbers of cells counted by algorithm compared to manual counting. Threshold 1: red and green 100-255, threshold 2: red 100-255, green 130-255.

Approach	Sample layout	Error Red (%)	Error Green (%)	Error Dead (%)	Error Live (%)
Particle count Threshold 1	2D	5 %	20 %	5 %	18 %
	3D	6 %	18 %	6 %	115 %
Particle count Threshold 2	2D	5 %	18 %	5 %	16 %
	3D	6 %	20 %	6 %	46 %

The error in counting green cells could be decreased with adjusting the used values of algorithm or other, additional image processing steps. It can be also concluded, that an algorithm to count double stained areas would be needed to complement the Particle Count algorithm.

It must be noted, however, that if the cells are cultured on 2D and have spread morphology, a situation presented in (Figure 8.11) has to be taken into account. In the figure dead fibroblasts have nuclei stained red and the cytosol around it stained green, although with a smaller intensity and uneven color. Simply counting areas that are stained with both stains would not recognize these areas as double stained, because green and red areas do not overlap. It is unusual to see such extreme case of double staining as in Figure 8.11, but should be considered as a limitation. A more expected staining result is clearly either green or red cells.

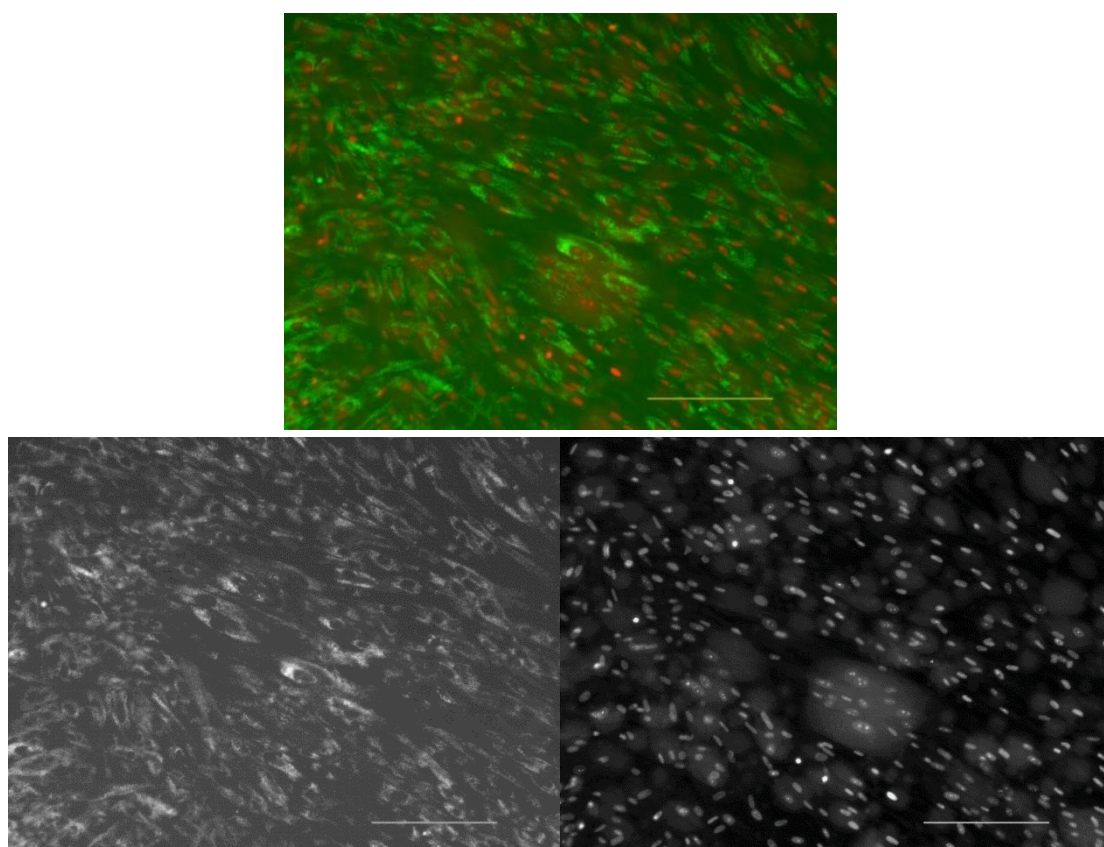


Figure 8.11 Above: RGB image of dead or damaged hFF cells. Red areas are nuclei and dotted, non-uniform green areas around the nuclei are the cytosols of cells. Below: Separate channels of the same image. It is evident from green channel (left) that there are gaps exactly in those locations where nuclei are seen in the red channel (right). Scale bar = 200 μ m.

Another setback of the algorithm was that the volume that is possible to be observed in hydrogel decreases with this method, as cells off the focus plane were filtered out. The extent of this happening depends on how the threshold values. A difficulty in counting cells automatically with Particle Count algorithm is finding the correct threshold values. Especially, determining values to filter out “false green” was challenging, because the green intensities of these cells were close to that of live cells. The threshold cannot be raised too much, because live cells that are slightly off focus but still visible (countable),

have lower intensity as well. In addition, the hydrogels were autofluorescent (in green). The thicker the hydrogel is between the objective lens and cells, the more the hydrogel will decrease the intensity that is observed from the cells. Therefore, the needed threshold values can differ between images.

8.2.6 Assessment of attachment and viability

Attachment and survival of cells on top of control materials and gellan gum are presented in Figure 8.12. Attachment of cells on different materials was compared to 2D, which had a comparison value 1. Attachment on GG 1.5% SPD was significantly greater than on PM and 2D. Even though viability was high on PDSM, attachment on PDMS was low, as expected. Both attachment and viability of cells on top of PM were higher on than on uncoated well plate and PDMS.

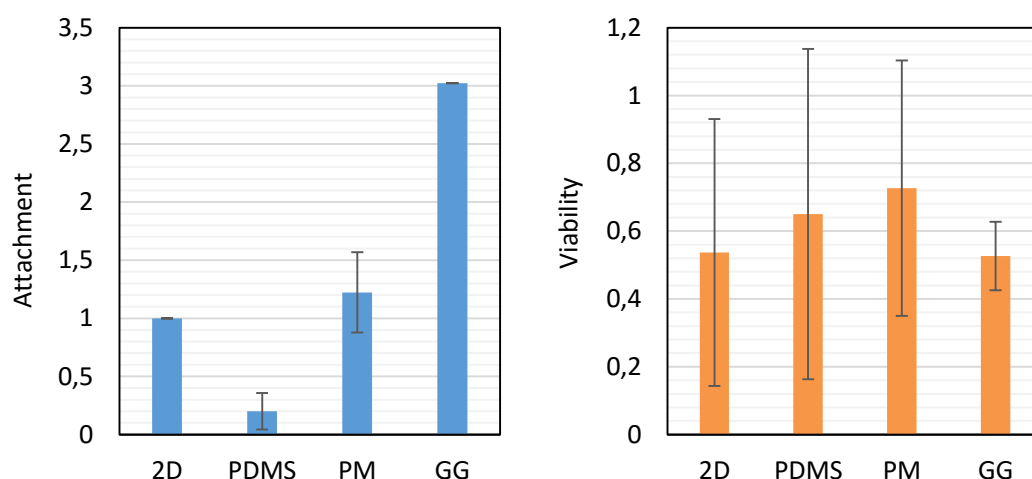


Figure 8.12 Attachment and viability of WI-38 cells on top of control materials and gellan gum. Error bars denote standard deviation. Number of analyzed images was n (2D, PDMS, PM) = 8, n (GG) = 5.

According to the assessed 3D samples, viability of cells encapsulated in PM was lower than in GG (Figure 8.13). Viability was also lower in PM than on 2D (but not necessarily statistically different). Although, the environment of cells on 2D is different than inside hydrogels, and therefore 2D can only be compared as a reference.

It is noteworthy, that standard variation in these results was very high, especially in case of viability assessment on OnGel samples. Possibly bigger number of images per sample would make the results more reliable. In addition, it can be concluded that PuraMatrix® can be used as a positive control for attachment and viability. Using PDMS as a negative control of viability on top of materials is questionable, because viability was higher than on 2D uncoated well.

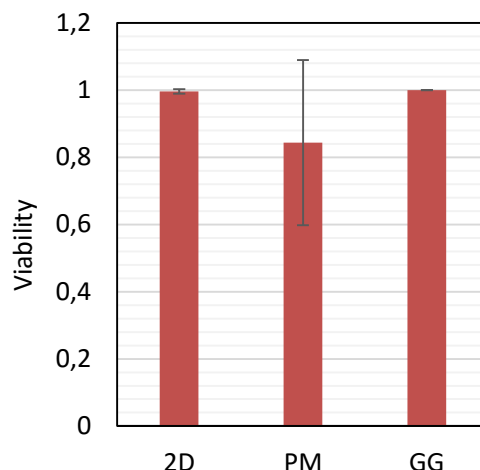


Figure 8.13 Viability of WI-38 cells encapsulated in PuraMatrix® (PM) and gellan gum (GG). 2D sample is shown as a reference. Number of analyzed images was n (2D and GG) = 6 and n (PM) = 9.

Because of different layouts, viability of cells on top (Figure 8.12) and encapsulated in hydrogels (Figure 8.13) cannot be directly compared. In addition, viability of cells on samples was analyzed 5 hours after sample preparation, while viability of cells encapsulated in samples was analyzed after 2 days. However, 2D samples can be compared between these two experiments, and it seems that cell viability after a few hours of culturing was nearly half of viability after 2 days. Also fluorescence images (Appendix 6) reveal that cells look healthier on 2D after longer culture time.

8.2.7 Cell behavior

Phase contrast images from 2D positive control showed that cells had a longitudinally spread out morphology before staining with Live/dead viability/toxicity kit. In images after staining, cells had retracted from this spread morphology and become more round. The retraction of cells increased over time, which was seen in three rounds of images taken with 70 min interval from the same location (two rounds after staining shown in Figure 8.14). Incubation time with Live/dead staining solution was 40 min and double concentration was used (0.10 μM EthD-1 and 0.20 μM Ca-AM solution).

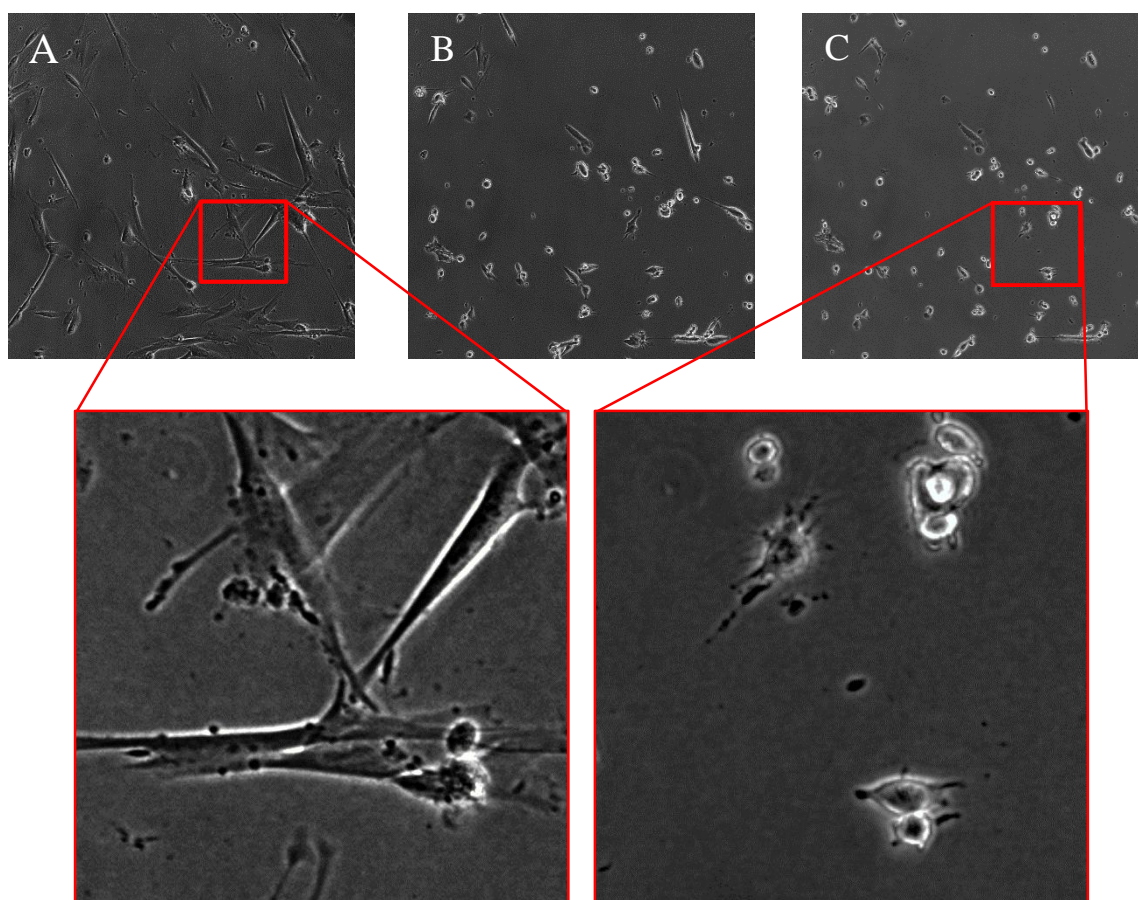


Figure 8.14 Phase contrast images of WI-38 cells on uncoated well. Same cells were imaged before staining (A), after staining (B) and 70 minutes later (C). Images were taken with 10x magnification (upper row; close-up in lower row).

This retraction of cells from their spread-out morphology was an interesting observation. Live/dead assay is an end-point analysis method, because the cells will eventually die after staining. However, cells should not die this fast, because the method detects cell viability and the incubation time was only 40 minutes. Staining with Live/dead kit was not used for morphological observations in this protocol, but spread out morphology indicates cell attachment to material [41]. Attachment, in turn, is generally considered a parameter for testing biocompatibility.

9. DISCUSSION AND FUTURE RECOMMENDATIONS

Several standards cover cytotoxicity and biocompatibility testing of materials or characterization of hydrogels for use in biomedical applications. These standards, which were introduced in this thesis, offer a good knowledge base for testing cytocompatibility of hydrogels. However, most standards describe the methods only in a general level, and methods used in the literature are varying. This thesis aimed to provide detailed instructions for first-step cytocompatibility screening of hydrogels by using one of the available methods, namely Live/dead staining and imaging. This method was chosen because it is easy, inexpensive and fast, and hydrogels do not have to be destructed for the analysis. Unlike in standards ISO 10993-5 [14] and ASTM F813 [33], cells were cultured on and encapsulated in hydrogels instead of under the test specimen. This layout represents better the final application of hydrogels as a cell culture substrate. In addition, reasoning for choosing a representable cell line for each step of the protocol was provided, so that the protocol could be used to test hydrogels specifically for different cell types.

For the first-step cytocompatibility screening protocol, a human fibroblast cell line WI-38 was chosen, which is a natural, finite cell line with a long life time. Variation occurs to some extent always when biological substances are used in experiments, but this can be minimized by using cell lines. Even though especially immortalized cell lines offer reproducible cell culture models, choosing a finite cell line is beneficial in biomaterial research because transformation of cells can cause alterations in growth characteristics, such as loss of anchorage dependence and contact inhibition [6].

In addition, using a human cell line was beneficial for two reasons. First, human fibroblasts have been found stabile [6], and second, the interviewed research groups of Bio-MediTech institute study human cells in their final applications. Therefore, more representable results can be obtained by using human cells from the first step on. Animal cells can be used in basic research, but results in their behaviour cannot be directly applied to human cells, and animal cells cannot be used in further clinical applications [78, p. 641].

WI-38 cells did not spread when cultured on top or encapsulated in hydrogels. It must be remembered, however, that the morphology cells have when growing on a 2D surface, is most likely not what should be expected from morphology of a cell in 3D. In general, in 3D environment human fibroblasts are spindle-shaped opposed to having flat morphology [60], and more natural morphology and behaviour is the aim with using 3D cell culture substrates.

The results in this experience showed round cells, and not yet even spindle-shaped cells. The culture time was quite short in this protocol, and in future experiment it is advised to increase the culture time. In addition, less elongated morphology and slower proliferation of cells grown in hydrogels compared to 2D has been previously shown [56], [60]. This is understandable, because the cells need to overcome impediments caused by the surrounding hydrogel, which acts as a physical barrier. Several properties of hydrogels, such as stiffness and presence of biological cues, affect the morphology and proliferation of cells in hydrogels. [7] More alarming behaviour was seen on 2D, where cells became round after staining, and the reason for that is unclear.

By culturing cells on top of hydrogels for few hours, attachment was primarily tested. At the same time, it was possible to calculate viability of cells on hydrogels as well. As discussed earlier (Chapters 6 and 7), attachment is analyzed after a short culture time, but for viability testing a longer culture time is usually needed. Therefore, it is not surprising that cells looked healthier and showed higher viability on 2D after longer culture time (48 h). This comparison shows that if cell viability is analyzed on top of hydrogels, 5h culture time is most likely too short to reliably assess viability of cells, and instead similar culture time has to be used as with cells encapsulated in hydrogels.

In addition, cells were often unevenly stained or cells had stained with both calcein and EthD-1. This made interpreting results difficult. Thus, the staining conditions with Live/dead cytotoxicity/viability kit should be further optimized. Another possible reason for the unclear appearance of cells may be in too low seeding density. Seeding densities under the recommended minimum of 2×10^4 cells / cm^2 was used in some experiments, because cells are difficult to count in higher densities. If higher seeding densities will be used in the future, it is recommended to stain the nuclei of cells with DAPI simultaneously with calcein-AM and EthD-1.

In future experiments, also other fluorometric or colorimetric analysing methods for viability, could be tried, which allow reading with a microplate. This might be a faster approach for screening. The reagent should not cause too high background reading with hydrogels. It should be noted that many colorimetric and fluorometric assays are destructive, meaning that the hydrogel has to be broken down for analysis. In addition, these methods usually require a standard curve, and existing data on interpreting result are optimized for 2D cultures [9].

In the chosen analysis method for this protocol, imaging and image analysis were the challenges related to adjusting analysis methods from 2D to 3D culture. Due to the nature of the samples, encapsulated cells were located at different depths in 3D samples, as expected. Because of this, only few cells were in focus at one time. This was also true in case of OnGel samples because of large topological variation. Cells were also unevenly

distributed in the hydrogels leaving some areas emptier. Because of these reasons, information retrieved from a single image was usually small.

In addition, even though BioStation CT was the more suitable for imaging hydrogels than ApoTome and Cell-IQ, it had many limitations in imaging options and increasing the number of images taken per sample may be time-consuming. On the other hand, the results of attachment and viability assessment had large standard variations and to improve the reliability and statistical significance of the results, it is suggested that the number of images taken per sample would be as high as feasible. Because of several aspects that were optimized during development of this protocol, the number of repeated testing was low with the final experimental parameters and settings. Further repeated studies are therefore needed as well.

The more automated analysis algorithms are found for analysing images and counting cells, the faster and more efficient the screening protocol will be. Therefore, the current algorithm presented in this thesis, could be further improved. In addition, there are number of other software aside FiJi that could be used for image analysis. For example, CL-Quant is a software produced by Nikon, which is especially designed to analyse images taken with BioStation CT. It is based on machine learning, and therefore it can be taught which cells should be counted. FiJi was chosen over CL-Quant in this thesis because FiJi is a commonly used open source software.

Another reason to analyse images with FiJi is that objective parameters for counting cells (based on size and intensity) can be given in FiJi. For example, teaching a machine learning based program to count encapsulated cells in hydrogel would require choosing cells subjectively in different depths. In FiJi, on the other hand, the same values can be used to all images. However, the more cells are processed with a machine learning program, the more accurate the recognizing and counting becomes. Since FiJi needed much work to find correct steps and values, and writing macros for counting cells, the amount of work to create an accurate counting algorithm in CL-Quant may not exceed the effort of creating an algorithm in FiJi. In addition, because CL-Quant is a program designed especially for BioStation CT images, even observing images (in RGB and different points) may be easier. Therefore, it is worthwhile to consider using CL-Quant instead of FiJi.

A negative control could be further searched for. PDMS was a successful negative control only for attachment. As a non-cytotoxic material, it does not cause a decrease in viability. In addition, because cells cannot be encapsulated inside PDMS, and therefore the control would not be similar to test samples, it was not used as a control in case of testing viability inside hydrogels. PuraMatrix[®] showed good results in viability and attachment, as expected. However, PuraMatrix[®] was difficult to handle and hydrogels were very inhomogeneous in thickness throughout the sample. Therefore, finding a better 3D positive control could also be considered.

The protocol presented as a result of this thesis has been already used in hydrogel cytocompatibility screening in BioMediTech (Tampere University of Technology). In future experiments, optimizing the cytocompatibility screening protocol should be continued with other parts suggested in Figure 8.1 (parts 1 C-D, 2 and 3). These include studies with more specific cells of each cell type (cells suggested in Table 7.2) and optimizing testing of proliferation and morphology of cells, and function of more specific cells.

10. CONCLUSIONS

Based on literature and interview, a three-phase cytocompatibility testing protocol was proposed, starting with a general cell line and ending with the intended cell type for the final application of the tested hydrogel. Most interviewed research groups shared at least requirements of using a human cell line and testing of viability of cells for the cytocompatibility screening of hydrogels. Attachment and viability screening with a general, fibroblast cell line, was optimized in practice. The final protocol, i.e. instructions for attachment and viability screening, is presented in Appendix 3.

A commercial human embryonic fibroblast cell line WI-38 was cultured on the surface and encapsulated in 3D macroscopic hydrogels. This finite cell line filled the set criteria in theory, but based in these experiments it is unclear whether the stability of WI-38 cells was sufficient for this protocol. Cell density, culture time, and staining concentrations should be further optimized for WI-38 cells.

Nikon BioStation CT proved to be the most suitable imaging system between the tested systems and imaging settings were found for attachment and viability testing. However, because BioStation CT had several limitations, it was not an optimal imaging system for screening three-dimensional hydrogels. Thus, it is suggested to continue the search for optimal imaging system. Maximum focusing range was achieved by using Greiner Bio-one CELLSTAR[®] 48-well plate, which has a lower bottom than multiwall plates of some other manufacturers. Hydrogels with volume of up to 250 μ l were entirely visible with this well plate, corresponding to effective working distance of 1600 μ m.

Several algorithms and parameter values were tested in FiJi software for counting cells. A macro was written for one part of the image analysis, which made the analysis more efficient. However, with the used parameter values, Particle Count algorithm was not accurate enough to count live and dead cell from fluorescence images. Cells were counted manually for assessing attachment and viability of cells on hydrogels and viability of cells encapsulated inside hydrogels.

As expected, PuraMatrix[®] and gellan gum were cytocompatible. Attachment and viability of cells on top of PuraMatrix[®] and gellan gum were better than on 2D. Viability of cells inside hydrogels did not significantly differ from 2D. Attachment of cells on PDMS was significantly smaller, as expected, but PDMS could not be used as a negative control in viability testing.

REFERENCES

- [1] A. S. Hoffman, "Hydrogels for Biomedical Applications," *Ann. N. Y. Acad. Sci.*, vol. 944, pp. 62–73, 2001.
- [2] A. Patel and K. Mequanint, "Hydrogel Biomaterials," in *Biomedical Engineering - Frontiers and Challenges*, R. Fazel, Ed. InTech, 2011, pp. 275 – 296.
- [3] "Standard Guide for Characterization of Hydrogels used in Regenerative Medicine." American Society for Testing and Materials (ASTM), F2900 – 11, West Conshohocken, p. 10, 2011.
- [4] W. P. Alberts B., Bray D., Hopkin K., Johnson A., Lewis J., Raff M., Roberts K., *Essential Cell Biology*, 3rd ed. Garland Science, Taylor & Francis Group, 2010.
- [5] K. C. Haug, E., Sand, O., Sjaastad, Ø. & Toverud, *Ihmisen fysiologia*, 1st ed. Porvoo: WSOY, 1995.
- [6] R. I. Freshney, *Culture of animal cells; A manual of basic technique*, 5th ed. New Jersey: John Wiley & Sons, 2005.
- [7] K. Bott, Z. Upton, K. Schrobback, M. Ehrbar, J. A. Hubbell, M. P. Lutolf, and S. C. Rizzi, "The effect of matrix characteristics on fibroblast proliferation in 3D gels," *Biomaterials*, vol. 31, no. 32, pp. 8454–8464, 2010.
- [8] A. Liedmann, A. Rolfs, and M. J. Frech, "Cultivation of human neural progenitor cells in a 3-dimensional self-assembling peptide hydrogel," *J. Vis. Exp.*, no. 59, p. e3830, Jan. 2012.
- [9] "Standard Guide for Quantitating Cell Viability Within Biomaterial Scaffolds." American Society for Testing and Materials (ASTM), F2739 - 08, West Conshohocken, p. 6, 2008.
- [10] M. Vert, Y. Doi, K.-H. Hellwich, M. Hess, P. Hodge, P. Kubisa, M. Rinaudo, and F. Schué, "Terminology for biorelated polymers and applications (IUPAC Recommendations 2012)," *Pure Appl. Chem.*, vol. 84, no. 2, pp. 377–410, 2012.
- [11] "Biological Evaluation of medical devices. Part 1: Evaluation and testing within a risk management process." Finnish Standards Association, SFS-EN ISO 10993-1, Helsinki, p. 21, 2009.
- [12] D. F. Williams, *Definitions in biomaterials*. Amsterdam: Elsevier, 1987.
- [13] D. F. Williams, "On the mechanisms of biocompatibility," *Biomaterials*, vol. 29, no. 20, pp. 2941–2953, 2008.
- [14] "Biological Evaluation of Medical Devices. Part 5: Tests for In Vitro Cytotoxicity." Finnish Standards Association, SFS-EN ISO 10993-5, Helsinki, p. 34, 2009.
- [15] H. Li, J. Yang, X. Hu, J. Liang, Y. Fan, and X. Zhang, "Superabsorbent polysaccharide hydrogels based on pullulan derivate as antibacterial release wound dressing," *J. Biomed. Mater. Res. - Part A*, vol. 98 A, no. 1, pp. 31–39, 2011.
- [16] F. Brandl, F. Sommer, and A. Goepferich, "Rational design of hydrogels for tissue engineering: Impact of physical factors on cell behavior," *Biomaterials*, vol. 28, no. 2, pp. 134–146, 2007.
- [17] Thermo Fisher Scientific, "Gibco® Cell Culture Basics," 2014. [Online]. Available: <http://www.lifetechnologies.com/fi/en/home/references/gibco-cell->

- culture-basics.html. [Accessed: 15-Jul-2014].
- [18] “WHO | Vaccine Procurement.” [Online]. Available: http://www.who.int/immunization/programmes_systems/procurement/en/. [Accessed: 26-Feb-2015].
- [19] S. P. Langdon, “Mammalian cell culture,” in *Molecular Biotechnology Handbook*, 2nd ed., R. Walker, J. M. and Rapley, Ed. Totowa, NJ: Humana Press, 2008, pp. 861 – 873.
- [20] American Type Culture Collection, “ATCC® ANIMAL CELL CULTURE GUIDE - tips and techniques for continuous cell lines,” 2014. [Online]. Available: <http://www.lgcstandards-atcc.org/en/Guides/Guides.aspx>. [Accessed: 17-Nov-2014].
- [21] ATCC, “ATCC: The Global Bioresource Center,” 2014. [Online]. Available: www.atcc.org. [Accessed: 10-Oct-2015].
- [22] RIKEN, “RIKEN BioResource Center.” [Online]. Available: <http://en.brc.riken.jp/>. [Accessed: 10-Oct-2015].
- [23] DSMZ, “Leibniz-Institut DMSZ-German Collection of Microorganisms and Cell Cultures.” [Online]. Available: <https://www.dsmz.de/>. [Accessed: 10-Oct-2015].
- [24] Public Health England, “European Collection of Authenticated Cell Cultures (ECACC).” [Online]. Available: <https://www.phe-culturecollections.org.uk/collections/ecacc.aspx>. [Accessed: 10-Oct-2015].
- [25] T. Tallheden, “Cell culture: harvest, selection, expansion, and differentiation,” in *Tissue Engineering*, C. Van Blitterswijk, Ed. Academic Press, 2008, p. 740.
- [26] L. Hayflick and P. S. Moorhead, “The serial cultivation of human diploid cell strains,” *Exp. Cell Res.*, vol. 25, no. 3, pp. 585–621, Dec. 1961.
- [27] K. Takahashi and S. Yamanaka, “Induction of Pluripotent Stem Cells from Mouse Embryonic and Adult Fibroblast Cultures by Defined Factors,” *Cell*, vol. 126, no. 4, pp. 663–676, 2006.
- [28] C. Wang, “Stem Cells,” *AccessScience*, 2012. [Online]. Available: <http://www.accessscience.com/content/Neural-stem-cells/800100#800100FG0010>. [Accessed: 18-Jul-2015].
- [29] R. S. Lappalainen, M. Salomäki, L. Ylä-Outinen, T. J. Heikkilä, H. Pihlajamäki, R. Suuronen, H. Skottman, and S. Narkilahti, “Similarly derived and cultured hESC lines show variation in their developmental potential towards neuronal cells in long-term culture Research Article,” *Regen. Med.*, vol. 5, no. 5, pp. 749–762, 2010.
- [30] J. Jukes, S. Both, J. Post, C. Van Blitterswijk, M. Karperien, and J. De Boer, “Stem cells,” in *Tissue Engineering*, C. Van Blitterswijk, Ed. Academic Press, 2008, p. 740.
- [31] F. Katagiri, M. Sudo, T. Hamakubo, K. Hozumi, M. Nomizu, and Y. Kikkawa, “Identification of active sequences in the L4a domain of laminin $\alpha 5$ promoting neurite elongation,” *Biochemistry*, vol. 51, no. 24, pp. 4950–4958, 2012.
- [32] ATCC, “Vero (ATCC CCL-81).” [Online]. Available: <http://www.lgcstandards-atcc.org/Products/All/CCL-81.aspx>. [Accessed: 06-Nov-2014].
- [33] “Practice for Direct Contact Cell Culture Evaluation of Materials for Medical

- Devices.” American Society for Testing and Materials (ASTM), F813 - 07, West Conshohocken, p. 5, 2012.
- [34] “Standard Test Method for Agar Diffusion Cell Culture Screening for Cytotoxicity.” American Society for Testing and Materials (ASTM), F895 - 11, West Conshohocken, p. 5, 2011.
- [35] ATCC, “NCTC clone 929 [L cell, L-929, derivative of Strain L] (ATCC CCL-1).” [Online]. Available: <http://www.lgcstandards-atcc.org/products/all/CCL-1.aspx#characteristics>. [Accessed: 27-Oct-2014].
- [36] ATCC, “WI-38 ATCC ® CCL-75™.” [Online]. Available: <http://www.lgcstandards-atcc.org/Products/All/CCL-75.aspx>. [Accessed: 06-Nov-2014].
- [37] ATCC, “MRC-5 ATCC ® CCL-171™.” [Online]. Available: <http://www.lgcstandards-atcc.org/Products/All/CCL-171.aspx>. [Accessed: 06-Nov-2014].
- [38] Public Health England, “General Cell Collection: WI 38.” [Online]. Available: http://www.phe-culturecollections.org.uk/products/celllines/generalcell/detail.jsp?refId=90020107&collection=ecacc_gc.
- [39] M. Amit, V. Margulets, H. Segev, K. Shariki, I. Laevsky, R. Coleman, and J. Itskovitz-Eldor, “Human Feeder Layers for Human Embryonic Stem Cells,” *Biol. Reprod.*, vol. 68, no. 6, pp. 2150–2156, 2003.
- [40] O. Hovatta, M. Mikkola, K. Gertow, A. M. Strömberg, J. Inzunza, J. Hreinsson, B. Rozell, E. Blennow, M. Andäng, and L. Ährlund-Richter, “A culture system using human foreskin fibroblasts as feeder cells allows production of human embryonic stem cells,” *Hum. Reprod.*, vol. 18, no. 7, pp. 1404–1409, 2003.
- [41] D. H. Nguyen, N. Q. Tran, and C. K. Nguyen, “Tetronic-grafted chitosan hydrogel as an injectable and biocompatible scaffold for biomedical applications.,” *J. Biomater. Sci. Polym. Ed.*, vol. 24, no. 14, pp. 1636–48, Jan. 2013.
- [42] M. Mori, P. V Almeida, M. Cola, G. Anselmi, E. Mäkilä, A. Correia, J. Salonen, J. Hirvonen, C. Caramella, and H. a Santos, “In vitro assessment of biopolymer-modified porous silicon microparticles for wound healing applications.,” *Eur. J. Pharm. Biopharm.*, vol. 88, no. 3, pp. 635–42, Nov. 2014.
- [43] ATCC, “CCD-1112Sk (ATCC® CRL-2429™),” 2014. .
- [44] B. Zavan, R. Cortivo, and G. Abatangelo, “Hydrogels and Tissue Engineering,” in *Hydrogels: Biological Properties and Applications*, R. Barbucci, Ed. Milan: Springer-Verlag, 2009, pp. 1–8.
- [45] L. Gasperini, J. F. Mano, and R. L. Reis, “Natural polymers for the microencapsulation of cells,” *J. R. Soc. Interface*, vol. 11, no. 100, pp. 1 – 19, 2014.
- [46] 3D Matrix Medical Technology, “PuraMatrix,” 2104. [Online]. Available: <http://www.puramatrix.com/puramatrix.html>. [Accessed: 10-Oct-2015].
- [47] 3D Matrix Medical Technology, “PuraMatrix,” 2104. .
- [48] L. Ylä-Outinen, T. Joki, M. Varjola, H. Skottman, and S. Narkilahti, “Three-dimensional growth matrix for human embryonic stem cell-derived neuronal cells,” *J. Tissue Eng. Regen. Med.*, vol. 8, no. 3, pp. 186–194, 2014.

- [49] Q. G. Wang, N. Hughes, S. H. Cartmell, and N. J. Kuiper, “The composition of hydrogels for cartilage tissue engineering can influence glycosaminoglycan profiles,” *Eur. Cells Mater.*, vol. 19, pp. 86–95, 2010.
- [50] C. J. Ferris, K. J. Gilmore, G. G. Wallace, and M. in het Panhuis, “Modified gellan gum hydrogels for tissue engineering applications,” *Soft Matter*, vol. 9, no. 14, pp. 3705–3711, 2013.
- [51] A. M. Smith, R. M. Shelton, Y. Perrie, and J. J. Harris, “An initial evaluation of gellan gum as a material for tissue engineering applications,” *J. Biomater. Appl.*, vol. 22, no. 3, pp. 241–254, 2007.
- [52] R. López-Cebral, P. Paolicelli, V. Romero-Caamaño, B. Seijo, M. A. Casadei, and A. Sanchez, “Spermidine-cross-linked hydrogels as novel potential platforms for pharmaceutical applications,” *J. Pharm. Sci.*, vol. 102, no. 8, pp. 2632–2643, 2013.
- [53] T. L. Riss, R. A. Moravec, A. L. Niles, T. J. Worzella, and L. Minor, “Cell Viability Assays,” In: *Sittampalam GS, Coussens NP, Nelson H, et al., editors. Assay Guidance Manual*, 2013. [Online]. Available: <http://www.ncbi.nlm.nih.gov/books/NBK144065/>.
- [54] American Type Culture Collection, “MTT Cell Proliferation Assay Instruction Guide.” pp. 1–6, 2011.
- [55] Molecular Probes, “LIVE/DEAD ® Viability/Cytotoxicity Kit for mammalian cells.” 2005.
- [56] J. H. Sung and M. L. Shuler, “A micro cell culture analog (microCCA) with 3-D hydrogel culture of multiple cell lines to assess metabolism-dependent cytotoxicity of anti-cancer drugs,” *Lab Chip*, vol. 9, no. 10, pp. 1385–1394, 2009.
- [57] ThermoFisher Scientific, “Calcein, AM, cell-permeant dye,” 2015. [Online]. Available: <https://www.thermofisher.com/order/catalog/product/C3100MP>. [Accessed: 15-Feb-2016].
- [58] ThermoFisher Scientific, “Ethidium Homodimer-1 (EthD-1),” 2015. [Online]. Available: <https://www.thermofisher.com/order/catalog/product/E1169>.
- [59] Roche, “Cell Proliferation ELISA , BrdU (colorimetric).” Roche, 2013.
- [60] E. Cukierman, R. Pankov, D. R. Stevens, and K. M. Yamada, “Taking cell-matrix adhesions to the third dimension,” *Science (80-.)*, vol. 294, no. 5547, pp. 1708–1712, 2001.
- [61] C. P. Pennisi, V. Zachar, L. Gurevich, A. P. Member, and J. J. Struijk, “The Influence of Surface Properties of Plasma-Etched Polydimethylsiloxane (PDMS) on Cell Growth and Morphology,” in *32nd Annual International Conference of the IEEE EMBS*, 2010, pp. 3804–3807.
- [62] H. Chen, Y. Liu, Z. Jiang, W. Chen, Y. Yu, and Q. Hu, “Cell-scaffold interaction within engineered tissue,” *Exp. Cell Res.*, vol. 323, no. 2, pp. 346–351, 2014.
- [63] American Type Culture Collection, “SH-SY5Y (ATCC® CRL-2266™),” 2014. [Online]. Available: http://www.lgestandards-atcc.org/products/all/CRL-2266.aspx?geo_country=fi. [Accessed: 03-May-2016].
- [64] AurnA Biomedical, “hNP1 Human Neural Progenitor Expansion Kit,” 2010. [Online]. Available: <http://www.arunabiomedical.com/index.php?id=26&productid=1>. [Accessed: 16-Apr-2016].

- [65] Cellular Dynamics International, “iCell® Neurons,” 2016. [Online]. Available: <https://cellulardynamics.com/products-services/icell-products/icell-neurons/>. [Accessed: 16-Apr-2016].
- [66] RIKEN BioResource Center, “RCB2280: HCE-T.” [Online]. Available: http://www2.brc.riken.jp/lab/cell/detail.cgi?cell_no=RCB2280&type=1. [Accessed: 03-May-2016].
- [67] ATCC, “ARPE-19 (ATCC® CRL-2302™),” 2014. [Online]. Available: http://www.lgcstandards-atcc.org/products/all/CRL-2302.aspx?geo_country=fi. [Accessed: 03-May-2016].
- [68] ATCC, “Saos-2 (ATCC® HTB-85™),” 2014. [Online]. Available: http://www.lgcstandards-atcc.org/products/all/HTB-85.aspx?geo_country=fi. [Accessed: 03-May-2016].
- [69] C. Mummery, A. Feijen, P. T. van der Saag, C. E. van den Brink, and S. W. de Laat, “Clonal variants of differentiated P19 embryonal carcinoma cells exhibit epidermal growth factor receptor kinase activity,” *Dev. Biol.*, vol. 109, no. 2, pp. 402–410, 1985.
- [70] C. Mummery, D. Ward, C. van den Brink, S. Bird, P. Doevendans, T. Opthof, a B. de la Riviere, L. Tertoolen, M. van der Heyden, and M. Pera, “Cardiomyocyte differentiation of mouse and human embryonic stem cells*,” *J. Anat.*, vol. 200, no. 3, pp. 233–242, 2002.
- [71] RIKEN BioResource Center, “RCB1127 : MC3T3-G2/PA6.” [Online]. Available: https://www2.brc.riken.jp/lab/cell/detail.cgi?cell_no=RCB1127. [Accessed: 03-May-2016].
- [72] H.-A. Kodama, Y. Amagai, H. Koyama, and S. Kasai, “Hormonal responsiveness of a preadipose cell line derived from newborn mouse calvaria,” *J. Cell Physiol.*, vol. 112, no. 1, pp. 83–88, 1982.
- [73] J. Schindelin, I. Arganda-Carreras, E. Frise, V. Kaynig, M. Longair, T. Pietzsch, S. Preibisch, C. Rueden, S. Saalfeld, B. Schmid, J.-Y. J.-Y. Tinevez, D. J. White, V. Hartenstein, K. Eliceiri, P. Tomancak, A. Cardona, K. Liceiri, P. Tomancak, and A. Cardona, “Fiji - an open source platform for biological image analysis,” *Nat. Methods*, vol. 9, no. 7, pp. 676–682, 2012.
- [74] J. Schindelin, C. T. Rueden, M. C. Hiner, and K. W. Eliceiri, “The ImageJ ecosystem: An open platform for biomedical image analysis,” *Mol. Reprod. Dev.*, vol. 82, pp. 518–529, 2015.
- [75] A. Kotsar, R. Nieminen, T. Isotalo, J. Mikkonen, I. Uurto, M. Kellomäki, M. Talja, E. Moilanen, and T. L. J. Tammela, “Biocompatibility of new drug-eluting biodegradable urethral stent materials,” *Urology*, vol. 75, no. 1, pp. 229–234, Jan. 2010.
- [76] Greiner Bio-one, “Customer Drawing 24 Well Multiwell Plate CELLSTAR(R).” 2015.
- [77] Greiner Bio-one, “Customer Drawing Cell Culture Multiwell Plate CELLSTAR(R), 48 Well.” 2015.
- [78] P. Dalton, A. Harvey, M. Oudega, and G. Plant, “Tissue Engineering of the nervous system,” in *Tissue Engineering*, C. Van Blitterswijk, Ed. Academic Press, 2008, p. 740.

APPENDICES

Appendix 1: Interview questions

Appendix 2: Interview results

Appendix 3: Protocol for cell attachment and viability testing

Appendix 4: Particle Count algorithm for FiJI

Appendix 5: Macro for opening images and merging channels in FiJI

Appendix 6: Fluorescence images

APPENDIX 1

INTERVIEW QUESTIONS FOR SELECTING A CELL LINE AND ANALYZING METHOD OF CELLS

Generally, a cell line chosen for this protocol should fill the following criteria:

1. commonly used and readily available, not too expensive
2. well characterized and standardized (identity, purity, safety)
3. relatively easy to culture, yet sensitive enough not to grow in an unsatisfactory hydrogel
4. robust, stable; as repeatable growth as possible
5. growth rate high enough so that it can be used in short time screening
6. adherent i.e. anchorage dependent cell line (not growing in solution, such as some hematopoietic, tumor and hybridoma cells).

Cell line vs. used cells, criteria

1. In addition to general criteria, what are other criteria for selecting the cell line relating to origin of the cell (see below)?
 - a. Species: should the cell be human or animal derived / does the species have any significance?
 - b. Age: should the cell be derived from a patient / animal of certain age (embryo / fetal / adult / iPS cell?)
 - c. Would it be better to use a finite or continuous cell line?
 - d. Immortal cells might have a drawback of having other transformations affecting the phenotype. Are transformed cells (for example, cells obtained with human telomerase reverse transcriptase (hTERT) transformation) representative in this case? How about tumor cells?
 - e. According to one source [17] the biggest advantage of using cell culture is the consistency and reproducibility of results that can be obtained from using clonal cells. On the other hand, a cell strain often acquires additional genetic changes subsequent to the initiation of the parent line [17]. Should clones be used?
2. Should the cells be pre-adapted to a certain growth medium or serum-free medium? Should serum be used (batch variation versus cost etc.)? Serum might disturb uniform gelation during gelation time, however after that serum can be present.
3. Which cell should the chosen cell line represent? Which cell line mimics the best cells that you use yourself?
4. Which cell line(s) that meets the above criteria would you recommend for this protocol? Which properties, advantages, and disadvantages it has?

Hydrogels with cells

5. In the future, in which applications you could imagine needing hydrogels in cell culture?
6. How should the cell-hydrogel combination be arranged; cells on top, under or inside the hydrogel?

Cell culturing and analyzing methods

7. Which amount of parallel samples is reliable? Is it enough to test with one cell line only, or should there be several cell lines?
8. What (gel) would you use as a positive and / or negative control?
9. Does the recommended cell line normally need a certain molecule to attach to the substrate (e.g. laminin for neurons)?
10. How long is the shortest possible culturing time in order to observe reactions toward a new material?
11. Which end-point analyzing method would you use? Is there a method you would use already during culturing to observe cells?

APPENDIX 2 (1/3) Interview results

	NEURO	CORNEA	RETINA	HEART	MESENCHYMAL STEM CELL
CELLS					
Species	human	human	human	not significant	human
Age	other than adult (blastoma can be from a child)	if cell line, not significant	if cell line, not significant	not significant	adult ok, young better
Finite / continuous	Continuous line better; if finite, proliferating enough for banking	continuous	continuous	Continuous line better, but they do not beat. Fibroblasts if finite.	continuous
Transformed	yes, as long as negative control found	yes	yes	yes	no
Tumor	yes, as long as negative control found	no	no	-	yes
Clone	not necessary	not recommended	not recommended	not necessary	not necessary
Should represent	any young CNS cell	corneal epithelial (CE) cell	retinal pigment epithelial (RPE) cell	differentiated cardiomyocyte	mesenchymal stem cell
(Mimicking) cells in use	iPS derived neurons, hNP1 (hESC derived neurons)	hiPS derived CE cells, human primary CE cells, HCE-T	hiPS derived RPE cells, human primary RPE cells, ARPE-19	primary rat cardiomyocytes, END2, PA6	mesenchymal stem cells, sarcomas, fibroblasts
Recommended cells	SH-SY5Y (neuroblastoma), hNP1 (hESC derived progenitor), iCell (hiPS derived neuron), fetal neural progenitors / neural stem cells	HCE-T	ARPE-19	Fibroblasts, continuous cardiomyocyte	fibroblasts, SAOS-2 (osteosarcoma), chondrosarcomas

APPENDIX 2 (2/3) Interview results

	NEURO	CORNEA	RETINA	HEART	MESENCHYMAL STEM CELL
SUBSTRATE					
Applications	3D cell culture, disease model, drug and toxicity testing. As a scaffold in transplantation therapy.	to mimic the structure of stroma	thin biomimetic substrate	3D cell culture, drug and toxicity testing. As a scaffold in heart patch.	3D cell culture
Arrangement of cells	on top, inside	on top only	on top only	on top, inside	inside
Positive control	3D: Puramatrix [®] . 2D: laminin coated well.	3D: Hydrogel not in use; try collagen. 2D: uncoated well.	3D: Hydrogel not in use. 2D: uncoated well.	3D: Puramatrix [®] , Matrigel [®] . 2D: gelatin coating	Cartilage: collagen. Soft tissue: Matrigel [®] , Tisel. 2D: Uncoated well
Negative control	3D: Hydrogel not in use (try unmodified PEG, chitosan, and unmodified cellulose). 2D: uncoated well.	3D: hydrogel not in use; try HA-PVA.		2D: Uncoated well	
Molecule for attachment	laminin	not with HCE-T	not with ARPE-19	gelatin, collagen (for cardiomyocytes)	no
Serum	serum-free preferred	in clinical use no serum; cell lines with serum	in clinical use no serum; cell lines with serum	serum-replacement (for cardiomyocytes)	serum is normally used

APPENDIX 2 (3/3) Interview results

	NEURO	CORNEA	RETINA	HEART	MESENCHYMAL STEM CELL
METHODS					
Parallels	3-5	3	3	3-5	5 (with which 3 repetitions first), later 3 parallels
Culture time	2 weeks	1 week	3-4 days (to detect the formation of mature RPE monolayer 28 to 42d)	1 week with fibroblasts	2 weeks (differentiation test 4 weeks)
Analyzing methods	a) Live/dead b) microscopy c) immunostaining d) RNA / protein isolation	a) Live/dead b) Microscopy and Presto blue proliferation assay c) Immunofluorescence staining d) (transepithelial resistance, gene expression)	a) Live/dead b) Microscopy and Presto blue proliferation assay c) Immunofluorescence staining d) (transepithelial resistance, gene expression)	a) Live/dead, b) number of cells / nuclei c) immunostaining d) immunostaining of KI67 e) time-lapse monitoring	a) microscopy and imaging (during growth) b) enzyme activity, immunochemical methods, PCR
To observe	a) viability b) morphology c) neuronal markers (identification), differentiation, apoptosis, migrational markers d) proliferation, genotype, phenotype	a) viability b) proliferation c) morphology d) (functionality)	a) viability b) proliferation c) morphology d) (functionality)	a) viability b) proliferation c) morphology d) cell division e) migration (+ attachment)	a) morphology, attachment b) proliferation (differentiation)

APPENDIX 3

PROTOCOL FOR TESTING CELL ATTACHMENT AND VIABILITY IN HYDROGELS

Attachment and viability testing share common instructions in most steps of this protocol. Steps that differ between those tests are specified in the protocol, otherwise the same steps are followed.

Attachment of cells is tested by culturing cells on hydrogels (named here OnGel samples). Viability of cells can be tested both encapsulated in hydrogels (3D samples) or on top of hydrogels (OnGel samples). 2D denotes uncoated well plate in this protocol. Hydrogels of 200 – 250 μ l final volume can be assessed with this protocol. Volumes and concentrations for sample preparation are calculated here for 200 μ l hydrogels.

The protocol includes the following main steps:

1. Preparation of materials and cell culture
2. Sample preparation
3. Phase contrast imaging in BioStation CT
4. Live/dead staining
5. Phase contrast and Fluorescence imaging in BioStation CT
6. Image Analysis in FiJi software
7. Quantitative analysis

1. Preparation of cells and materials before experiment

- 1.1 Grow WI-38 cells at least one week after thawing. WI-38 cells are subcultured twice a week with 1:2 ratio (or with seeding density of $2-4 \times 10^4$ cells / cm^2).
 - Medium for WI-38 cells (“WI-38 medium”) contains DMEM-F12 medium supplemented with 10% FBS, 1.25% Glutamax, and 0.5% Penicillin/Streptomycin.
- 1.2 Prepare stock solutions and dilutions of hydrogels and crosslinkers that will be tested. Sterilize unsterile solutions by sterile filtering, if applicable.
- 1.3 For attachment test: prepare poly(dimethylsiloxane) (PDMS) discs with around 1 mm thickness or smaller, and 8.5 mm diameter. (Diameter has to be smaller than the diameter of 48-well). Sterilize PDMS discs by autoclaving in 121 °C for 15 min.

2. Sample preparation

2.1 Warm up WI-38 medium and DMEM –F12 medium to 37 °C.

2.2 Prepare cell suspensions.

- Wash a T75 bottle of WI-38 cells two times with 10 ml DPBS. Detach cells with 2.5 ml trypsin, let it affect for 5-10 min. Stop trypsinization with 7.5 ml WI-38 medium (or DMEM-F12 medium if unsupplemented medium is needed for sample preparation).
- Count cells and prepare required concentrations of cell suspensions (see Table 1). Note that for encapsulated PuraMatrix® (PM) samples, cells are suspended in 10% sucrose solution. Cells for test samples may be diluted to media according to their respective instructions.
- Keep the temperature as close to 37 °C as possible while working at all times, and allow sufficient change of gases for cells (if needed, leave the cap untightened).

Table 1 Required concentrations of cell suspension, which are prepared in step 2.2. Presented volumes of the cell suspensions are needed to prepare samples with indicated final cell densities (step 2.3). Values for encapsulated (3D) sample layout is given only for PM; concentration and volume of cell suspension for test hydrogel are prepared according to their respective instructions, so that the final cell density would be equal to cell density in PM. Area of CELLSTAR® 48 well is 1.13 cm² and volume of hydrogels is 200 µl.

Sample layout	Concentration (cells / ml)	Volume (µl)	Final cell density	
			(cells / cm ²)	(cells / µl of gel)
2D, PDMS, OnGel	45200 - 67800	500	$2-3 \times 10^4$	-
3D (PM)	1.2×10^6	100	-	600

2.3 Prepare samples and controls into CELLSTAR® 48-well plate (Greiner Bio-one).

In all tests, leave one row of wells on each side of the well plate empty (for better imaging results). Prepare at least 3 replicates (parallel samples) of all samples and controls.

- For testing attachment, PDMS is used as the negative control. Positive controls are uncoated well (2D) and PM (OnGel layout, cells on top).
- For testing viability of cells on top of hydrogel, 2D is used as a reference and PM (OnGel layout, cells on top of hydrogel) is used as positive control.
- For testing viability of cells encapsulated in hydrogel, 2D is used as a reference and PM (3D layout, cells encapsulated in hydrogel) is used as positive control.

Attachment test

- a) PDMS discs are simply placed in the bottom of the wells. (Handle PDMS discs with tweezers at all times, do not touch PDMS discs with gloves, because they leave a stain on PDMS.) Transfer 500 μl of cell suspension in 2D control wells and on PDMS discs so that cell density on 2D and PDMS is $2\text{-}3 \times 10^4$ cells/cm².
- b) Prepare PM hydrogels with final volume of 200 μl according to PuraMatrix[®] instructions. In brief, transfer 200 μl of PM stock solution (1 mg/ml) into a well and, very carefully, add 400 μl of WI-38 medium for crosslinking. The medium needs to be added extremely carefully and slowly along the side of the well. Refresh medium twice within one hour.
- c) Prepare test hydrogels according to their respective instructions (for example, refer to Chapter 8.1.1.2.). Prepare all hydrogel samples with final volume of 200 μl .
- d) After sufficient crosslinking, add 500 μl of cell suspension on the hydrogels (PM and test samples). Final cell density on all samples should be $2\text{-}3 \times 10^4$ cells/cm².
- e) Add water to empty wells.
- f) Leave the plate in incubator or in BioStation CT for a few hours (minimum 2 h).

Viability test of cells on top of hydrogel

Prepare samples and controls according to instructions for attachment test, except for PDMS, which is not used, and culture cells in incubator for 1-3 days after sample preparation.

Viability test of cells encapsulated in hydrogel

- a) PDMS discs are simply placed on the bottom of the wells (do not touch PDMS discs with gloves). Transfer 500 μl of cell suspension in 2D control wells and on PDMS discs so that cell density on 2D and PDMS is $2\text{-}3 \times 10^4$ cells/cm².
- b) Prepare all hydrogel samples with final volume of 200 μl (for example, refer to Chapter 8.1.1.2.). Cell density in encapsulated samples (PM and test hydrogels) should be 600 cells/ μl of hydrogel.
- c) Prepare PM hydrogels according to PuraMatrix[®] instructions. In brief, mix 100 μl of cell suspension (cells in 10% sucrose) and 100 μl of PM stock solution (1 mg/ml). Transfer the mixture (200 μl) into a well and, very carefully, add 400 - 500 μl of WI-38 medium for crosslinking. The medium needs to be added extremely carefully and slowly along the side of the well. Refresh medium twice within one hour.

- d) Encapsulate cells to test hydrogels according to their respective instructions. Add 400 - 500 μ l of fresh WI-38 medium on the samples after sufficient crosslinking.
- e) Add water to empty wells.
- f) Leave the plate in incubator for 1-3 days (or place in BioStation for time-lapse imaging). If a longer culture time is desired, medium has to be refreshed every three days.

2. Phase contrast imaging (BioStation CT)

Place the well plate to BioStation CT half an hour before start of imaging to allow temperature equalize between well plate and BioStation CT. Condensation droplets will form under the well plate, and they disturb imaging, before the temperature has equalized. Use “Standard 48 well plate” as the well plate option.

The same imaging points are imaged with phase contrast microscope (Ph channel) before staining, and with Ph and fluorescence microscope (FL channels) after staining with Live/dead staining solution. Imaging with Ph channel before staining is optional in terms of the attachment and viability tests presented here, but this step makes setting imaging points faster after the staining and images may be useful for qualitative analysis.

Imaging points are set the same way for both attachment and viability tests; settings are dependent only on sample layout. Use the settings described in Table 2 for imaging samples and controls with phase contrast channel. Autofocus may be used with hydrogel samples, but it is unreliable with these samples. In that case, check images taken with autofocus in the beginning of the test to ensure images are focused to cells (inside or on the sample).

Another option to settings in Table 2 would be to image 2D, PDMS and 3D sample with Full Scan ja Tiling functions (see Chapter 8.2.4). Full Scan gives more images at the same time per one Z level, but all coordinates cannot be saved for a new experiment and one Z level is imaged at one time. Therefore, the Full Scan imaging is useful after staining.

Table 2 Settings for imaging points in different sample layouts. *Autofocus may be feasible, if sample is homogenous and surface is even.

Setting	2D	PDMS	OnGel	3D
Observation points	5 default	custom (Figure 1)	custom (Figure 1)	custom (Figure 1 and Table 4)
Channel	Ph	Ph	Ph	Ph
Magnification	10x	10x	10x	10x
Focusing	autofocus	custom	custom*	custom *
Copying points	automatically set, no need	no	no	yes
Z stack	no	no	no	no

When custom points are used, set the imaging points in samples by using the well plate map in Figure 1. The map is helpful in navigating in the samples by moving with arrows: each square corresponds to the area seen in the control panel of BioStation CT in the live mode (10x magnification).

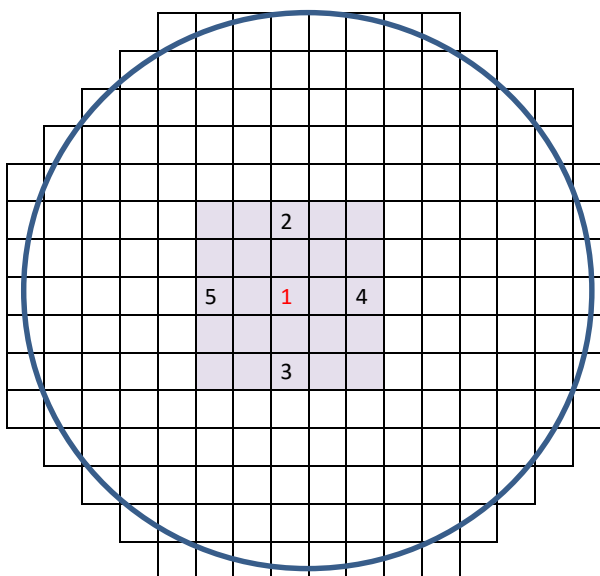


Figure 1. Well map for setting custom points. Each square corresponds to the area of well visible in "Live mode" at each time with 10x magnification.

Images that are obtained from the points marked in the well map (Figure 1) are named with x, y coordinates listed in Table 3. Other imaging points can be used, and especially for 3D samples the number of custom points is recommended to be larger than 5. However, points should be set to the colored area marked in Figure 1.

Table 3 Coordinates of imaging points in Figure 1, according to their distance from the center point of well. The imaging points are named in this way in resulting image files. In BioStation CT, these coordinates are not visible, but the distances are equal to the coordinates shown in BioStation CT.

Point	Coordinates (picture files)	
	x	y
1	000000	000000
2	000000	001520
3	000000	-001520
4	001520	000000
5	-003040	000000

Z values for custom points in Figure 1 can be chosen according to Table 4, according to the respective sample volume. These Z coordinates are given as examples, based on the average Z values on the surface of gellan gum gels in earlier experiments. Imaging points are set lower than those values, not to image above hydrogel samples. However, other Z values can be used if needed.

Table 4 Examples of Z values that can be set for points in 200 μ l or 250 μ l samples.

Point	200 μ l	250 μ l
1-2	3200 μ m	3400 μ m
3-5	3400 μ m	3700 μ m

Z = 3150 μ m is the estimated average Z coordinate for well bottom in the middle of the well. Therefore, Z coordinates can be safely set to two levels, Z₁ = 3200 μ m and Z₂ = 3400 in case of 200 μ l hydrogel, and Z₁ = 3200 μ m and Z₂ = 3600 in case of 250 μ l hydrogel.

Note: BioStation changes $\Delta Z = 0$ μ m corresponding to Z = 3500 μ m when returning from New experiment mode into Live observation mode. Therefore, it is more useful to set points according to Z value, instead of using ΔZ .

Before scheduling the experiment, select the option Holder → Save to save the set options. Schedule the experiment to obtain phase contrast images.

3. Live/dead staining

Prepare a solution from LIVE/DEAD® cytotoxicity/viability kit (ThermoFisher Scientific) by mixing 5 μ l EthD-1 (stock 2 mM, final 0.1 μ M) and 2 μ l calcein-AM (stock 1 mM, final 0.2 μ M) into 10 ml PBS, 37 °C (work protected from light). Aspirate medium

from wells very carefully, avoiding disruption of hydrogels. Add 500 μ l of staining solution to each well. Incubate in BioStation CT (37 °C) for 30 - 45 min before imaging.

4. Fluorescence imaging

Check that condensation droplets under the well plate have disappeared, as they disturb or even prevent imaging. Droplets can be wiped off gently with tissue paper, if incubation time tends to become too long. Observe cells with fluorescence channels in live mode to determine correct excitation times for each channel. To make the next step faster, the chosen excitation times can be set as personal options in main menu.

In New experiment mode, use either “Previous setting” or load the previously saved holder to retrieve previously set imaging points and their imaging settings. Now, add fluorescence channels to settings of each well (Ch2 for live and Ch4 for dead cells in our laboratory, filter cubes can be changed depending on equipment). In addition, see that the excitation times are correct for each sample. Schedule the experiment for obtaining phase contrast and fluorescence images.

5. Image Analysis in FiJi software

Analyze fluorescence images obtained in the previous step with ImageJ software, FiJi distribution. Use a macro Smart_J_worker (Appendix 5) to open and process images (all coordinates from one sample, one magnification, and one time point). Count the numbers of live cells (L_i) and dead cells (D_i) in each fluorescence image. Green cells are live and red cells are dead. If there are cells stained both with green and red stains, count them as dead cells.

6. Quantitative analysis

Numbers of live cells (L_i) and dead cells (D_i) in each image that were obtained in step 6 are used here for calculating attachment and viability. For each sample, calculate the average numbers of live cells and dead cells in an image with equations 1 and 2. In one sample, the average number of live cells in an image is

$$\bar{L} = \frac{1}{n} \sum_{i=1}^n L_i , \quad (1)$$

and the average number of dead cells in an image is

$$\bar{D} = \frac{1}{n} \sum_{i=1}^n D_i , \quad (2)$$

where i = index of the image and n = number of images analyzed from the sample type.

Assessment of attachment

Attachment of cells to test material is compared to attachment on uncoated well plate (2D positive control). Attachment is calculated according to equation (3). The average number of cells attached in one sample is represented by the average number of cells per image in the sample (\bar{L} for live cell; \bar{D} for dead cells; and $\overline{(L + D)}$ for all cells). When s denotes sample and 2D denotes 2D positive control, attachment on a sample is:

$$\begin{aligned} Attachment_s &= \frac{\text{cells on sample}}{\text{cells on 2D}} = \frac{\text{average (cells per image on sample)}}{\text{average (cells per image on 2D)}} \\ &= \frac{(\bar{L} + \bar{D})_s}{(\bar{L} + \bar{D})_{2D}} = \frac{\bar{L}_s + \bar{D}_s}{\bar{L}_{2D} + \bar{D}_{2D}} \end{aligned} \quad (3)$$

Using attachment values calculated for each sample, calculate the average attachment and standard deviation for each material. Uncoated well plate (2D positive control) has a comparison value of 1.

Assessment of viability

Viability of cells (both in 3D samples and OnGel samples) is calculated by dividing the total number of live cells with total number of all cells (dead and live) in a sample. The number of analyzed images is the same for both numbers, and viability can be calculated with average numbers of cells (live or all) per image. (This way same numbers can be used as above for attachment.) The viability is calculated for each sample according to equation (4).

$$\begin{aligned} Viability_s &= \frac{(\text{live cells})_s}{(\text{live cells} + \text{dead cells})_s} \\ &= \frac{\sum_{i=1}^n L_i}{\sum_{i=1}^n (D_i + L_i)} = \frac{\frac{1}{n} \sum_{i=1}^n L_i}{\frac{1}{n} \sum_{i=1}^n D_i + \frac{1}{n} \sum_{i=1}^n L_i} = \frac{\bar{L}}{\bar{L} + \bar{D}} \end{aligned} \quad (4)$$

Using viabilities of each sample, calculate average viability for each material and their standard deviations. The viability of cells in tested hydrogel is compared to that of cells in 3D positive control, PuraMatrix®.

APPENDIX 4

PARTICLE COUNT ALGORITHM FOR FIJI

Before counting cells with this algorithm (or after step 1), it is advised to estimate the needed threshold values for green and red channel and the size of cells that will be counted. (Refer to Chapter 8.1.4.)

1. Open images and create RGB stack

- a. Use a macro Smart_J_worker (Appendix 5) to open images (all coordinates from one sample, one magnification and one time point).

OR

- b. If merged RGB images have been saved already earlier (by using Smart_J_worker, for example) select File / Import / Image Sequence. Select one image in the folder where all imaged you want to analyze are saved. With default settings, all images in the folder will be opened.

OR

- c. For taking this step manually (not recommended) choose for each individual points:
 - i. Open images, green and read channel: File / Open...
 - ii. Merge the channels: Image -> Color -> Merge Channels.
 - iii. Choose the correct file for each color. Untick “create a composite”. One RGB type image has been formed.
 - iv. Create an RGB stack: Image -> Type -> RGB Stack. A stack of three images is formed, in 8-bit format. Save the file and close. Repeat for all points in the sample and continue by importing all RGB stacks.

2. Separate into stacks of channels

- a. Select Image / Color / Separate channels. This will create 3 stacks, one for each channel.
- b. Close the stack of Blue channel, it will not be analyzed.

3. Adjust threshold

- a. For each stack, the threshold is set separately (allows choosing same or different threshold values). Choose one stack at a time, and select Image/Adjust/Threshold. For example:
 - i. threshold when analyzing red channel: 100-225,
 - ii. threshold when analyzing green channel: 130-225
 - iii. Method: default, color: B&W
 - iv. Tick “dark background” and “stack histogram”
 - v. Select “Apply”
- b. A new window opens for converting stack to Binary. Choose the following settings.
 - i. Method: Default
 - ii. Background: Dark
 - iii. Other boxes not selected (If it is preferred to check that thresholds were set correctly, tick “List Thresholds”.)
- c. Now the stack has been converted to binary masks, where the images have only values 0 (background) or 255 (cells).
- d. Repeat adjusting threshold (step 3) to the second channel.

4. (Optional step: Separate cells that are together

- a. Select Process/Binary/Watershed.
 - i. Use default settings
- b. Watershed makes 1 px line between areas that FiJi considers two different particles.)

5. Count particles

- a. Select one stack of channels at a time and use the Analyze Particles plugin: Analyze / Analyze particles. Settings:
 - i. Size: for example, 40 px² – infinity
 - ii. Circularity: 0.00 – 1 (1 being a perfect circle)
 - iii. Show: outlines
 - iv. Tick: Display results, Clear results, Summarize, Exclude on Edges
 - v. Untick: Add to Manager, Include holes, Record starts, In situ Show
- b. This step will produce a Summary window which shows the number of particles counted in the stack (either green or red channel). The Summary table can be saved or values can be copied for further calculations.
- c. Repeat step 5 to the stack of second channel.

APPENDIX 5

MACRO FOR OPENING IMAGES AND MERGING CHANNELS IN FIJI

BioStation CT has a very intricate way of dividing images into folders. This is very helpful for knowing the origin of the image, but screening pictures with FiJi (and manually) becomes slow because of this, as each image that was taken was located in individual folders behind a long path. A macro, “Smart_J_worker”, was written to more efficiently open images in FiJi from their respective folders and to merge the green and red channels. This macro was written by MSc Boris Kashentsev.

The macro opens all images from one sample, that were desired to analyse at one time (Figure below):

- all coordinates imaged with the same magnification (and fluorescent channels)
- one time point of experiment
- one time point of imaging round
- both green and red channels.

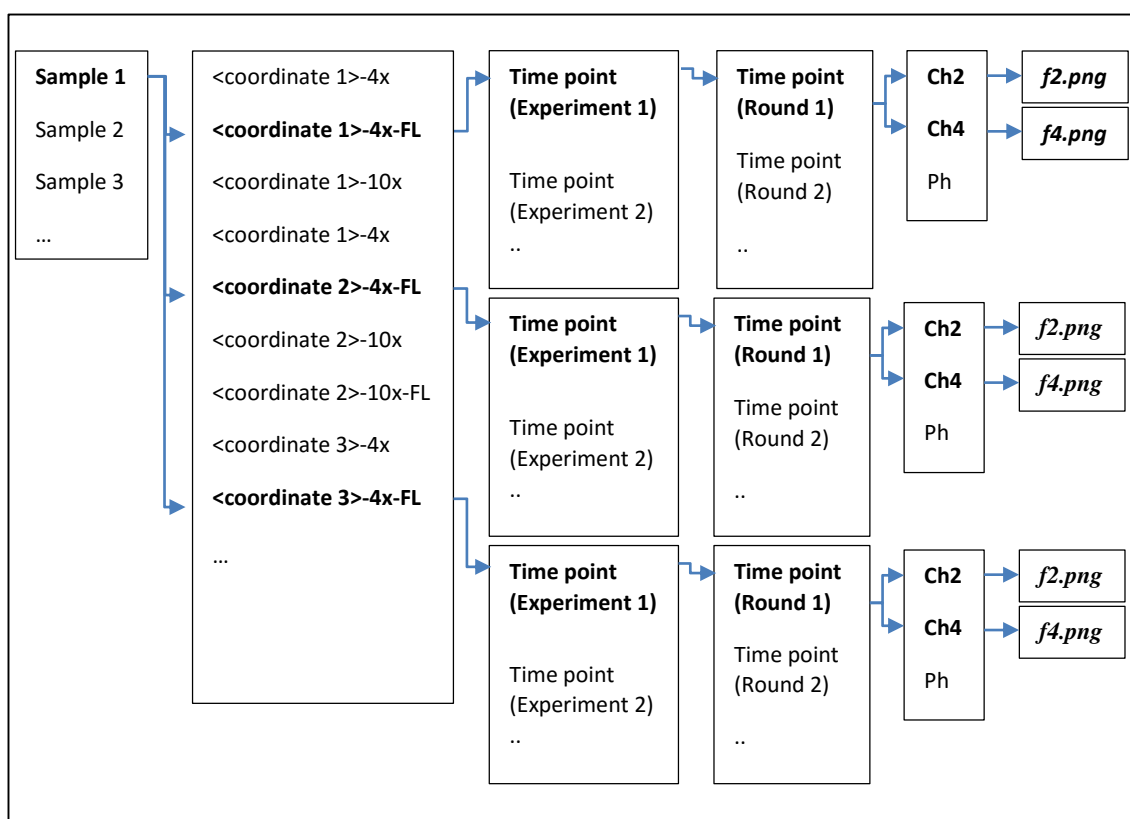


Figure: Distribution of images to folders after downloading from BioStation CT. The macro for FiJi opens images (.pgn) at the same time from: one sample, all coordinates imaged with the same magnification and fluorescent channels, one time point of experiment, one time point of imaging round, from both green and red channels. The macro also merges the correct green and red channels and makes an RGB stack.

The macro merges the correct green and red channels and makes a stack of these RGB format images (all coordinates in one stack). The images can be automatically saved, in which case a new folder is created for the resulting images. The macro also enables opening all imaging rounds at a time.

The code of the macro can be saved as a .txt file and used for image analysis in FiJi by selecting Plugins/Macros/Run. Note that before using the macro, a black image is needed as the blue channel (because RGB image is formed). The black image should be 1000x1000 pixel, named "blue.png" saved in the folder named in the code row 114 (for example, "C:\\pictures"). The macro asks for the location of images that will be analyzed. The code of the macro is below.

```

1  dir = getDirectory("Choose the channel folder containing one of the
   images you want to process.");
3
   dirComponents = split (dir, "\\");
5
   Dialog.create("Smart Choice");
7  Dialog.addRadioButtonGroup("Choose the folder of current coordinate:",
   dirComponents,
9   dirComponents.length,
   1,
11  dirComponents[0]);
   Dialog.addRadioButtonGroup("Choose the folder of the imaging round (time
13 stamp):",
   dirComponents,
15  dirComponents.length,
   1,
17  dirComponents[0]);
   Dialog.addCheckbox("Save to folder", false);
19 Dialog.addCheckbox("Analyze all time points",false);
   Dialog.show();
21
   coordinatesDir = Dialog.getRadioButton;
23 timeStamp = Dialog.getRadioButton;
   toSave = Dialog.getCheckbox();
25 toAllRoundTimes = Dialog.getCheckbox();

27 for(i = 0; i < dirComponents.length; i++){
   if(dirComponents[i] == coordinatesDir){
29     indexOfCoord = i;
   }
31   if(dirComponents[i] == timeStamp) {
     indexOfTime = i;
33   }
   }
35
   coordinatesDirComponents = split(coordinatesDir, "-");
37 magnification = coordinatesDirComponents[coordinatesDirCompo-
   nents.length-2];
39
   dirBeforeCoor = dirComponents[0];
41 for(i=1; i<indexOfCoord; i++){
     dirBeforeCoor = dirBeforeCoor + "\\\" + dirComponents[i];

```

```

43 }

45 listOfDir = getFileList(dirBeforeCoor);
   index=0;
47 for(i = 0; i < listOfDir.length; i++){
   if(indexOf(listOfDir[i], "-"+magnification+"-")!=-1 && indexOf(lis-
49 tofDir[i], "-FL")!=-1){
   if(index == 0){
51     listOfNeededDir = listOfDir[i];
   index = 1;
53   } else {
   listOfNeededDir = Array.concat(listOfNeededDir, lis-
55 tofDir[i]);
   }
57   }
59 }

   dirBeforeTime = "";
61 for(i = indexOfCoor + 1; i < indexOfTime; i++){
   if (dirBeforeTime == "")
63     dirBeforeTime = dirComponents[i];
   else
65     dirBeforeTime = dirBeforeTime + "\\\" + dirComponents[i];
67 }

   //print(dirBeforeTime);
69
   if (dirBeforeTime == "")
71     listOfRoundDir = getFileList(dirBeforeCoor + "\\\" + coordi-
   natesDir);
73 else
   listOfRoundDir = getFileList(dirBeforeCoor + "\\\" + coordinatesDir
75 + "\\\" + dirBeforeTime);

77 index = 0;
   for(i = 0; i < listOfRoundDir.length; i++){
79     //print(listOfRoundDir[i]);
   if (indexOf(listOfRoundDir[i], "\/") != -1){
81     //print("Went through: " + listOfRoundDir[i] + " index: " +index
   );
83     myArray = split(listOfRoundDir[i], "\/");
   if(index == 0) {
85     correctList = myArray[0];
   index = 1;
87     }
   else
89     correctList = Array.concat(correctList, myArray[0]);
   }
91 }
   listOfRoundDir = correctList;
93

   if(!toAllRoundTimes){
95     listOfRoundDir = Array.concat(timeStamp,"");
   }
97 //Array.show(listOfRoundDir);

99 for (j = 0; j <listOfRoundDir.length; j++){
   if(listOfRoundDir[j] != ""){
101     setBatchMode(true);

```

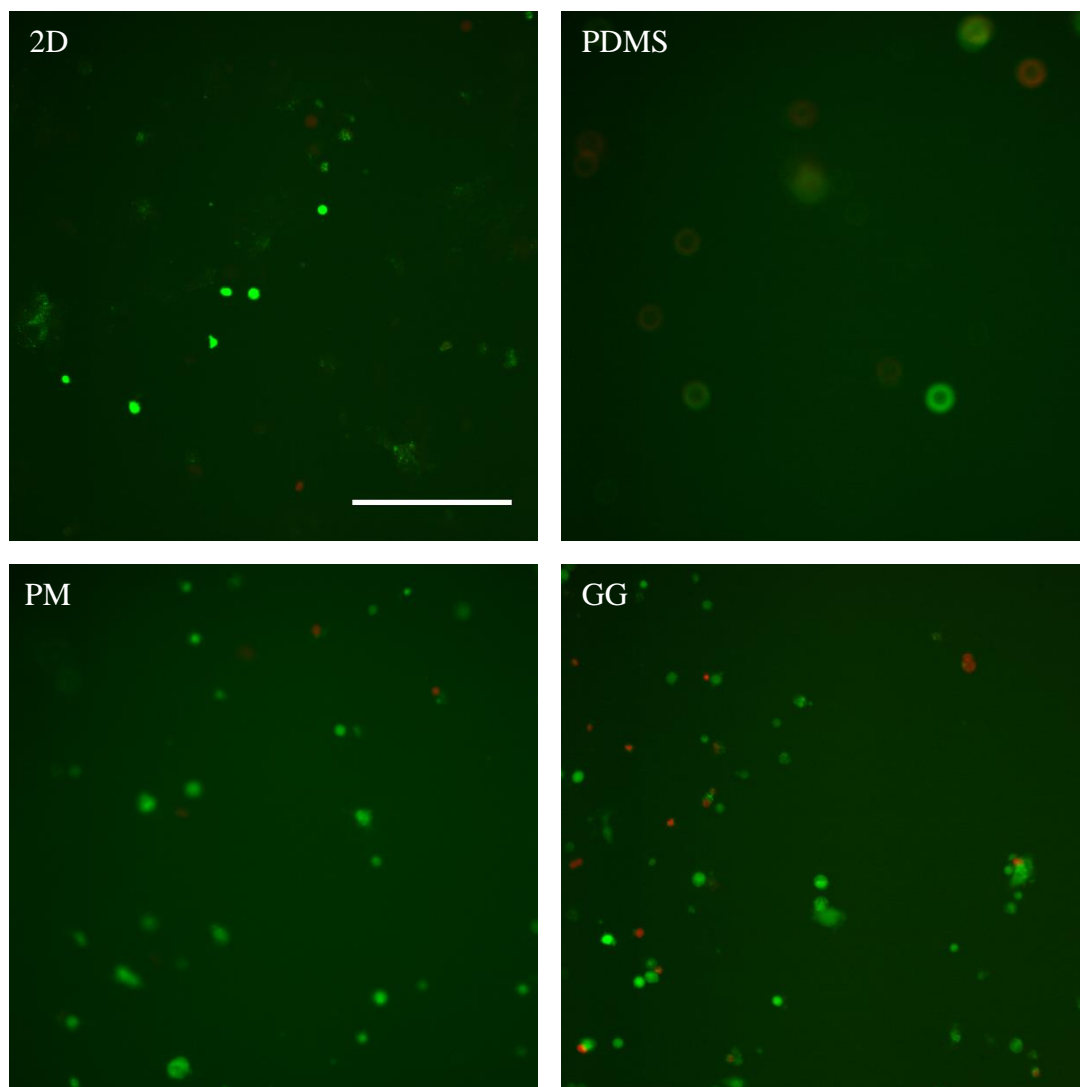
```

        stack = 0;
103     for (i = 0; i < listOfNeededDir.length; i++){
            showProgress(i+1, listOfNeededDir.length);
105         if(dirBeforeTime == "")
            dir = dirBeforeCoor + "\\\" + listOfNeededDir[i] + "\\\"
107 + listOfRoundDir[j] + "\\\";
            else
109                 dir = dirBeforeCoor + "\\\" + listOfNeededDir[i] + "\\\"
+ dirBeforeTime + "\\\" + listOfRoundDir[j] + "\\\";
111                 ch2dir = dir + "Ch2";
                    ch4dir = dir + "Ch4";
113 //Change the variable of blueDir to the location where file blue.png is
saved. The file has to be 1000 x 1000 px black image.
115                 blueDir = "C:\\pictures";
                    ch2file = getFileList(ch2dir);
117                 ch2file = ch2file[0];
                    ch4file = getFileList(ch4dir);
119                 ch4file = ch4file[0];
                    blueFile = "blue.png";
121                 open(ch4dir + "\\\" + ch4file);
                    open(ch2dir + "\\\" + ch2file);
123                 open(blueDir + "\\\" + blueFile);
                    run("RGB Merge...", "red=["+ch4file+"] green=["+ch2file+"]
125 blue=["+blueFile+"]");
                    index = indexOf(ch4file, "f4");
127                 name = substring(ch4file, 0, index);
                    if (toSave == 1)
129                 {
                        File.makeDirectory(dirBeforeCoor + "\\\" + magnification
131 + "-RGB\\");
                            File.makeDirectory(dirBeforeCoor + "\\\" + magnification
133 + "-RGB\\\" + listOfRoundDir[j] + "\\");
                                saveAs("png", dirBeforeCoor + "\\\" + magnification + "-
135 RGB\\\" + listOfRoundDir[j] + "\\\" + name);
                                    }
137                 width=getWidth();
                    height=getHeight();
139                 run("Copy");
                    close();
141                 if (stack==0) {
                            newImage("RGB Stack", "RGB Black", width, height, lis-
143 tofNeededDir.length);
                                stack = getImageID;
145                 }
                    selectImage(stack);
147                 setSlice(i+1);
                    run("Paste");
149                 setMetadata(name);
            }
151
        setSlice(1);
153     run("Select None");
        setBatchMode(false);
    }
}

```

APPENDIX 6 (1/2)

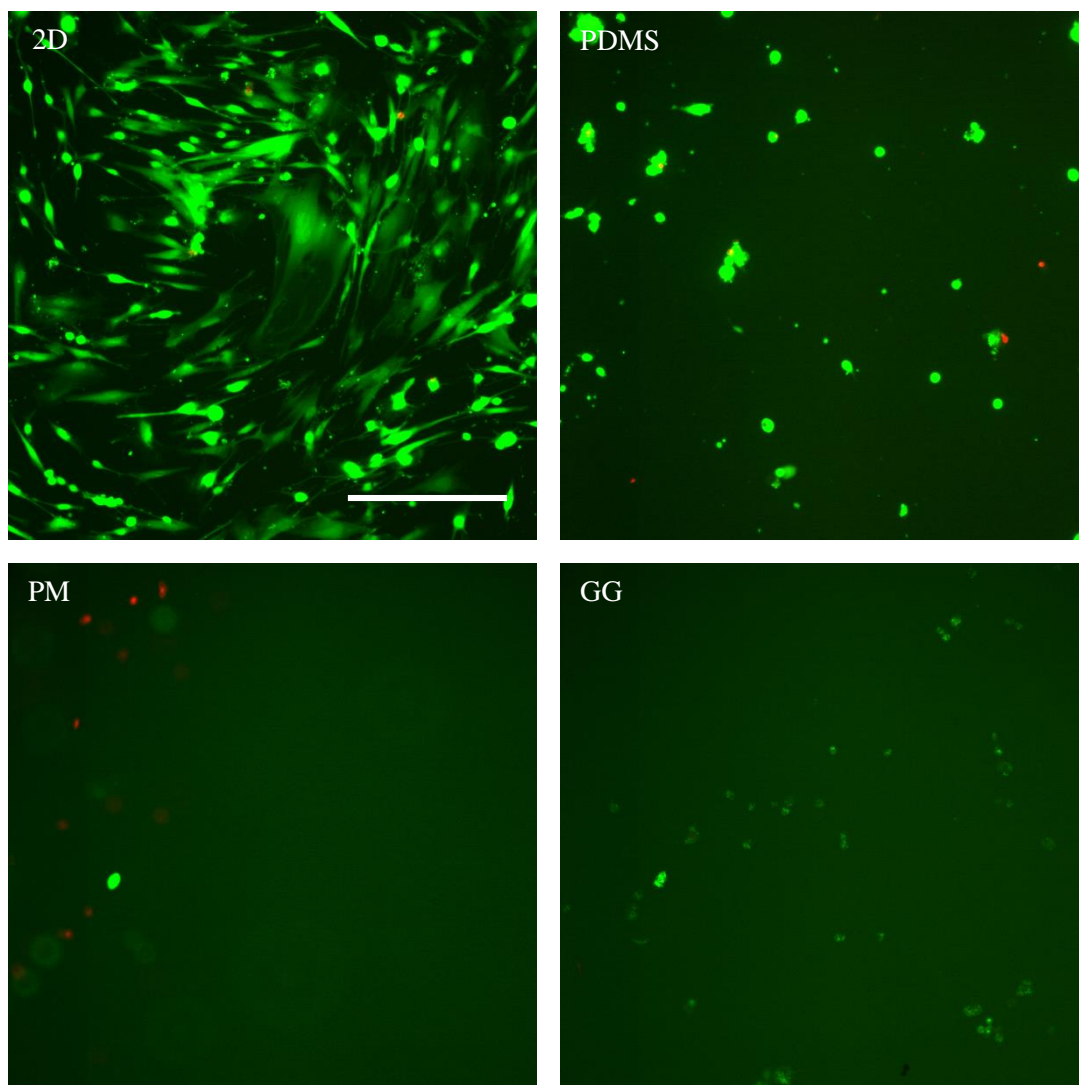
FLUORESCENCE IMAGES



Fluorescence images of cells cultured on uncoated well (2D), PDMS disc, and PuraMatrix[®] (PM) and gellan gum (GG) hydrogels. Cells were cultured 5 h before staining. Scale bar = 200 μ m.

APPENDIX 6 (2/2)

FLUORESCENCE IMAGES



Fluorescence images of cells cultures on uncoated well plate (2D) and PDMS disc, and encapsulated in PuraMatrix[®] (PM) and gellan gum (GG) hydrogels. Cells were cultured 2 d before staining. Scale bar = 200 μ m.